

EFFECT OF CASTOR OIL, MORINGA SEED OIL AND
CANOLA OIL AS LUBRICITY ENHANCERS FOR DIESEL
FUEL

Andrew Osei Sakyi

EFFECT OF CASTOR OIL, MORINGA SEED OIL AND
CANOLA OIL AS LUBRICITY ENHANCERS FOR DIESEL
FUEL

by

Andrew Osei Sakyi

A dissertation submitted in partial fulfilment of the requirements for the
degree

Master of Engineering (Chemical Engineering)

In the

Department of Chemical Engineering

University of Pretoria

12 July 2021

EFFECT OF CASTOR OIL, MORINGA SEED OIL AND CANOLA OIL AS LUBRICITY ENHANCERS FOR DIESEL FUEL

Synopsis

The amphiphilic qualities of plant oils that emerge from their fatty acid makeup lead to improved lubricity. To produce diesel that is friendlier to the environment requires severe hydrotreating, unfortunately the same process also reduces the lubricity of the fuel. Adding petroleum based lubricity additives to the fuel may improve diesel lubricity but also present the challenge of being environmentally unfriendly or expensive. Plant oils such as castor oil, moringa oil and canola oil offer a green and relatively inexpensive approach to lubricating hydrotreated diesel fuels. This work reports on lubricity tests carried out on diesel fuel treated with castor oil, moringa oil and canola oil as lubricity enhancers to investigate lubricating abilities of the resulting mixtures. The high frequency reciprocating rig (HFRR) which is generally accepted as a universal test apparatus for determining the lubricity of diesel fuels was used. The diesel fuel was treated with these plant oils up to a concentration of 1 % (w/w).

The friction coefficient (COF) and the amount of wear that occurred was measured and the wear scar surfaces were also evaluated. Factors that influence wear were also taken into consideration.

The following findings were made from this study:

- Castor oil, moringa oil and canola oil can function as diesel lubricity enhancers. Increase in plant oil concentration in diesel stimulated a stable film formation and improved the tribo-characteristics of the fuel.
- A concentration of less than 1 % (w/w) of any of the three plant oils investigated in diesel (i.e. castor oil, moringa oil or canola oil) was enough to cause the wear scar diameter (WSD) of the fuel to reduce appreciably. As reference, the wear scar diameter (WSD) of the untreated diesel fuel after HFRR tests was 897 μm . However, at 1 % (w/w) of each plant oil in the diesel fuel, the observed reduction in WSD was 221.2 μm (castor oil), 339.06 μm (moringa oil), and 281.84 μm (canola oil).
- Castor oil has comparatively better lubrication in diesel than moringa oil and canola oil owing to its hydroxyl functional group that increases both the viscosity and polarity of the oil. A concentration of less than 0.2 % (w/w) of castor oil in diesel was enough to bring the WSD of the fuel down to below the maximum allowable limit of 460 μm as specified in ISO 12156.
- Viscosities of castor oil, moringa oil and canola oil have a significant effect on performance as a lubricity enhancers.
- Friction coefficient for diesel treated with castor oil, moringa oil and canola oil increases with increasing temperature because at high temperatures, the lubricant film formed by fatty acids tends to be less stable and breaks down more easily. As expected, increase in temperature also causes an increase in wear, for all three mixtures.
- Lubricating ability of moringa oil is much lower compared to castor oil and canola oil. Mild to severe abrasive wear was observed for diesel treated with moringa oil.

- Moisture in the atmosphere affects the repeatability of the friction and wear tests. This occurs because of the formation of an oxide layer on the metal surface that involves water. Upon keeping a close humidity range of 50 % - 55 % in the test chamber an improvement in repeatability of the test results was observed.

Keywords: plant oil, biodegradability, diesel fuel, lubricity enhancer.

Acknowledgements

I would like to show my utmost gratitude to the friendly agents at the petroleum companies who assisted with the supply of untreated diesel fuel used in this research.

A big thank you as well to Mr and Mrs Sakyi and prof. Philip de Vaal for their advice and assistance in this research work.

Table of contents

Synopsis	ii
Acknowledgements	v
Nomenclature	xii
1. Introduction	1
1.1. Background	1
1.2. Problem statement	3
1.3. Objectives	4
1.4. Method, scope and limitations	5
2. Literature	6
2.1. Regimes of lubrication	6
2.1.1. Hydrodynamic lubrication	7
2.1.2. Elastohydrodynamic lubrication	10
2.1.3. Mixed lubrication	11
2.1.4. Boundary lubrication	11

2.2.	Surface layer characterization	14
2.2.1.	Deformed layer	16
2.2.2.	Chemically reacted layer	16
2.2.3.	Physisorbed layer	17
2.2.4.	Chemisorbed layer	18
2.3.	Molecular science of lubricity additives.....	18
2.3.1.	Tribo-chemical reactions	19
2.3.1.1.	Oxidation of plant oils.....	21
2.4.	Friction	24
2.4.1.	Laws of friction	25
2.4.1.1.	Adhesion	26
2.5.	Wear.....	28
2.5.1.	Variations of wear	29
2.5.1.1.	Adhesive wear.....	29
2.5.1.2.	Corrosive wear	31
2.5.1.3.	Abrasive wear.....	32
2.5.1.4.	Fatigue wear.....	33
2.6.	Diesel fuel lubricity model	34
2.7.	Wear scar corrections.....	36

2.8.	Diesel production	38
2.8.1.	International diesel specifications	39
2.8.2.	Diesel properties	43
2.8.2.1.	Cetane number	43
2.8.2.2.	Flash point.....	43
2.8.2.3.	Aromatic content	43
2.8.2.4.	Sulphur content.....	44
2.8.2.5.	Lubricity.....	44
2.8.2.6.	Oxidative stability.....	45
2.8.2.7.	Cloud point.....	45
2.8.2.8.	Pour point	46
2.9.	Additive technology.....	46
2.9.1.	Plant oils as lubricity enhancers	47
2.9.1.1.	Castor oil	50
2.9.1.2.	Canola oil.....	52
2.9.1.3.	Moringa oil.....	53
2.9.2.	Physical properties of plant oils.....	56
2.9.2.1.	Molecular structure of fatty acids.....	56
2.9.2.2.	Viscosity	58
2.9.2.3.	Viscosity index (VI)	60
2.9.2.4.	Density	61
3.	Experimental work.....	65
3.1.	Apparatus	66
3.1.1.	High frequency reciprocating rig (HFRR).....	66

3.1.1.1. WS1.4 correction.....	69
3.1.2. Ultrasonic cleaner	71
3.1.3. Viscometer	72
3.1.4. Relative humidity control	72
3.1.5. Optical microscope.....	73
3.2. Materials and chemicals.....	73
3.3. Experimental method.....	76
3.3.1. Filtering process (ASTM D6217)	76
3.3.2. Cleaning of test specimen	77
3.3.3. HFRR test procedure	77
3.3.4. Wear scar measurement	78
3.3.5. Calculating averages and standard deviations.....	79
4. Results and discussion	80
4.1. Effect of plant oil concentration on lubrication	81
4.1.1. Friction coefficient	81

4.1.2. Diesel lubricity model.....	89
4.2. Effect of temperature on lubrication.....	93
4.2.1. Friction coefficient	93
4.2.2. Wear mechanism	100
4.3. Effect of load on lubrication	104
4.3.1. Friction coefficient	105
4.3.2. Wear mechanism	113
5. Conclusions and recommendations	118
5.1. Physical properties	118
5.1.1. Molecular structure.....	119
5.1.2. Viscosity	119
5.1.3. Viscosity index (VI)	119
5.1.4. Density	120
5.2. Effect of temperature on lubrication.....	120
5.2.1. Friction coefficient	120

5.2.2. Wear mechanism	121
5.3. Effect of load on lubrication	121
5.3.1. Friction coefficient	121
5.3.2. Wear mechanism	121
5.4. Effect of plant oil concentration on lubrication	122
5.4.1. Friction coefficient	122
5.4.2. Wear mechanism	123
6. References	124
Appendix A - Humidity control.....	131
Appendix B – Standard deviations (error bars)	131
Appendix C – Wear scars at 0.2 % (w/w) plant oil in diesel	132

Nomenclature

A	Surface area (Nominal)	m^2
A_a	Apparent area	m^2
A_r	Real area	m^2
AVP	Average water vapour pressure	kPa
E	Activation energy	J
F_{res}	Resultant force	N
F	Force	N
f	Frictional force	N
H_R	Relative humidity	%
h	Thickness	mm
h_o	Initial thickness	mm
h_i	Final thickness	mm
L	Load	N
MWSD	Mean wear scar diameter	μm
η	Dynamic viscosity	Pa·s
P	Pressure	Pa
P_{water}^*	Saturation pressure of water	Pa
P_{water}	Partial pressure of water	Pa
R	Universal gas constant	kJ/kmol·K
SO _x	Sulphur oxides	-
T	Temperature	K
τ_a	Shear strength for dry contact	$N \cdot m^{-2}$
τ_l	Shear strength for lubricated contact	$N \cdot m^{-2}$
u	Speed	$m \cdot s^{-1}$
μ	Friction coefficient	-
W	Weight	N
WR%	Percentage wear reduction	%
WS1.4	Wear scar corrected to 1.4 kPa	μm
γ	Fraction of unlubricated area	-

1. Introduction

In this chapter a discussion of important theories describing the problem associated with severely hydrotreated fuels are discussed in brief. The objectives of this research and the methodology used in achieving these objectives are also discussed. The subsequent chapter (chapter 2) discusses relevant literature concerning friction, wear and lubrication. Diesel properties, international diesel specifications and an overview of additive technology are also presented in chapter 2. Chapter 3 discusses the methods that were used to explore the underlying principles of how boundary films are adsorbed, reacted, and desorbed as an effect of the concentration, temperature and load. The materials and equipment used in this investigation are also listed and discussed. In chapter 4 all experimental results are presented and discussed. The experimental and modelling results together bring an understanding to the behaviour of castor oil, moringa oil and canola oil in reducing wear. Chapter 5 concludes with derived understandings based on results from the experimental work and makes recommendations for further research and studies.

1.1. Background

Diesel fuel sourced from crude oil has good inherent lubricity. This is due to aromatic, unsaturated and polar oxygenated compounds that are naturally present in the feedstock (Agarwal *et al*, 2013). To reduce air pollution due to the presence of SO_x in exhaust fumes and the consequential acid rain having devastating effect on the ecosystem, stringent requirements have been put in place to limit the amount of sulphur in fuels. As a result, during diesel production

hydrotreating is carried out to remove sulphur ([Figure 1.1](#)). Hydrotreating for sulphur removal is called hydrodesulphurization (Stolten & Emonts, 2016). In this process the feedstock is deaerated and mixed with hydrogen, preheated in a fired heater (316 °C – 427 °C), and then charged under pressure (up to roughly 6 900 kPa) through a fixed-bed catalytic reactor.

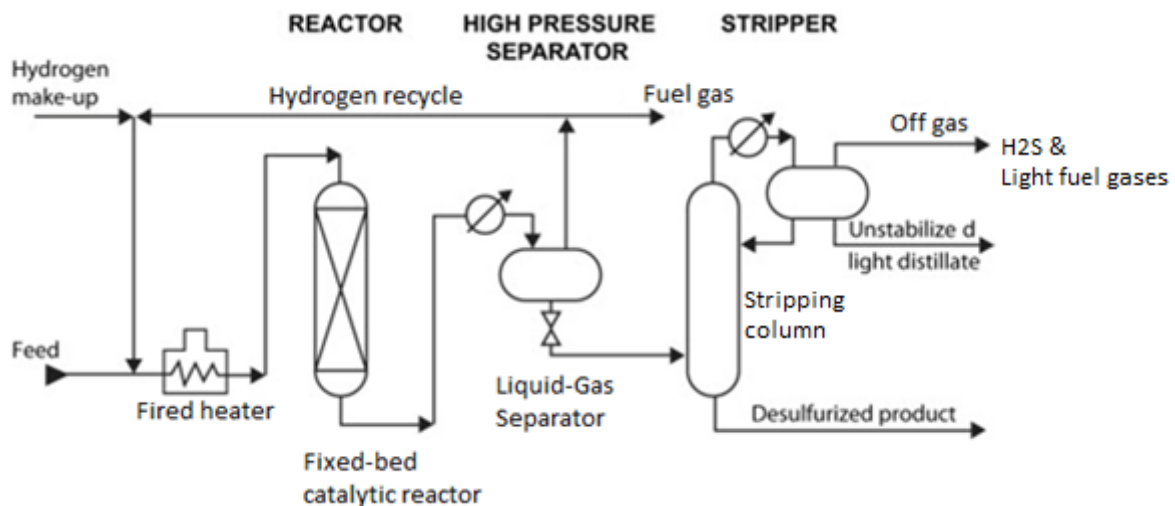


Figure 1.1: Schematic of distillate hydrotreating (Stolten & Emonts, 2016)

In the fixed-bed catalytic reactor, the reaction that takes place removes environmentally hazardous elements such as sulphur and nitrogen compounds in the feedstock by converting these contaminants to H₂S and NH₃. The products from the reaction leave the reactor and are cooled to a low temperature before entering a liquid/gas separator.

The hydrogen-rich gas from the high-pressure separation is recycled to combine with the feedstock, and the low-pressure gas stream rich in H₂S is sent to a gas-treating unit where H₂S is removed. The purified gas is then appropriate to use as a fuel in refinery furnaces. The liquid stream is the product from hydrotreating and is normally sent to a stripping column for removal of H₂S as an off-gas together with other undesirable components ([Figure 1.1](#)).

Catalytic hydrotreating is necessary in diesel production. The reasons are that the process can remove about 90 % of impurities such as sulphur, nitrogen and oxygen from liquid petroleum fractions. These impurities can have a negative impact on the catalyst used for hydrotreating. The contaminants can also affect the quality of the finished product negatively (Stolten & Emonts, 2016).

Most importantly hydrotreating is used to ensure that the fuel produced complies with current environmental legislation on pollution. The sulphur content in fuels is of primary concern as sulphur is considered a major pollutant. The first European emission standard for diesel issued in 1992 stipulated a maximum sulphur content of 2 000 ppm, and this was also applied in several parts of the world including South Africa. Nonetheless, in striving to produce environmentally safe fuels, the new regulation (Euro 6) stipulate sulphur should not be found in excess of 10 ppm (Hultema *et al*, 2019: 7). South Africa still maintains a maximum sulphur content of 50 ppm but even this looks likely to change in the near future (SANS 342, 2016).

1.2. Problem statement

The challenge associated with diesel production is to produce diesel that is friendlier to the environment and this requires severe hydrotreating (Stolten & Emonts, 2016). The hydrotreating is aimed at removing sulphur from the crude oil, but unfortunately the process also removes (chemically converts) the polar compounds and unsaturated compounds that give lubricity to the fuel. Polar compounds and unsaturated compounds are lubricity enhancers naturally found in diesel. Their removal leads to loss of lubricity or poor lubricity in the final diesel product (Agarwal *et al*, 2013; Knothe & Steidley, 2005; LePera, 2000).

Using diesel fuel that has poor lubricity may cause severe wear on machine parts, increased diesel consumption, increased emissions, and possible damage to fuel injector pumps of compression ignition engines (Agarwal *et al*, 2013).

In seeking to remedy the problem of lubricity deficiency in diesel fuels after hydrodesulphurisation, different techniques can be undertaken, one of which is adding lubricity enhancers to the fuel (Agarwal *et al*, 2013). Most fuel manufacturers use various lubricity additives to increase fuel lubricity to acceptable levels after hydrodesulphurisation, but those additives also present a possible problem of being environmentally unfriendly or expensive (Agarwal *et al*, 2013).

1.3. Objectives

Plant oils have unique characteristics that can enhance the lubricity behaviour of diesel. They are environmentally friendly and possess unique characteristics that can substitute various additives in use today. In this study the objectives were to:

- Determine contributions that castor oil, moringa oil and canola oil can make to the lubricity of diesel fuel.
- Determine concentrations of castor oil, moringa oil and canola oil at which appreciable lubricity is reached with diesel with respect to international lubricity standards.

1.4. Method, scope and limitations

The HFRR tribometer was used as a bench test for all the friction and wear tests. The viscosities of castor oil, moringa oil and canola oil were determined using the Anton Paar SVM 3000/G2 Stabinger viscometer. The diesel fuel used in this research work was obtained from a crude oil sourced refinery. It contained no fuel additives. The certificate of analysis for the fuel is presented in the Experimental section of this report.

Plant oils suffer defects as potential lubricants because of oxidative and thermal instability. This is due to the presence of unsaturated fatty acids in the oil which leads to significantly higher reactivity (Bongfa *et al*, 2015). Consequently, the plant oils originally contained minute quantities of antioxidants such as rutin, beta-sitosterol and moringine for stability. The plant oils were used as received from the supplier. The product specification for the oils are presented in the [Experimental](#) section of this report.

2. Literature

In this section a discussion of important literature concerning friction, wear and lubrication is given. A short overview of the different regimes of lubrication is given together with diesel properties and production. International diesel specifications are also presented, and the chapter ends with an overview of additive technology.

Plant oils possess unique advantages compared to other lubricating fluids (Guo *et al*, 2016). The work done by Argawal *et al* (2013) suggested that addition of free fatty acids found in plant oils to low lubricity diesel fuel at additive levels enhance fuel lubricity. What is more, Guo *et al* (2016) mentions that the good lubrication property of plant oils is determined by the basic structure of its molecules and chemical components. Plant oil molecules can form an adsorption film on a metallic surface; the fatty acid component of plant oils can react with such metal surface to form a monofilm of metallic soap. This formed monofilm can influence anti-friction and anti-wear behaviour throughout the various regimes of lubrication (Guo *et al*, 2016).

2.1. Regimes of lubrication

During the first industrial revolution, lubricants became increasingly important in ball and journal bearings (Stachowiak, 2017). The ability to reduce both friction and wear has been the two most significant elements in increasing component efficiency and life span. [Figure 2.1](#) is known as the Stribeck curve. It shows the effect of load, fluid viscosity, and speed on friction coefficient (μ). The

4 regimes of lubrication (1-hydrodynamic, 2-elastohydrodynamic, 3-mixed and 4-boundary) are shown in [Figure 2.1](#) and explained in the next section.

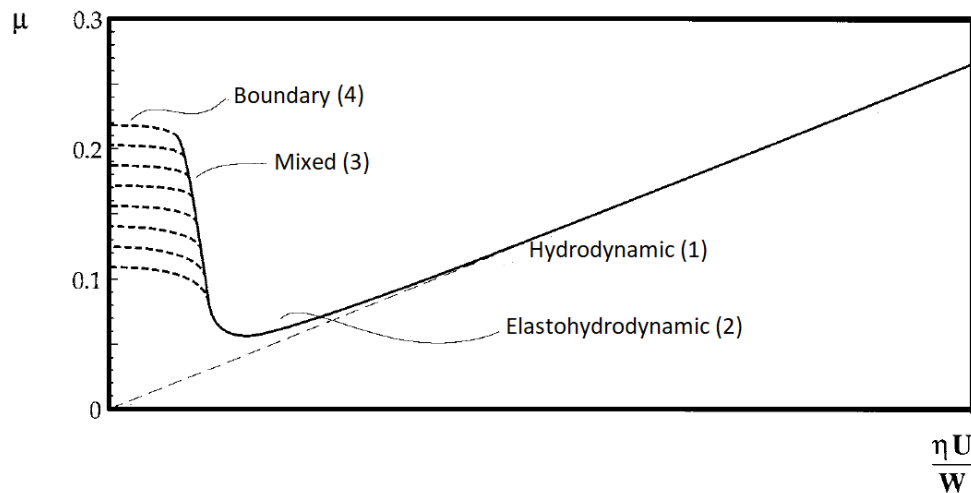


Figure 2.1: Stribeck curve showing the four lubricating regimes (Stachowiak & Batchelor, 2006: 185 and Zhang et al, 2016).

The parameter on the horizontal axis of the Stribeck curve ([Figure 2.1](#)) is termed the Hersey number (Zhang *et al*, 2016). The Hersey number is a key parameter which is derived as the product of fluid viscosity (η) and speed (u) over the applied load (W).

2.1.1. Hydrodynamic lubrication

Hydrodynamic lubrication is defined as the lubrication mechanism achieved when a viscous film of sufficient thickness is compressed between two surfaces and the hydrodynamic pressure generated is sufficient to prevent the surfaces from touching (Stachowiak & Batchelor, 2006: 104). This is represented as region (1) in [Figure 2.1](#). The imperfections of the solid surfaces are the cause of friction for the vast majority of surfaces encountered in nature and used in industry. The aim of hydrodynamic lubrication is to apply a suitable lubricant to

the contact zone between rubbing solids and form a thin liquid film. This film prevents the surfaces from direct contact, reducing friction and, as a result, wear (Stachowiak & Batchelor, 2006: 104).

The mechanism of hydrodynamic lubrication can be explained with [Figure 2.2](#). Consider a tilted block that moves in the longitudinal direction from rest over a surface that is covered with a liquid film of thickness h (shown in [Figure 2.2c](#)). Because the block is tilted with respect to the surface, as the block or gear moves over the surface it traps the liquid between the gap or entrains the liquid film. This liquid must pass into a narrowing gap and be squeezed between the contact surfaces to create enough (hydrodynamic) pressure to sustain the load (Arakeri & Sreenivas, 1996).

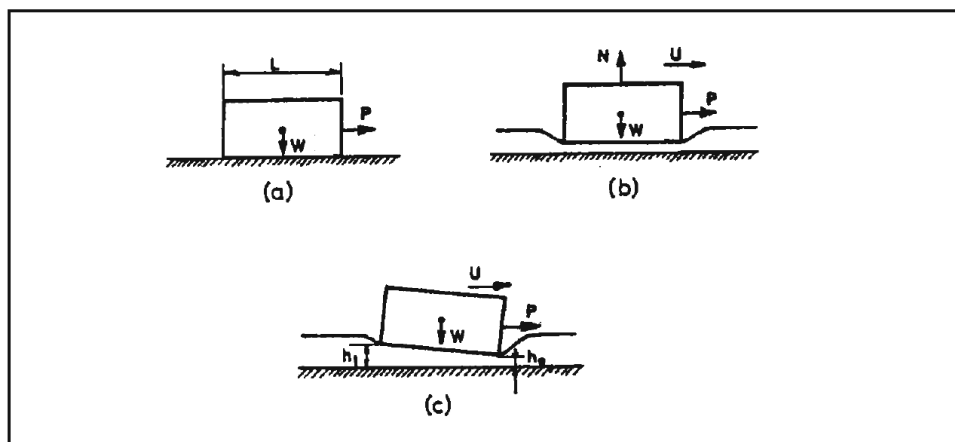


Figure 2.2: Rectangular block sliding to the right under different conditions demonstrating hydrodynamic lubrication (Arakeri & Sreenivas, 1996)

If the block is positioned as in [Figure 2.2a](#) the force required to cause motion at a constant speed should be equal to the frictional force so that the resultant force in the direction of motion will be zero (i.e. $F_{Res} = F - f$). That force is given by [Equation 2.1](#) (Arakeri & Sreenivas, 1996).

$$F = \mu W \quad (2.1)$$

μ is the friction coefficient and W is the weight of the block. If to improve on lubrication of the block in [Figure 2.2a](#) a liquid film is introduced so that the setup takes the form of [Figure 2.2b](#). The force now required to cause motion at a constant speed is given by [Equation 2.2](#) (Arakeri & Sreenivas, 1996). Note that this force must also equal the frictional force (i.e. $F_{Res} = 0$) to achieve constant speed.

$$F = \frac{\eta Au}{h} \quad (2.2)$$

η is the dynamic viscosity of the fluid, A is the contact area, h is the liquid film thickness and u is the entrainment speed. Note that the required force (F) in [Figure 2.2b](#) for constant motion is now a function of entrainment speed (u), but even if the fluid flows at a low speed such that the force required to cause constant motion in [Figure 2.2b](#) decreases significantly the reduction in frictional force is still pointless because the fluid cannot support the weight of the block. The liquid will flow out of the sides under the weight. It is not enough for the frictional force to decrease but equally important is the fact that the fluid should be able to support the weight of the block. Both conditions are realised when the block tilts forward as it moves ([Figure 2.2c](#)).

Two key principles are important for hydrodynamic lubrication if the images in [Figure 2.2](#) are compared. They are the motion that is required to entrain the liquid or sweep it along and the dragging of the liquid into a narrowing gap or a constriction. Because if either component is missing the liquid will not be able to support the load. Consequently, in hydrodynamic lubrication it is important

for the contacts to be of convergent shape to allow the liquid film to be entrained. This creates a pressure that is sufficient to support the load (Arakeri & Sreenivas, 1996).

The conditions under which hydrodynamic lubrication occur are summarized below (Arakeri & Sreenivas, 1996).

- The first condition is that the Reynolds number be small, i.e., when $\rho u h_o / \eta \leq 1$. Here, ρ is the density of the fluid in the gap. A low Reynolds number indicates that viscous forces are important and are the reason why the fluid drags in and the subsequent pressure build-up. The two surfaces should have sufficient relative velocity so that a lubricating film capable of carrying the load can be formed.
- The second condition is that there be an angle of the narrowing passage (angle of tilt as shown in [Figure 2.2c](#)) and it be small.

2.1.2. Elastohydrodynamic lubrication

Elastohydrodynamic lubrication is a type of fluid-film lubrication in which the hydrodynamic film generation mechanism is facilitated by surface elastic deformation and lubricant viscosity increases as a result of high pressure (Bhushan, 2013: 402). This is represented as region (2) in [Figure 2.1](#). When the contact pressure increases and the sliding speed decreases, the fluid is no longer entrained as effectively and the film thickness reduces to the same order as the roughness or surface distortions of the contacting bodies, so that it can no longer be assumed that the surfaces are smooth (Bhushan, 2013: 402).

The higher the pressure on the fluid, the more its viscosity increases because the molecules are forced together and the more difficult it becomes to extrude the liquid. Moreover, because of the significant rise in fluid viscosity, the possibility for asperities to deform each other elastically through the film without touching becomes higher. This causes an increase in the contact area, while preventing wear (Bhushan, 2013: 407-408).

2.1.3. Mixed lubrication

The mixed lubrication regime is the intermediate zone between the boundary lubrication regime and the elastohydrodynamic lubrication regime. In this regime, the applied load is partly carried by the interacting asperities and the remaining part by the fluid film (Bhushan, 2013: 403). Region (3) of the Stribeck curve represents the mixed lubrication regime ([Figure 2.1](#)).

In this regime surface roughness significantly affects the performance of the contact (Bhushan, 2013: 403). It is rare for sliding systems to operate exclusively in the boundary lubrication regime, unless the sliding velocity and the fluid viscosity are extremely low. Most practical systems operate in the mixed lubrication regime where the load is carried by both boundary films and hydrodynamically-generated pressure (Bhushan, 2013: 403).

2.1.4. Boundary lubrication

Boundary lubrication is lubrication by a liquid lubricant under conditions where the solid surfaces are so close together that appreciable contact between opposing asperities is possible ([Figure 2.3](#)) (Bhushan, 2013: 403). This is

represented as region (4) in [Figure 2.1](#). The friction and wear in boundary lubrication are determined predominantly by interaction between the solids and between the solids and the liquid (Bhushan, 2013: 403).

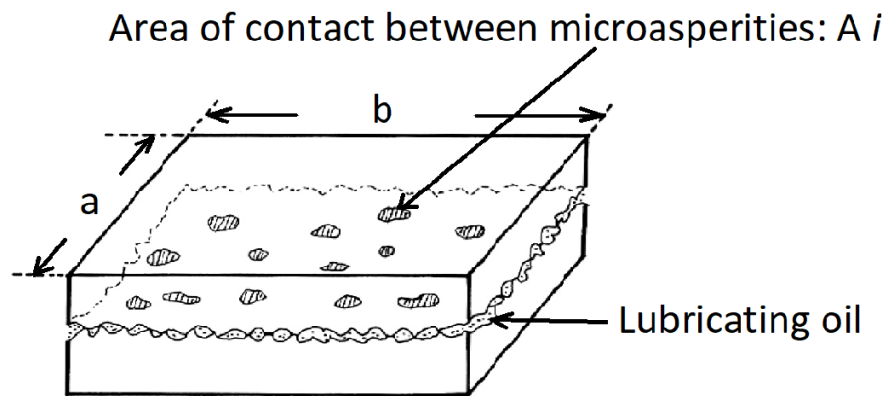


Figure 2.3: Friction surface contact between two solid bodies (Hironaka, 1984)

This lubrication behaviour is observed when the viscosity of the lubricant becomes low and film thickness very thin, load is extremely high and sliding speed is extremely low (Bhushan, 2013: 403). This thin layer of lubrication becomes the last line of defence in which the lubricant's physical and chemical interaction with the solid surface controls friction and wear. In other words, in boundary lubrication, because the thickness h of the oil film between the friction surfaces is less than their surface roughness r , metallic contact occurs over the entire surface, causing wear as shown in [Figure 2.3](#).

In the boundary lubrication regime viscosity plays a minor role against wear. This is because when the load becomes extremely high the viscosity of the fluid is insufficient to sustain a film between the sliding surfaces. Boundary lubrication regime is considered the regime that controls component life. For this reason, the HFRR instrument operates under boundary lubrication conditions (worst

case scenario) to examine the lubricity capabilities of diesel fuels (ISO 12156). On a more microscopic level a cross section of [Figure 2.3](#) is shown in [Figure 2.4](#).

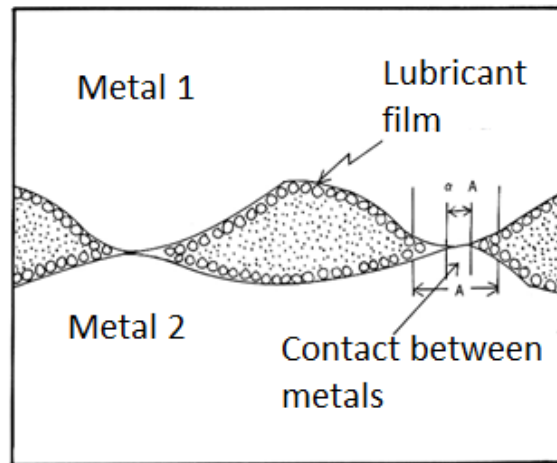


Figure 2.4: Friction surface contact model (B) (Hironaka, 1984)

A schematic of two sliding surfaces solid [1] and solid [2] under specific operating conditions for load and sliding speed is shown in [Figure 2.5](#). For different types of wear such as oxidative wear to occur it would involve interactions between solid [1] or solid [2] and lubricant [3] or atmosphere [4]. Usually the oxide layers that form on the surface serve as a protective film to reduce friction and wear. On the contrary adhesive and abrasive wear occurs between the solid [1] and solid [2] alone.

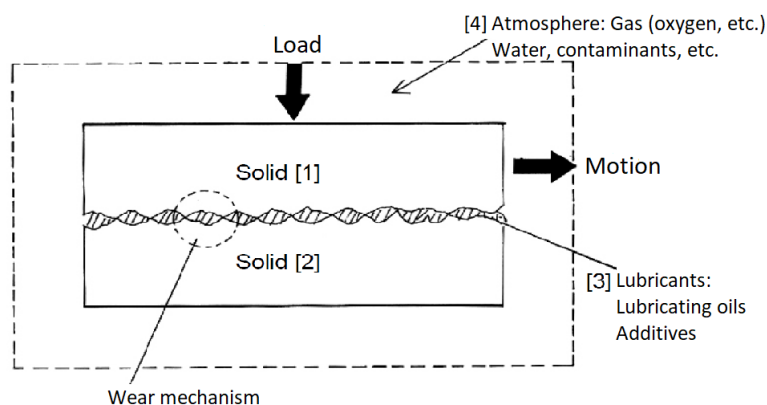


Figure 2.5: Wear under boundary lubrication (Hironaka, 1984)

Plant oils consist of fatty acids which are composed of two parts, a tail, and a head. The tail consists of long hydrocarbon chains and the head, polar groups that are acidic. The polar end of the fatty acid is what adsorbs physically or chemically onto friction surfaces to form lubricating films that prevent metal-metal contact and reduce friction and wear (Quinchia *et al*, 2014).

Long chain fatty acids such as stearic acids (C18), oleic acids (C18) and ricinoleic acids (C18) can be found in plant oils and are typical lubricity enhancers. Plant oils that contain high percentages of saturated fatty acids such as stearic acids are set to be good additives for lubricity in diesel. This is because these saturated fatty acids can align themselves in a compact formation to form stronger films that can withstand load (Patel *et al*, 2016).

On the contrary polyunsaturated fatty acids such as linolenic and linoleic have many double bonds present that create bends in their structure. Consequently, the molecules are unable to align themselves in a compact manner to create strong lubricating films like the saturated fatty acids (Mosarof *et al*, 2016).

2.2. Surface layer characterization

No solid surface, no matter how smooth in appearance, is completely even. All solid surfaces contain irregularities of various magnitudes (Bhushan, 2013: 9). Most surfaces used for tribological tests are prepared by mechanical techniques and they contain defects resulting from fracture, heating, plastic deformation, and contamination (Bhushan, 2013: 9). Even surfaces that were formed by cleavage are rarely defect free. Tribological surfaces that are mechanically

abraded and machined to give a smooth finish are still extremely rough on atomic scale.

The nature of a surface, describing its hills and valleys or irregularities, is termed topography and the hills or rough projections on the surface are termed asperities. Besides these asperities present on the surface, the surface on its own may contain contaminant layers of atomic dimensions (< 3 nm) thick (Bhushan, 2013: 10). These contaminants come about because of exposure to air. The surrounding atmosphere (air) may contain gases, water vapour or even hydrocarbons that may adsorb onto the surface to form thin films (Bhushan, 2013: 10).

Friction and wear are affected by the presence of these surface films. Adsorbed films on the surface have a major impact on surface interactions, even if they are only a fraction of a monolayer. These thin monolayers influence the tribo-characteristics of the surface such as friction coefficient and resistance to wear, erosion, oxidation, and corrosion.

[Figure 2.6](#) shows details of solid surfaces from a tribological perspective, indicating surface texture and typical surface layers. The subsequent section will go through the details of the various surface layers.

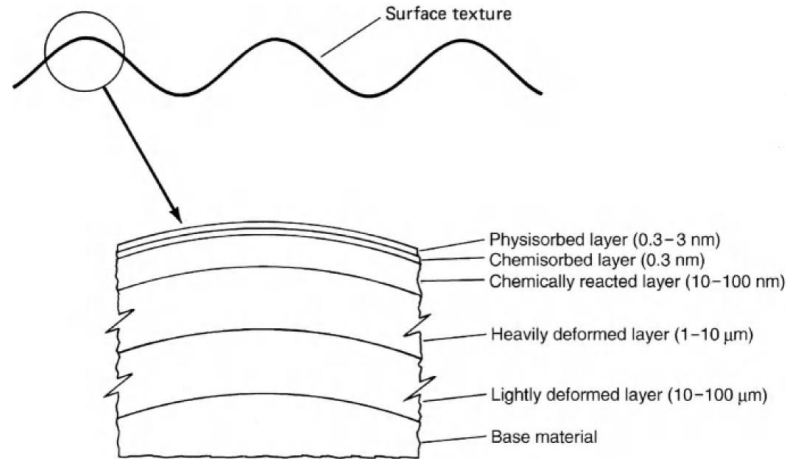


Figure 2.6: Solid surface details, surface texture (vertical axis magnified) and typical surface layers (Bhushan, 2013: 10).

2.2.1. Deformed layer

The surface layer properties of a metal can differ distinctly from the rest of the material because of the forming processes that were used to prepare the surface. The microstructure, and defects of a solid often vary as a function of depth into the material or spatially across the material (Bhushan, 2013: 11). The way a material is prepared speaks a lot. For instance, on surfaces that have undergone machine processes such as grinding, polishing etc. the surface layers are plastically deformed with or without a temperature gradient and become highly strained. This strained layer is termed the deformed layer (Bhushan, 2013: 11).

2.2.2. Chemically reacted layer

As its name suggests, a chemically reacted layer occurs because of a reaction taking place on the surface. This layer forms because of exposure to a gas, mostly air (Bhushan, 2013: 11). Various factors influence how this layer forms and its depth on the surface depends on factors such as temperature, surface

reactivity, atmospheric conditions and how long the surface was exposed (Stachowiak & Batchelor, 2006: 370-371).

2.2.3. Physisorbed layer

Physisorption is the physical bonding of liquid or gas molecules to the surface of a solid that a liquid or gas comes into contact with. This occurs due to weak Van der Waals forces and results in the formation of a thin film on the surface of the solid called a physisorbed layer (Bhushan, 2013: 12).

In any solid structure the majority of the atoms that make up the solid are surrounded on all sides by other atoms. On the other hand, atoms on the surface of the solid are not fully bound. They are exposed to the environment. These surface atoms are reactive due to Van der Waals interactions, causing them to attract liquids, vapours, and gases to correct for their atomic force imbalance (Stachowiak & Batchelor, 2006: 370-373). When adsorption happens, the attracted molecules fill in the pores on the solid's surface. The most common components of adsorbate layers are water vapour molecules, oxygen, or hydrocarbons from the atmosphere that are concentrated and physically adsorbed onto the surface of the metal (Bhushan, 2013: 12).

[Figure 2.7](#) shows a schematic of physisorption on the surface of a metal. The molecule depicted is a diatomic molecule bonding itself to the surface, much like will occur for oxygen. Both oxygen atoms of the diatomic molecule will bond to the already contaminated surface in this situation (Bhushan, 2013: 11).

2.2.4. Chemisorbed layer

A chemical reaction occurs between the surface and the adsorbate in chemisorption. At the adsorbent surface, new chemical bonds are formed. The bonds formed are stronger than the weak Van der Waals forces holding a physisorbed layer in place as such it is more difficult to remove a chemisorbed layer ([Figure 2.7](#)) (Bhushan, 2013: 12).

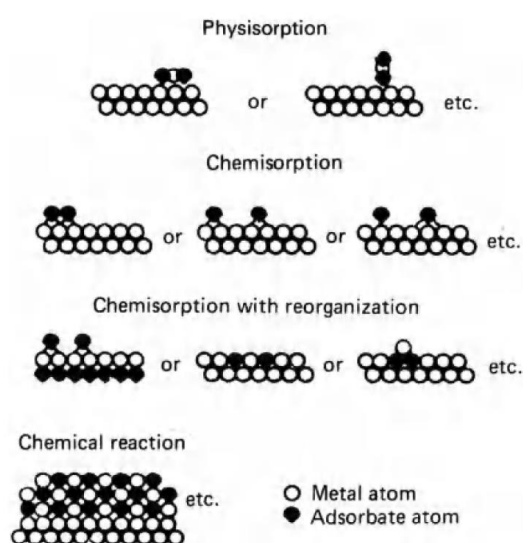


Figure 2.7: Physisorption, chemisorption, and a chemical reaction are depicted in schematic diagrams (Bhushan, 2013:11).

The chemisorbed layer is however limited to a monolayer. Chemisorption stops as soon as the surface is filled with a layer. From this point any successive layer is formed either by physisorption or chemical reaction (Bhushan, 2013: 12).

2.3. Molecular science of lubricity additives

A lubricity additive is an organic material that is added to minimize friction and wear between surfaces in direct contact, thereby lowering the heat produced

when the surfaces move (Schaschke, 2014: 226). Lubricity additives/enhancers perform key roles that contribute to a better and efficient functioning of highly processed diesel fuels. Examples are:

- Controlling friction - this is one of the primary roles of lubricity enhancers. Reducing friction and preventing seizure are essential in most applications (Minami, 2017). Generally, lubricant-to-surface friction is much smaller than surface-surface friction for a system with no lubrication. If friction is reduced in a system a primary benefit is reduction in heat generation (Minami, 2017).
- Reducing wear - reducing wear is another role of lubricity enhancers in fuel. This is achieved by keeping the surfaces in motion apart. In the case of plant oils this is achieved when the polar heads of the fatty acids adsorb onto the metal surface whereas the hydrocarbon tail extends out to separate the sliding surfaces.

2.3.1. Tribo-chemical reactions

Tribo-chemical reactions refer to the chemistry that takes place between lubricants and the sliding surfaces under lubricated conditions (Minami, 2017). This chemistry involves the conversion of molecules to others under specified operating conditions and reactions that would occur independently under the temperatures and pressures in the contact (Minami, 2017).

All chemical reactions generally need energy to occur. A chemical reaction may specifically be defined as rearrangement of atoms within or between molecules and is accompanied with breaking and making of chemical bonds (Kotz *et al*,

2015: 16). In tribo-chemical reactions mechanical energy is converted to chemical energy (Minami, 2017). [Figure 2.8](#) summarizes the potential driving forces (energy sources for chemical reactions) for tribo-chemical processes.

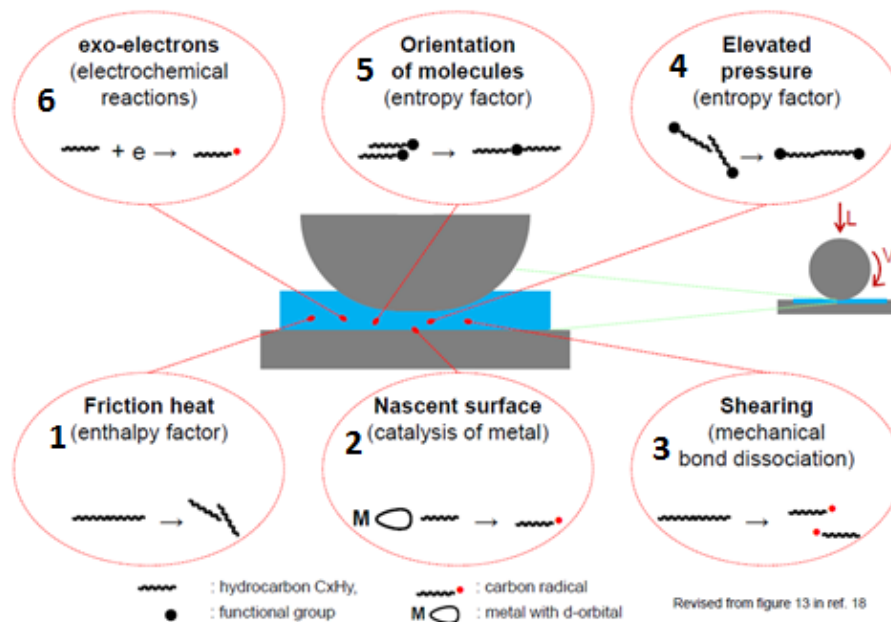


Figure 2.8: Possible sources of energy for chemical reactions at the tribo-contact (Minami, 2017).

For the initiation of tribo-chemical reactions, six different driving forces are considered (Minami, 2017). From [Figure 2.8](#) each of the possible driving forces numbered 1 to 6 generally comes about as follows (Minami, 2017):

1. Friction heat - majority of chemical reactions that occur in tribo-chemistry are initiated because of high temperature. Heat provides energy for molecules to move or collide with each other for a reaction to start. It is estimated that sliding surfaces can reach temperatures as high as 250 °C - 450 °C (Minami, 2017).

2. Nascent surfaces – a nascent surface is a fresh or new surface which is exposed because of wear taking place on the solid surface. This nascent surface can become a chemically active site for reactions.
3. Shearing – shearing can cause dissociation of chemical bonds due to mechanical action (Minami, 2017). Radicals can be formed from these dissociations and this can initiate a chemical reaction.
4. Elevated pressure – when pressure is extremely high lubricant molecules are pressed together. Since what is needed for a reaction to start is collision between molecules and correct orientation of molecules, chances are a reaction is likely to start when pressure is increased.
5. Orientation of molecules – even if molecules collide but not in the correct orientation no reaction will take place. The functional groups of the molecules need to collide in the right orientation for a reaction to occur.
6. Exo-electrons – Sliding surfaces have the potential to release exo-electrons. These electrons have insufficient energy to facilitate chemical reactions, but they can create radical intermediates that can be used in subsequent chemical reactions. (Minami, 2017).

2.3.1.1. Oxidation of plant oils

The oxidative degradation of organic compounds that occurs spontaneously under aerobic conditions without the use of reagents, catalysts, or driving forces is known as autoxidation (Minami, 2017). Plant oils typically exhibit relatively poor oxidative stability, and therefore it is important to examine the impact of oxidation on the performance of the three plant oils as lubricity enhancers.

The level of saturation of the fatty acids in any plant oil is one of the key factors in determining its oxidative stability. Fatty acids with high numbers of double bonds (e.g. linolenic and linoleic acids) or triple bonds lack stability against oxygen. This is because the triple bond represents a region of higher inter-atomic electron density. The inter-atomic electron density for triple bonds is higher than that for double bonds, whose electron density is likewise higher than single bonds. In other words, more electrons can be found in the vicinity where the double/triple bond is located compared to the vicinity where a single bond is located. Therefore, a double bond is more likely to be attacked by an electron-seeking species because it has many electrons available (high electron density) compared to a single bond. A triple bond is worse than a double bond because it has a higher electron density than a double bond. Consequently, electrons binding multiple bonded atoms e.g. double/triple bonds are more vulnerable to attack by electron-seeking species such as electrophiles (radicals) (Kotz *et al*, 2015: 126).

Radicals are problematic, because they have an unpaired valence electron, and these unpaired electrons make radicals highly reactive and therefore unstable (Klein, 2017: 436-438). Consequently, multiple bonded atoms e.g. double/triple bonds are less stable against oxidative attack than single bonded atoms. [Figure 2.9](#) shows a step by step process of how the autoxidation of unsaturated fatty acids occurs in plant oils.

• Initiation	Initiator \rightarrow Free Radicals (R^\bullet)
• Propagation	$R^\bullet + O_2 \rightarrow ROO^\bullet$ $ROO^\bullet \rightarrow ROOH + R^\bullet$
• Autocatalysis	$ROOH \rightarrow RO^\bullet + HO^\bullet$
• Termination	$R^\bullet + R^\bullet \rightarrow R-R$ $ROO^\bullet + R^\bullet \rightarrow ROOR$

Figure 2.9: Simplified model of the auto-oxidation of fatty acids found in plant oils (Ahmed *et al*, 2016).

The initiation step is the creating of a free radical (R^\bullet) from the fatty acids in the plant oil. It happens when a hydrogen atom is removed from the fatty acid and turns it into a radical (Ahmed *et al*, 2016).

The formed radical reacts with oxygen to produce a peroxy radical (ROO^\bullet). The peroxy radical that is formed also removes a hydrogen atom from another fatty acid molecule and the reaction starts all over again (i.e. propagation stage repeats). During the propagation steps, hydroperoxide molecules ($ROOH$) are formed that may break down into alkoxy (RO^\bullet) and hydroxyl radicals plus water. This is known as the autocatalysis stage (Ahmed *et al*, 2016).

The oxidation process ends when two free radicals combine to form a non-radical product. The rate of oxidation increases in relation to the degree of unsaturation. Fatty acids such as linolenic acid are found to oxidise 25 times faster than oleic acid and twice as fast as linoleic acid (Minami, 2017).

2.4. Friction

Friction is resistance to motion (Bhushan, 2013: 199). Frictional force can be useful or detrimental, depending on the perspective upon which one considers it. Friction is required in some applications, such as vehicle brakes and clutches, and frictional power transfer (such as belt drives) and so is maximized (Bhushan, 2013: 199). In systems that have sliding or rolling machine parts however friction causes wear which deteriorates materials.

Inter-surface adhesion, surface roughness, surface deformation, and surface contamination all contribute to friction. As a result of the difficulty of these interactions, calculating friction from first principles is impractical, necessitating the use of analytical methods for theory formulation and study (Rothbart & Brown, 2006: 7.6). [Figure 2.10](#) shows a schematic of a body experiencing friction as it slides on a surface.

If L is the normal reaction of the body sliding on the surface, which is equivalent to the weight (W) of the block. The frictional force required to initiate or maintain motion can be described by [Equation 2.1](#) (Bhushan, 2013:200):

$$f = \mu W \quad (2.1)$$

where μ is the friction coefficient. μ can be μ_s or μ_k depending on whether the object is stationary or moving.

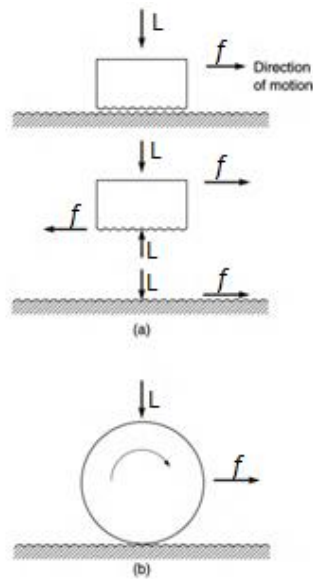


Figure 2.10: Schematic illustrations of (a) a body sliding on a surface with a free body diagram, and (b) a body rolling on a horizontal surface; L is the normal load (force) and f is the frictional force (Bhushan, 2013: 200).

2.4.1. Laws of friction

There are two fundamental laws of friction that generally hold true for several experimental conditions (Rothbart & Brown, 2006: 7.2). According to Rothbart and Brown (2006), these fundamental laws of friction correlate well with actual tests performed on clean and lubricated contacts. They are

1. Frictional force is directly proportional to the normal force between the sliding surfaces but is independent of the load.
2. Frictional force between the two sliding surfaces is independent of the apparent area of contact.

Bhushan (2013) proposed that in the case of two metallic surfaces sliding against each other, pressure build up occurs at individual contact spots which brings about local welding. Furthermore, the contacts that are formed experience high shear forces because of the sliding motion of the two surfaces (Bhushan, 2013: 207-209). Because of the proximity of the surface asperities, adhesion occurs, which leads to plastic deformation on a micro-scale. Generally, plastic deformation is the major type of deformation that occurs between two metallic surfaces in contact, consequently high friction, and wear result.

2.4.1.1. Adhesion

If two metal surfaces are placed in contact, they do not really touch over the entire apparent area of contact. Generally, they are supported by the irregularities (asperities) that are on the surfaces. Consequently, contact takes place at the tips of these asperities and as a result friction and wear originate at these points.

As the surfaces are compressed, the asperities deform in elastic and plastic modes, expanding the contact area between the two surfaces until the contact area is large enough to accommodate the load (Bhushan, 2013: 207-208). As the load increases the plastically deformed area propagates upwards to the surface until the whole contact area is plastically deformed and the average contact pressure is round about three times the yield strength of the material, in most cases. If an asperity radius of 1 μm is assumed, a load of less than 1 mN is sufficient to cause plastic deformation (Stachowiak & Batchelor, 2006:468).

In [Figure 2.11](#) a schematic showing how contact occurs between two metal surfaces, is presented. To obtain the real area of contact (A_r), it will entail adding up all the contact areas on the surface. Consequently, the real area is only a fraction of the apparent area (A_a) (Bhushan, 2013: 207-208).

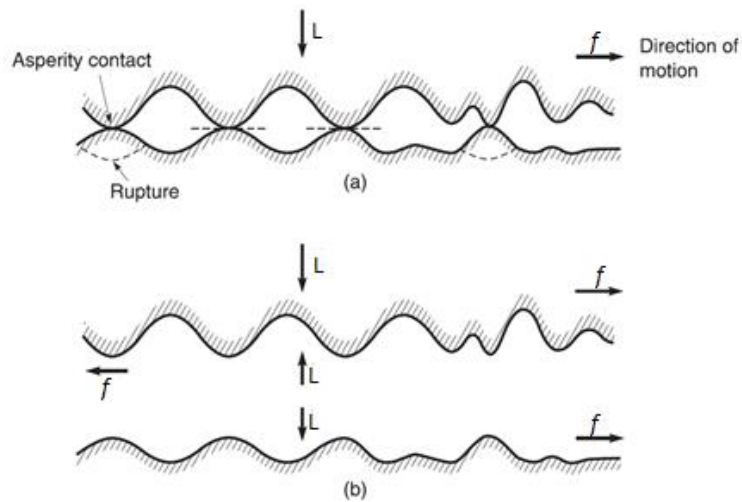


Figure 2.11: Schematic of (a) two rough surfaces in a sliding contact and (b) a corresponding free body diagram (Bhushan, 2013: 207).

For a dry contact, the frictional force is defined according to [Equation 2.3](#) as (Bhushan, 2013: 208):

$$f = A_r \tau_a \quad (2.3)$$

and for a contact with a partial liquid film ([Equation 2.4](#)) (Bhushan, 2013: 208),

$$f = A_r [\gamma \tau_a + (1 - \gamma) \tau_l] \quad (2.4)$$

and ([Equation 2.5](#))

$$\tau_l = \frac{\eta u}{h} \quad (2.5)$$

where τ_a and τ_l are the average shear strengths of the dry contact and of the lubricant film, respectively. γ is the fraction of the unlubricated area, η is the dynamic (absolute) viscosity of the lubricant, u is the relative sliding speed; and h is the liquid film thickness. A contribution to friction due to adhesion is always present at an interface. The existence of a lubricating film may result in the formation of adhesive bridges in boundary lubricated conditions and viscous effects may become significant, in some cases even dominating the overall force of friction. Hence, controlling friction and wear in the boundary lubrication regime is important. Two main strategies exist in reducing boundary friction and wear; lubricant additives and surface coatings (Bhushan, 2013: 208).

Lubricant additives such as plant oils can deter excessive friction and enhance fuel lubricity using fatty acid molecules. These fatty acid molecules contain polar head groups and non-polar tail groups. Friction reduction is achieved by the adsorption of vertically oriented, single monolayers of these fatty acids on each surface, which separates the sliding surfaces (Agarwal *et al*, 2013).

2.5. Wear

Wear is the steady removal or deformation of material from solid surfaces that causes damage under conditions of load and relative motion (Bhushan, 2013: 315). Wear mainly occurs as a progressive loss of material resulting from the mechanical interaction of the sliding surfaces under the influence of load (Bhushan, 2013: 315). Wear is most likely to occur in the boundary lubrication regime, where metal-metal contact is possible. In majority of the cases surface interactions at asperities lead to wear. As the two surfaces slide over each other the material on the contacting surface is displaced so that properties of the solid

body, at least at or near the surface, are altered, but little or no material is lost. As sliding between the two surfaces continues material may be removed from one surface and may be transferred to the mating surface or may break loose as a wear particle (Bhushan, 2013: 315). For a lubricated contact, the wear is controlled by the lubricating film and therefore the wear behaviour as a function of time approaches a steady state or a constant value. From a tribological perspective it is better to avoid wear than high friction. High friction does not necessarily mean that high wear rates will be experienced (Bhushan, 2013: 315).

The different variations of wear are discussed in the subsequent sections.

2.5.1. Variations of wear

2.5.1.1. Adhesive wear

The mode of wear that often has the most detrimental effect on sliding or oscillating metals in contact is adhesive wear. Adhesive wear is a severe form of wear that has a high rate of wear and a high, unstable friction coefficient (Bhushan, 2013: 316). As solid surfaces slide over each other, they make intimate contact over a number of small junctions. These junctions continue to form and split during sliding, and a wear particle is formed if a junction does not break along the original interface (Bhushan, 2013: 316).

Adhesive wear is undesirable for the following reasons (Stachowiak & Batchelor, 2006: 553)

- The loss of material would inevitably cause the mechanism's output to deteriorate.

- Large wear particles may form in tightly fitting sliding parts, causing the mechanism to seize prematurely

Adhesive wear is particularly common in metals, which explains its practical importance. In metals, adhesive wear is caused by lubricant failures on sliding surfaces. This is because this type of wear is associated with the breakdown in the lubricant's fundamental role of providing some form of separation between the sliding surfaces (Bhushan, 2013: 316). [Figure 2.12](#) shows an image of adhesive wear in metals.

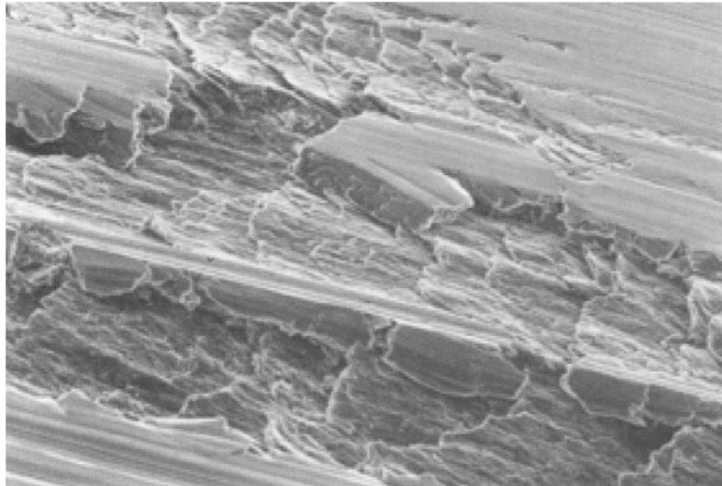


Figure 2.12: Adhesive wear has worn the surface of the Al-Si alloy. Note the formation of wear particles (Stachowiak & Batchelor, 2006: 568).

The best way to control adhesive wear is by the introduction of a lubricant or a reaction film.

2.5.1.2. Corrosive wear

Corrosive wear is a form of material deterioration that involves both corrosion and wear mechanisms. When sliding takes place in a corrosive setting, this happens. The gas or liquid in the corrosive setting reacts chemically with the surface that has been exposed as a result of the sliding process. The most corrosive medium in the air is oxygen. As a result, chemical wear in the air is commonly referred to as oxidative wear. (Bhushan, 2013: 359). [Figure 2.13](#) shows a photograph of corrosive wear in metals.

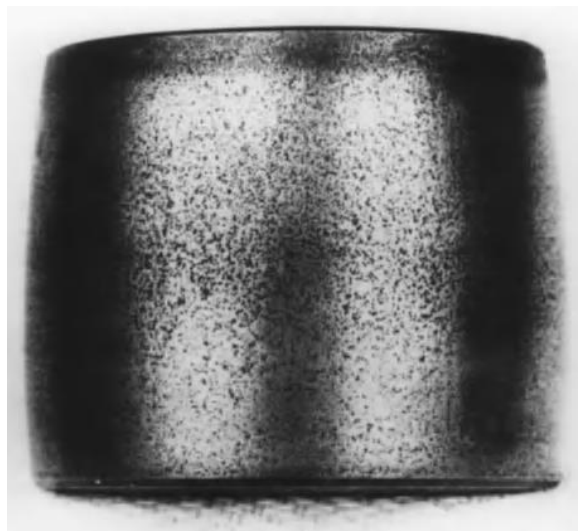


Figure 2.13: SEM micrograph of 52100 quenched and tempered roller bearing after corrosive wear (Bhushan, 2013: 360).

When a surface corrodes, the corrosion products usually remain on the surface, slowing down further corrosion. However, if continuous sliding occurs, the sliding motion eliminates surface deposits that would otherwise protect against further corrosion, causing corrosion to occur more quickly (Bhushan, 2013: 359). Corrosive wear is generally characterised by a reduction in friction coefficient.

2.5.1.3. Abrasive wear

Abrasive wear occurs whenever a material is loaded to or slides over a harder material or a material of equal hardness. In abrasive wear the hard, rough surface usually produces grooves on the softer material after sliding (Bhushan, 2013: 328). Abrasive wear in metals usually happens by one of three mechanisms: cutting, wedge formation and ploughing. [Figure 2.14](#) shows abrasive wear in metals.

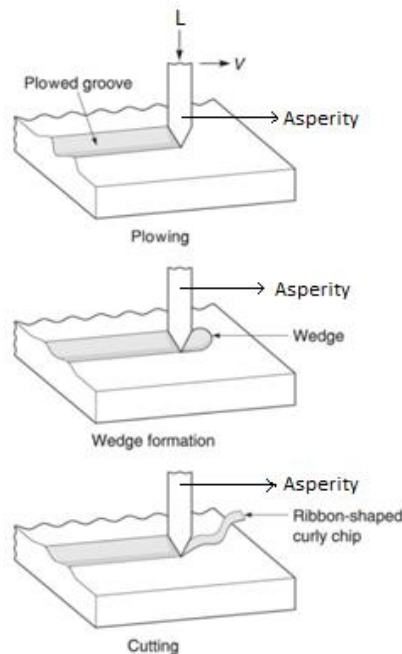


Figure 2.14: Schematics of abrasive wear processes because of plastic deformation by three deformation modes (Bhushan, 2013: 331).

Asperities of the harder material can cut the softer material, removing shavings or chips from the surface like the process of machining. Sliding of the harder asperities can also cause grooves in the softer material although no material is removed from the surface. This is called ploughing and is characterised by

material being displaced to the sides of the grooves (Bhushan, 2013: 329). It may also be caused by third-body wear, which is caused by loose abrasive particles rolling between two soft sliding surfaces or particles embedded in one of the opposing surfaces (Stachowiak & Batchelor, 2006: 501).

Since abrasive wear occurs when the abrading layer is rougher and harder than the abraded surface, it can be avoided by the introduction of a lubricant. At minimum, a good lubricant should be able to keep the surface asperities on both surfaces apart. Therefore, for any lubricated contact, if abrasive wear still occurs it generally is an indication of an inadequate lubricant, irrespective of the wear scar size.

2.5.1.4. Fatigue wear

When a material is exposed to cyclic loading, such as metal wheels on tracks or a ball bearing in a machine, surface-fatigue wear occurs, causing progressive and localized structural damage (Bhushan, 2013: 342). Fatigue wear occurs when surface and subsurface cyclic shear stresses or strains in the softer material of an articulation exceed the fatigue limit for that material. A simpler way to put it is if the applied load is higher than the fatigue strength of the material fatigue is likely to occur. Fatigue wear causes extreme plastic deformation in most cases (Bhushan, 2013: 343-345). [Figure 2.15](#) shows an image of fatigue wear.



Figure 2.15: Subsurface fatigue wear occurring on a 52100-ball bearing race (Bhushan, 2013: 344).

2.6. Diesel fuel lubricity model

A model that estimates the lubricity behaviour of diesel treated with lubricity additives was proposed by Fox (2007). In the model it is proposed that the pattern followed for wear scar diameter reduction on the HFRR for diesel fuel lubricity is an inverse sigmoidal curve. The model puts forward that anti-wear additives solubilized in diesel fuel adsorbed as a film on metal surfaces. The adsorption may either be by chemisorption or physisorption and occurs at the polar end of the additive molecules. [Figure 2.16](#) represents the inverse sigmoidal curve proposed by Fox.

According to the model, for low concentrations of the lubricity additive an incomplete coverage of film forms on the metal surface. This formed film is not compact and broad enough to support the load and sustain anti-wear action. This is marked as region I on [Figure 2.16](#). In this region little reduction in wear

occurs because the primary role of the lubricant in being able to keep the sliding surfaces apart is not realized.

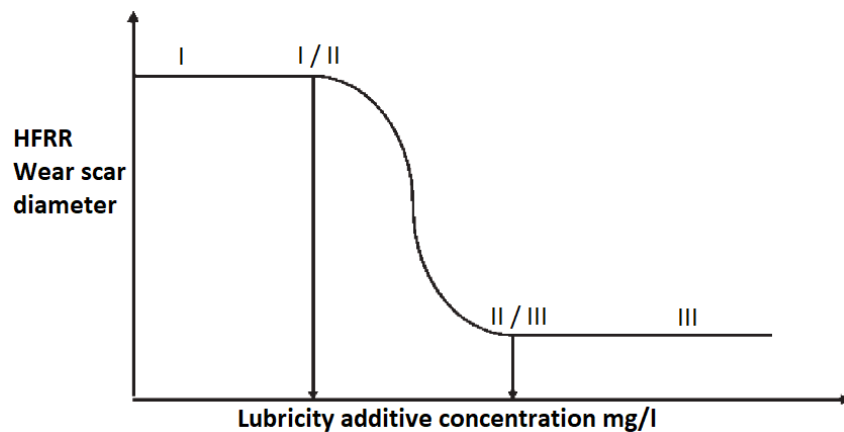


Figure 2.16: HFRR wear scar diameter reduction against lubricity additive concentration (Fox, 2007).

When the concentration of the additive is further increased to region II an improvement in wear reduction occurs. A coherent but still incomplete, additive film forms on the metal surfaces. The incomplete additive film partially separates the sliding metal surfaces because of the slightly higher fuel additive concentration and therefore it can support anti-wear action better than in region I (Fox, 2007). Consequently, slightly reducing the overall wear scar diameter. If additive concentration is even increased further to region III, enough additive will be available in the diesel so that the polar heads of the molecules are able to adsorb fully onto the metal surface to form a complete film. Hence the curve flattens in region III. This complete film can now support anti-wear action more (Fox, 2007). There is a possibility that a multilayer of additive film may form upon continual addition of additive, but neither the friction nor the wear will be highly affected by the formation of a multilayer.

2.7. Wear scar corrections

When the diesel lubricity test was first developed on the HFRR, it was discovered that at 60 °C, better fuel differentiation was obtained than at 25 °C. It was found to have arisen because of variations in relative humidity. The effect of humidity on wear tests was reduced when the amount of fuel to be measured was increased from 1 to 2 mL. Under moist conditions, a better correlation was obtained. Discrimination was found to be poor in extremely dry conditions (Davenport, 1996).

The ISO standard considered the effect of humidity on lubrication after a series of tests were conducted. The tests investigated the effects of relative humidity on lubrication by testing 24 different fuels at 60 % RH (≈ 1.9 kPa) and 85 % RH (≈ 2.7 kPa) at 25 °C ambient air temperature. From the results, of the 24 fuels tested, 22 of them had a larger wear scar at 85 % RH than at 60 % RH. The remaining 2 had a slightly smaller wear scar at 85 % RH than at 60 % RH (Davenport, 1996).

Following this, a Round robin testing cycle ranging from 0.8 kPa to 2.2 kPa was performed on 12 fuels with low sulphur content to determine the impact of relative humidity on lubrication (Davenport, 1996). The following were the results:

- 2/12 fuels, including the high lubricity reference, showed no response.
- 10/12 fuels showed increased mean wear scar diameter (*MWSD*) with increasing water vapour pressure.

- For the 12 fuels analyzed, the average difference in *MWSD* per change in water vapour pressure was 60 $\mu\text{m}/\text{kPa}$.
- The response of the high lubricity reference was nearly flat (3 m/kPa).

As a result, ISO adopted a correction of 60 m/kPa , and 1.4 kPa was chosen as the standard (Langenhoven, 2014). The humidity correction factor is specified as 60 m/kPa (HCF). This is shown in [Equation 2.6](#) and stipulated in ISO 12156. Based on the deviation from the standard water vapour pressure of 1.4 kPa, this equation provides a linear modification of the wear scar (Langenhoven, 2014).

The range for allowable water vapour pressures for [Equation 2.6](#) was changed from 0.8 - 2.2 kPa to 0.8 - 2 kPa. This range is shown in [Figure 3.2](#). The water vapour pressure of 1.4 kPa was selected as the standard because this is the midpoint of the new proposed allowable range of water vapour pressure (Davenport, 1996).

$$WS_{1.4} = MWSD + 60(1.4 - AVP) \quad (2.6)$$

$WS_{1.4}$ represents the corrected wear scar diameter, $MWSD$ is the mean wear scar diameter and AVP is the average water vapour pressure of the test. Test results will only be valid if laboratory conditions are within the specified range.

According to ISO 12156, for unknown diesel fuels the HCF value should be set to 60. Consequently, an HCF value of 60 was used in all the experimental tests in this study.

2.8. Diesel production

Diesel is one of the products commonly produced from crude oil. Crude petroleum is an unrefined petroleum commodity made up of hydrocarbon deposits and other organic materials that occurs naturally (Reedijk & Poeppelmeier, 2013: 529). It is subjected to refining by continuous fractional distillation to produce useful different fractions. The different fractions, thus obtained contain hydrocarbons of different chain lengths. The diesel fraction comprises of hydrocarbon chains C_9 - C_{22} in length with a boiling range of $250\text{ }^{\circ}\text{C}$ - $350\text{ }^{\circ}\text{C}$ (Reedijk & Poeppelmeier, 2013: 526). [Figure 2.17](#) shows fractional distillation of crude oil.

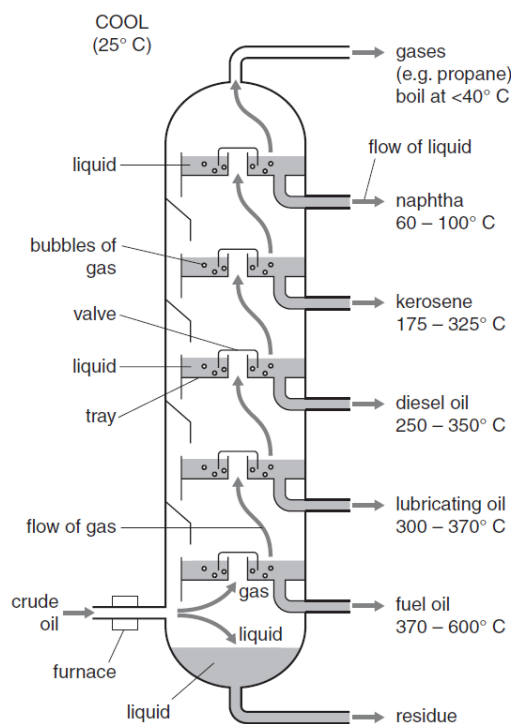


Figure 2.17: Refining of crude oil (adapted from Jechura, 2018)

Diesel fuel has a lot of specifications that are quite opposite to petrol (gasoline). Due to the fact that diesel fuel is used in compression-ignition engines, it is important that it auto-ignites. However, in petrol it is critical to prevent fuel auto-ignition so that spark-ignition can be properly timed for optimal engine efficiency (Reedijk & Poeppelmeier, 2013: 529). The quality of the diesel fuel is imperative for many internal engine components including fuel pumps and injectors especially in performing its role as both fuel and lubricant. When the lubricity of the fuel is not to a satisfactory level excessive wear and metal damage occurs leading to shortened service life of the engine. Therefore, the role of additive packages in final fuel formulation is just as important as the properties of the base fuel. This is because these additives are crucial for engine protection (Reedijk & Poeppelmeier, 2013: 529).

2.8.1. International diesel specifications

The guidelines that are used in Europe and several parts of the world for diesel fuel are the European fuel specifications and the specifications associated with the five categories specified in the World-wide fuel charter (WWFC). Of the two, the European fuel specification is legislated, while the WWFC establishes a generic collection of guideline requirements to assist refiners, motor manufacturers, and policymakers in reaching a consensus on possible future fuel specifications. The most recent edition of the WWFC for diesel published in October 2019 is given in [Table 2.1](#) (Hultema *et al*, 2019: 1).

European emission standards regulate petrol and diesel fuel separately. In 1992, the first European emissions standards were adopted, and the rules were nowhere near as rigorous as they are today. Over the years, the regulations have

become stricter and the limits lowered. [Table 2.2](#) shows the Euro standards for diesel from past to present.

Table 2.1: Specifications for diesel fuel from the WWFC. (Hultema *et al*, 2019: 53-61).

Specification	Category 1	Category 2	Category 3	Category 4	Category 5
Viscosity at 40 °C (cSt)	2.0-4.5	2.0-4.0	2.0-4.0	2.0-4.0	2.0
Flashpoint (°C), min	55	55	55	55	55
Lubricity at 60 °C (µm), max	460	460	460	400	400
T95 distillation point (°C), max.	370	355	340	340	340
Total aromatics (mass %), max.	-	25	15	15	15
Polycyclic aromatics (mass %), max.	-	5	2	2	2
Sulphur (mg/kg), max.	2000	300	50	10	10
Cetane number, min	48	51	53	55	55
Cetane index, min	45	48	50	52	52
Density at 15 °C (kg/m ³)	820-860	820-850	820-840	820-840	820

Table 2.2: Euro emissions standard for diesel fuel (Hultema *et al*, 2019: 7-53)

Euro Standard	Date	Sulphur limit (ppm)	CO (g/km)	NOX (g/km)	PM (g/km)	HC+NOX (g/km)	PN
Euro 1	July 1992	2 000	2.72	-	0.14	0.97	-
Euro 2	Jan 1996	500	1.0	-	0.08	0.7	-
Euro 3	Jan 2000	350	0.64	0.50	0.05	0.56	-
Euro 4	Jan 2005	50	0.50	0.25	0.025	0.30	-
Euro 5	Sep 2009	10	0.50	0.180	0.005	0.23	6.0×10 ¹¹
Euro 6	Sep 2015	10	0.50	0.08	0.005	0.17	6.0×10 ¹¹

From [Table 2.2](#) Euro 6 is a substantial improvement over Euro 5 in terms of NO_x limits. The specification for NO_x limit decreases from 0.18 g/km to 0.08 g/km, a reduction of 56 %. The requirement for the NO_x limit was first introduced in Euro 3 at 0.5 g/km, and by Euro 6 a reduction of about 84 % is realised. This has major implications for control technologies, because for the first time emission control had to be incorporated after treatment for NO_x. The same principle applies to the particle mass (PM) and particle number (PN) standards. Limits on particle mass emissions for diesel fuel have been significantly decreased since the Euro 1 standards were first introduced. Currently, the Euro 6 particle mass limits reflect a 96 % reduction from the Euro 1 limits for diesel fuel. The Euro 6 particle mass limits are now so low that measurement precision and sensitivity are a challenge, and this has led to the implementation of PN limits that are easier to measure (Hultema *et al*, 2019: 7).

Sulphur content is another major environmental pollutant that is addressed in the European emission standards. The current sulphur content specified in Euro 6 is 10 ppm. However according to the South African national standards for

automotive fuels (SANS 342, 2016) a sulphur content of 50 ppm is still acceptable on the fuel market. These increasing restrictions on the sulphur content in diesel fuel requires extreme hydrotreating techniques that severely affects the diesel’s lubricity. The use of lubricity enhancing additives become key in maintaining the functionality of the diesel as a lubricant.

The WWFC has set higher standards for aromatic material, T95 boiling point, lubricity at 60 °C, and cetane specifications. The more rigorous WWFC guidelines are primarily motivated by pollution reduction and environmental effects, and they may well signal future legislative directions (Hultema *et al*, 2019: 51). The WWFC guidelines for diesel are established for five different categories of fuel quality ([Table 2.3](#)).

Table 2.3: Categories of fuel defined by the sixth edition of World-wide fuel charter (Hultema *et al*, 2019: 51).

Category	Description
1	Markets with little or minimum criteria for pollution regulation. The majority of the requirements are based on basic vehicle/engine performance criteria.
2	Markets with strict pollution controls or other requirements, such as Euro 2 or US Tier 1 fuel.
3	Markets with advanced pollution control or other demands necessitated by technology in the year 2000, such as Euro 3 and Euro 4.
4	Markets with more stringent pollution control standards, such as Euro 4 and US EPA Tier 2 fuel, would require sophisticated after-treatment technologies to meet potential needs.
5	Markets with advanced emission control and fuel efficiency standards, such as those that require US 2017 light duty fuel economy, US heavy duty fuel economy, and so on.

2.8.2. Diesel properties

2.8.2.1. Cetane number

This is a measure on how well diesel fuel ignites. A standard (direct injection) diesel engine is easier to start the higher the cetane number is. The cetane number also indicates the percentage (by volume) of cetane (n-Hexadecane) in a combustible mixture (containing cetane and 1-methylnapthalene) with ignition characteristics similar to the diesel fuel under test (Schaschke, 2014: 61).

2.8.2.2. Flash point

The flashpoint of any liquid is the lowest temperature at which it will produce sufficient vapour to form a flammable mixture in air. If there is an ignition source present, a lower flashpoint temperature makes it easier to ignite the air. For any given material the higher the flashpoint the safer it is to handle the material (Janes & Chaineaux, 2013).

2.8.2.3. Aromatic content

If a molecule has at least one benzene ring, it is classified as aromatic (IUPAC, 2016). As a result, aromatics can be categorized as a wide range of molecules with widely different fuel properties. Consequently, fuel specifications, such as the WWFC, distinguish between complete aromatics and polynuclear aromatics (aromatics with three or more benzene rings).

The flame temperature during combustion is determined by the total aromatic content, with a higher aromatic content resulting in higher NO_x emissions. The

total aromatic content of diesel fuel is also related to its density, so there is a relationship between particulate emissions and aromatic content (Hultema *et al*, 2019: 77). Furthermore, high aromatic content generally yields poor fuel quality, giving a low cetane number to the diesel (Hultema *et al*, 2019: 78). Nonetheless, the presence of aromatic compounds also contribute to the lubricity of the fuel.

2.8.2.4. Sulphur content

Over the years this fuel specification in diesel has changed the most. A sharp drop from 500 ppm to 10 ppm is observed in the current Euro 6 specification. This is mostly due to the raised concern and awareness about SO_x emissions, particularly SO₂ emissions. Studies show that the harmful effect of SO₂ on vegetation extends beyond acid rain, which earlier made sulphur emissions a contentious political problem (Surawski *et al*, 2017).

The presence of sulphur in automotive fuels triggers an increase in the release of other harmful compounds to the atmosphere. Sulphur content in the exhaust system of diesel engines reduces catalytic conversion capability, resulting in increased emissions of nitrous oxides (NO_x), carbon monoxide (CO), hydrocarbons, and volatile organic compounds (VOCs) (Surawski *et al*, 2017).

2.8.2.5. Lubricity

Lubricity is a measure of the fuel's ability to reduce friction and wear (Schaschke, 2014: 226). For the majority of diesel fuel injector pumps, lubricity is essential, since these pumps are reliant on the fuel to lubricate their moving parts. The

formation of a lubricating film by the fuel between the sliding solid surfaces prevents the metal components from wear. Inadequate lubricity in diesel can result in excessive pump wear or possibly machine failure.

Prior to desulphurization diesel fuel possesses lubricity which is inherent. Unfortunately, after desulphurization this natural lubricity is lost. The natural lubricity of diesel is not a function of sulphur in the fuel. Instead, it is due to the presence of trace levels of polar substances such as oxygen, nitrogen, aromatics, and olefinics in diesel fuel prior to desulphurization. These compounds created protective layers on the metal surfaces as a natural lubricant (Hultema *et al*, 2019: 86). To resolve lubricity deficiency in highly processed fuels inexpensive lubricity enhancers such as plant oils can be used instead of changing the fuel refining process (Guo *et al*, 2016).

2.8.2.6. Oxidative stability

Oxidative stability refers to the susceptibility of the diesel fuel to oxidation. It is a property that describes how the constituent compounds react with oxygen. The rate of oxidation is accelerated by high temperatures, water, and acids. Oxidation generally leads to an increase in the diesel fuel's viscosity and deposits of varnish and sludge (Kotz *et al*, 2015: 126).

2.8.2.7. Cloud point

The temperature at which paraffin a natural component in diesel fuel, begin to form cloudy wax crystals is termed the cloud point temperature (Dehaghani & Rahimi, 2018).

2.8.2.8. Pour point

The temperature at which the paraffin in the fuel crystallizes to the point that the fuel gels up and becomes resistant to flow is known as the pour point. (Dehaghani & Rahimi, 2018).

2.9. Additive technology

Additives are chemical compounds added to lubricating oils to provide the finished product specific qualities (Schaschke, 2014: 6). Some additives give the lubricant new and useful properties, while others improve existing properties and slow down the rate at which undesirable changes occur in the material throughout its service life (Minami, 2017).

Although there is no rigorous definition as to the quantity of a substance that constitute an additive, as opposed to a blending component, it is generally accepted that an additive is something added at less than 1 % (w/w). As a result of this low concentration, the physical properties of the fuel, such as density, viscosity, and volatility should not change significantly (Minami, 2017).

Over the years, advancement in design and manufacture of engines have been realized and oil additives have been identified that solves a variety of engine related problems such as excessive wear and/or friction. Plant oils have unique characteristics that lubricate surfaces to reduce wear and/or friction.

2.9.1. Plant oils as lubricity enhancers

Plant oils are derived from plant sources. The main constituent is triglyceride molecules (shown in [Figure 2.18](#)). Triglyceride molecules are formed by single-molecule glyceride and three-molecule straight-chain fatty acids that are connected to the glycerine molecule through an ester bond. Although mineral oil-based additives are also used as lubricity additives in fuels, several plant oils have unique characteristics that makes them perform well as lubricity enhancers in various petroleum-based products (Quinchia *et al*, 2014). Certain plant oils possess good lubricity, good anti-corrosion, better viscosity–temperature characteristics, and low evaporation loss in industrial applications. Furthermore, plant oils are eco-friendly and renewable therefore can substitute synthetic and mineral oil-based additives in many applications.

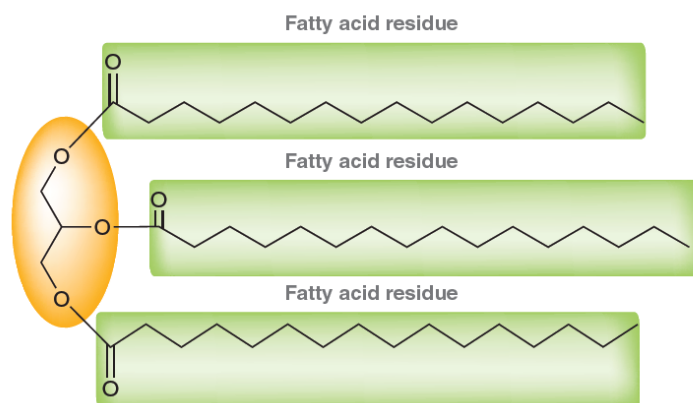


Figure 2.18: Triglyceride structure (Klein, 2017: 1193).

In the triglyceride structure of fatty acids, the chain length is typically between 14 and 22 carbon atoms, with various degrees of unsaturated bonds. The level of saturation in the fatty acid chain of the triglyceride molecule is key to the

behaviour of the plant oil as a lubricity enhancer. If the fatty acid chains are saturated (only single bonds), the oil attains a good oxidation stability, but cold flow properties of the oil become poor. If the fatty acid chains of the oil are polyunsaturated (contains many double or triple bonds) the oxidative stability is adversely affected while cold flow properties become better. On the other hand, if the fatty acid chains are monounsaturated (contains only one unsaturated bond in the structure) the properties of the oil lie between the two extremes. Quinchia *et al* (2014) stated that some of the physical properties of the plant oils such as viscosity index can be correlated with the fatty acid composition in the oil which in turn can be utilized to develop models to predict these physical properties. According to Quinchia, the pour point and cloud point of the oils are influenced by the amount of saturated, monounsaturated, or polyunsaturated fatty acids present and not by their chain lengths. Therefore, a low amount of saturated fatty acids with a good combination of monounsaturated fatty acids and polyunsaturated fatty acids favours low pour point and cloud point temperatures. [Figure 2.19](#) shows the molecular structures of different fatty acids found in various plant oils. Plant oils generally contain different percentages of these fatty acids ([Table 2.4](#)).

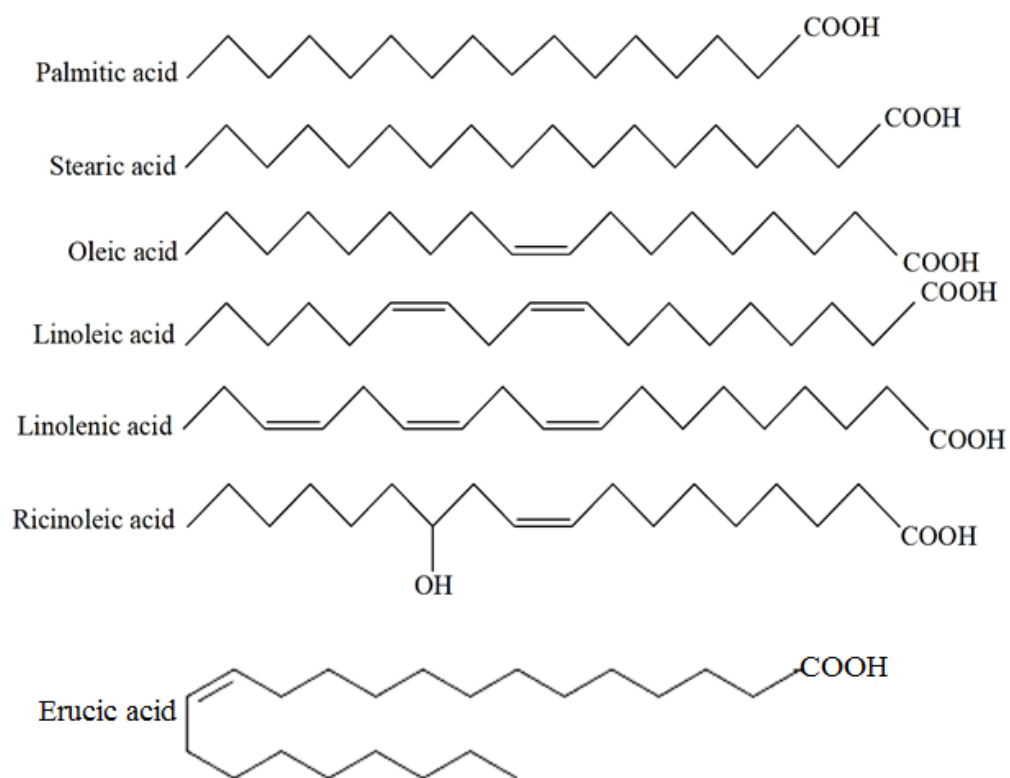


Figure 2.19: Molecular structure of fatty acids in plant oils (Rustan & Drevon, 2005)

Of the three oils under study (i.e. castor, moringa and canola oil), castor oil is unique. It contains 90.85 % of a specific monounsaturated fatty acid known as ricinoleic acid. The molecular structure of ricinoleic acid contains a hydroxyl group (i.e. an –OH group) which makes castor oil more polar than the other plant oils investigated (Patel *et al*, 2016). The triglyceride molecular structure of castor oil is also shown in [Figure 2.20](#).

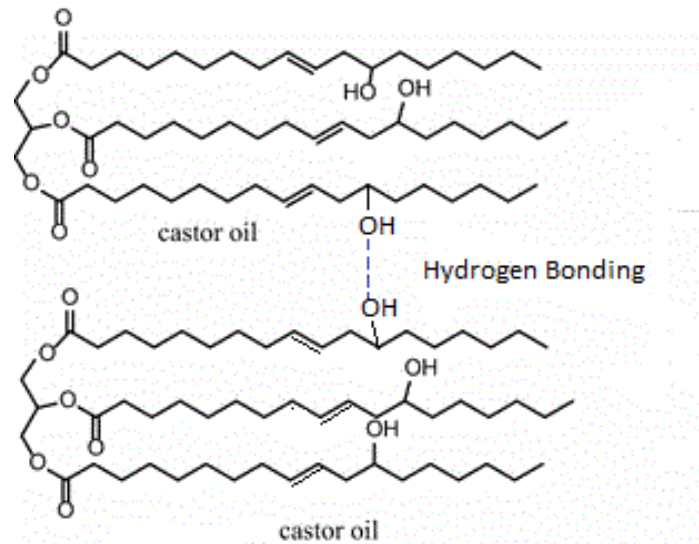


Figure 2.20: Molecular structure of castor oil (Asadauskas *et al*, 1997).

In the subsequent sections a brief concept about castor oil, canola oil and moringa oil is discussed. Comparison between the three plant oils in terms of their physical properties as well as their compositions is done and discussed.

2.9.1.1. Castor oil

Castor is one of the world's oldest crops; however, it just makes a small contribution of about 0.15 % to plant oils produced in the world (Patel *et al*, 2016). The oil produced from this crop is of importance to the global specialty chemical industry because it is a major commercial source of a hydroxylated fatty acid (Patel *et al*, 2016).

Castor oil is a viscous fluid with a pale yellowish colour. The castor beans are cultivated for their seeds ([Figure 2.21](#)). The oil is obtained by pressing the seeds of the castor oil plant. In South Africa, the plant is majorly cultivated in the Western Cape. The oil was selected for this research work because castor oil has

excellent lubrication and a high viscosity which is desirable in automotive lubrication (Patel *et al*, 2016) [Table 2.5](#) details the physical properties of castor oil.



Figure 2.21: Castor bean and seeds (Laurent, 2010)

Castor oil's distinct structure provides remarkable properties, making it suitable for various industrial applications. It has a high content of ricinoleic acid ([Figure 2.20](#)). The $-OH$ group in the ricinoleic acid structure makes castor oil a natural polyol. An organic compound with several hydroxyl groups is known as a polyol. Ricinoleic acid has two hydroxyl groups. This gives the oil some oxidative stability and a relatively high shelf life compared to other oils by preventing peroxide formation (Patel *et al*, 2016).

The $-OH$ group in ricinoleic acid structure also provides a functional group position for a wide range of chemical reactions, such as halogenation, dehydration, alkoxylation, esterification and sulphation. Consequently, this unique functionality increases the utilisation of castor oil in many industrial applications such as lubricants manufacturing and paint production.

2.9.1.2. Canola oil

Canola oil is a plant oil extracted from a rapeseed variety with a low erucic fatty acid content. Naturally cultivated rapeseed oil contains 43 % erucic acid. However, erucic fatty acid is harmful for human consumption. For that reason, the amount of erucic acid in rapeseed oil is significantly reduced to 2 % or less to produce canola oil (Herbst, 2015).

As per international regulated standard the official definition for canola is (Herbst, 2015):

“Seeds of the genus Brassica (Brassica napus, Brassica rapa or Brassica juncea) from which the oil shall contain less than 2 % erucic acid in its fatty acid profile and the solid component shall contain less than 30 micromoles of any one or any mixture of 3-butenyl glucosinolate, 4-pentenyl glucosinolate, 2-hydroxy-3-butenyl glucosinolate, and 2-hydroxy-4-pentenyl glucosinolate per gram of air-dry, oil-free solid”.

The fatty acid composition of the oil can be genetically regulated, and this has been used to create products that are specifically formulated for use, example in food production or lubricant manufacturing. Canola oil was selected for this research work because it is popular in Europe for making biodiesel (Herbst, 2015). Its popularity necessitates research into its performance as a lubricity enhancer. [Figure 2.22](#) shows an image of canola seeds used to produce canola oil.

The density of the oil is influenced by the fatty acid constituents. Monounsaturated fatty acids (MUFA) and polyunsaturated fatty acids (PUFA) have a lower density than saturated fatty acids (Herbst, 2015). High saturated fatty acid content in the oil causes sedimentation at low temperatures (Herbst, 2015). The existence of unsaturated C=C bonds in the molecular structure of plant oils is responsible for their mediocre oxidative stability when compared to synthetic additives. Particularly, when there is presence of polyunsaturated compounds such as linoleic and linolenic acids in the oil.



Figure 2.22: Canola seeds (Barnes, 2017)

2.9.1.3. Moringa oil

Moringa oleifera is a fast-growing, drought-resistant plant of the *Moringaceae* family. It is native to the sub-Himalayan regions. Moringa oil is rich in monounsaturated fatty acids compared to other conventional plant oils (Mosarof *et al*, 2016). Its fatty acid profile is primarily oleic acid ([Table 2.4](#)).

The level of polyunsaturated fatty acids such as linoleic and linolenic in the oil is insignificant (< 1 %), therefore, it possesses a substantial resistance to oxidative degradation for a plant oil (Mosarof *et al*, 2016). The oil was selected for this

research study because it has good lubricity and grows in arid grounds. These grounds are not suitable for food cultivation. Hence, moringa oil does not take up lands used for food cultivation (Mosarof *et al*, 2016).

[Figure 2.23](#) shows an image of moringa seeds.



Figure 2.23: Moringa seeds (Kajal, 2019).

The composition of plant oils is vital to their functionality as lubricity enhancers. It primarily determines their tribological behaviour as lubricants. [Table 2.4](#) presents typical fatty acid composition of castor oil, moringa oil and canola oil. The values presented in the table are mean values and those in parenthesis are ranges reported in the literature. Looking at the table, high contents of polyunsaturated fatty acids (PUFA), such as linoleic acid and linolenic acid are present in canola oil and this is usually a sign of low oxidation resistance in the oil. High amounts of oleic and erucic acid is ideal in terms of improving oxidative stability because they are monounsaturated fatty acids (MUFA) (Mosarof *et al*, 2016). High amounts of palmitic and stearic acids indicate poor cold flow properties but good oxidative resistance since these fatty acids are saturated (SFA).

Table 2.4: Plant oil composition. SFA – saturated fatty acid, MUFA– monounsaturated fatty acid & PUFA – polyunsaturated fatty acid. (Mosarof *et al*, 2016, Herbst, 2015, Patel *et al*, 2016).

Fatty acid	Type	Castor oil	Moringa oil	Canola oil
Palmitic acid (%)	SFA	0.72 (0 – 1.3)	6.65 (5.40 - 9.07)	4.3 (3.6 – 4.75)
Stearic (%)	SFA	0.64 (0.5 – 1.2)	6.09 (2.68 - 6.15)	1.8 (1.43 – 2.59)
Arachidic (%)	SFA	-	3.98 (2.14 – 4.08)	0.6 (0.5-0.99)
Behenic (%)	SFA	-	5.85 (4.57 – 7.10)	0.5 (0.3 – 0.6)
Oleic acid (%)	MUFA	2.01 (0 – 5.5)	73.85 (67.79- 79.50)	61.6 (57.5 – 64.5)
Gadoleic acid (%)	MUFA	-	1.99 (0 – 2.64)	-
Erucic acid (%)	MUFA	-	-	0.11 (0 – 0.2)
Vaccenic (%)	MUFA	-	-	4.99 (1.5 – 3.5)
Ricinoleic acid (%)	MUFA	90.85 (84.2 - 94)	-	-
Eicosanoids (%)	PUFA	-	-	1.7 (1.12 – 1.9)
Linoleic acid (%)	PUFA	4.73 (4.3 – 7.3)	0.99 (0 - 1.29)	18.6 (16.32 – 22.67)
Linolenic acid (%)	PUFA	0.97 (0 – 1.0)	-	9.1 (7.54 – 11.47)
SFA (%)		1.36 (1 – 2.5)	22.6 (17.24 – 23.79)	7.3 (6.3 – 7.65)
MUFA (%)		92.8 (85 - 95)	75.84 (71.70 – 80.70)	62.49 (61.9 – 64.1)
PUFA (%)		5.7 (2 - 7)	1.0 (0.41 – 2.20)	29.4 (28.7 – 31.3)

Values are mean values and those in parenthesis are ranges reported in the literature.

2.9.2. Physical properties of plant oils

In this section the effects of the physical properties of castor oil, moringa oil and canola oil on lubrication performance are analysed and discussed. The discussion covers molecular structures of fatty acids, viscosity influence, viscosity index and density, among others. It was important to determine these properties to be able to design the friction and wear testing experiments that were conducted on the HFRR.

2.9.2.1. Molecular structure of fatty acids

Plant oils can exert lubricating and wear resisting effects between two frictional surfaces. On the metal surface effective molecules in plant oils undergo physical and chemical adsorption and then successfully form lubricating oil film that inhibits wear. These characteristics are linked to the adsorptive property and reactivity of the molecules, as well as the characteristics of the formulated oil film, which also is associated to the molecular structure (Debnath *et al*, 2014).

The major component of plant oils is a triglyceride formed by single-molecule glyceride and three-molecule straight-chain fatty acids. The fatty acids occupy approximately 90 % of the triglyceride structure and connects to glycerine molecules through an ester bond ([Figure 2.18](#)). The chain length of fatty acids in plant oils is usually between 14 and 22 carbon atoms with varying degrees of unsaturated bonds. For saturated fatty acids, if the carbon fatty acid chain length is longer than 16, the number of carbons in the molecular structure does not influence the friction performance. However, if the fatty acid is unsaturated, the adsorption film cannot be compact because of the presence of a double

bond. That is, the molecules are unable to align themselves in straight line formation on the metal surface because the double bond creates a bend in the molecular structure. Therefore, the molecular cohesion of fatty acids is important. Consequently, the lubrication performance of the fatty acids with more carbon atoms is better than that of fatty acids with fewer carbon atoms (Debnath *et al*, 2014).

Castor oil is a kind of plant oil that has a number of distinct properties. Ricinoleic acid glyceride is the most important ingredient of castor oil ([Figure 2.20](#)). The ricinoleic acid glyceride constitute about 90.85 % of castor oil. The remaining 9.15 % are oleic, linoleic acid glyceride, stearic acid glyceride, as well as a small quantity of other fatty acids. Most plant oils including castor, moringa and canola oil have a -COOH functional group and therefore are polar. The unique feature in castor oil is that a second functional group i.e. an -OH group is located on the 12th carbon atom of the ricinoleic acid. As a result, the polarity of castor oil is stronger than moringa and canola oil, and the oil exhibits a prominent metal adsorptive property and superior lubrication performance. The -COOH group is more polar than the -OH group because of the presence of two oxygen atoms. The -OH is polar due to its hydrogen bonding capabilities and the presence of one oxygen atom in the molecule (Klein, 2017: 9-11, 905-910).

Therefore, the molecular structure of the fatty acids in plant oils play a key role in its performance as a lubricity enhancer. Another parameter greatly influenced by molecular structure is viscosity and viscosity indexes (VI) of the oil.

2.9.2.2. Viscosity

The internal friction of a fluid substance is measured by viscosity, which is a fluidity index (Schaschke, 2014: 403). Fluidity is a significant factor affecting lubrication efficiency, and higher viscosities typically result in higher oil film strength. Generally, an increase in carbon chain length increases both viscosity and viscosity index. Castor oil had the highest viscosity of all the plant oils tested at room temperature. The dynamic viscosity of castor oil reached 657.93 cP under room temperature.

The lubrication performance of castor oil, moringa oil and canola oil increases as dynamic viscosity increases. When the dynamic viscosity of the plant oil is extremely low, the lubricating film that forms is thin. On the contrary, when dynamic viscosity of the plant oil becomes exceedingly high, flow nearly stagnates, and the lubricating performance becomes poor. During the sliding motion on the HFRR, variations in temperature are experienced which alters viscosity of the plant oil.

[Figure 2.24](#) shows the relationship between dynamic viscosity with rising temperature for diesel, castor oil, moringa oil and canola oil. The dynamic viscosities were measured using the Anton Paar SVM 3000/G2 Stabinger viscometer at atmospheric pressure (Anton Paar, 2011: 14) according to ASTM D7042.

[Figure 2.24](#) shows that the dynamic viscosity of the diesel and the plant oils decrease with increase in temperature. The reason behind this result is because fluid viscosity is a comprehensive representation of the gravitational force and

momentum transfer between molecules (Welty *et al*, 2014: 83-87). The average speed of the random motion of the fluid molecules decrease when temperature decreases.

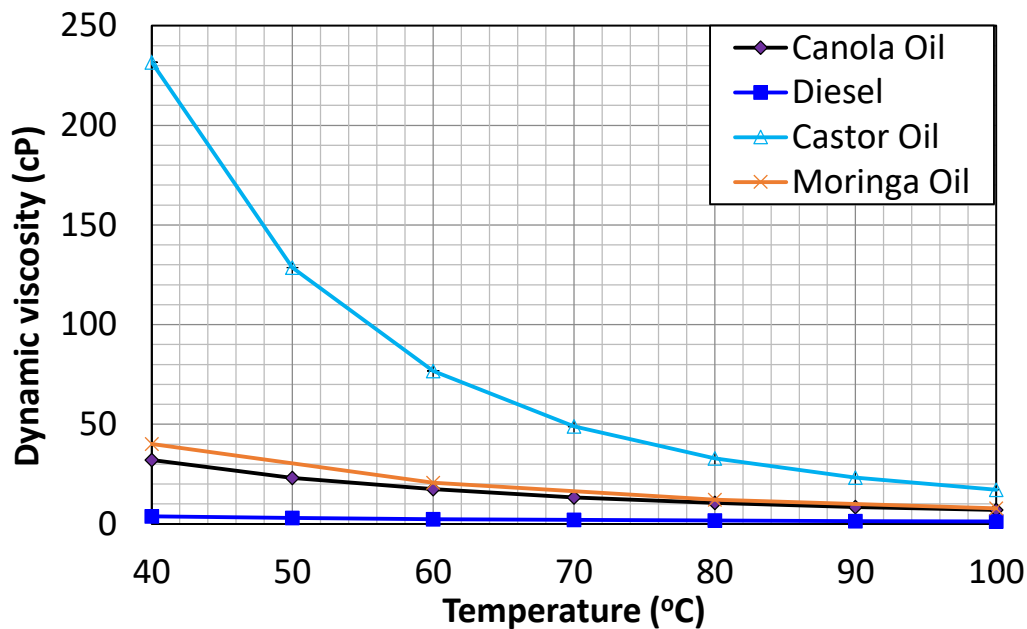


Figure 2.24: Relationship between dynamic viscosity and temperature for diesel, castor oil, moringa oil and canola oil (Guo *et al*, 2016).

This is because high temperature/heat gives energy to the molecules so when temperature is low, the molecules lack energy to move. As the temperature rises, the distance between molecules increases as well, so the molecules now have more energy to travel apart, and the acting force between them decreases. Consequently, viscosity is reduced as seen in [Figure 2.24](#) (Welty *et al*, 2014: 84).

Another observation to note from the figure is that when the temperature is low, the viscosity changes quickly, while when the temperature is high, the viscosity changes slowly. This means that plant oils have stronger viscosity-temperature properties at higher temperatures. This will be an advantage when

they are blended with the diesel fuel. This is because it is undesirable in a diesel engine for fuel viscosity to change too much with a small drop in temperature

Furthermore, [Figure 2.24](#) shows that the viscosity of castor oil is significantly higher than diesel and the other plant oils. This behaviour will affect its performance as a fuel lubricity enhancer.

2.9.2.3. Viscosity index (VI)

The viscosity index indicates how viscosity is affected by temperature, as was discussed from [Figure 2.24](#). It characterizes the viscosity-temperature behaviour of lubricating oils. The lower the VI, the more temperature fluctuations influence viscosity.

The criteria for assessing the best lubricity enhancer is generally the least viscous oil which still forces the two moving surfaces apart to achieve "fluid bearing" conditions. Many lubricant applications demand that the lubricant work under a variety of conditions. Particularly in diesel engines where the diesel treated with these plant oils will be needed to reduce friction between engine components when the engine is started from very low temperatures to temperatures as high as 200 °C or whenever the engine is running.

In that case, the best lubricity enhancer should have the highest VI because that oil will remain stable and not vary much in viscosity over a wide temperature range. The ASTM standard for calculating VI is ASTM D2270 and it requires measurement of the oil's kinematic viscosities at 40 °C and 100 °C. The Anton Paar SVM 3000/G2 Stabinger viscometer was used to measure the kinematic

viscosities of the three plant oils at 40 °C and 100 °C. The VI's of the three plant oils were then calculated according to ASTM D2270. The results are tabulated in [Table 2.5](#).

Table 2.5: Properties of castor oil, moringa oil and canola oil at atmospheric pressure. These laboratory results were obtained using the Anton Paar SVM 3000/G2 Stabinger viscometer (Guo *et al*, 2016, Quinchia *et al*, 2014).

Plant oil	ν (cSt) 40 °C	ν (cSt) 100 °C	Density (ρ) at 40 °C (g/cm ³)	VI
Castor oil	244.88	18.91	0.9459	86
Moringa oil	44.76	9.18	0.8974	193
Canola oil	35.49	8.15	0.9040	215

Canola oil has the highest VI value of 215 indicating it is least affected by temperature changes.

2.9.2.4. Density

The densities of diesel, castor oil, moringa oil and canola oil where examined next using the Anton Paar SVM 3000/G2 Stabinger viscometer. From the plot in [Figure 2.25](#), the observed trend is density decreases with temperature. This is because as temperature increases so does the kinetic energy of the molecules. The higher the temperature the more kinetic energy will be available to the molecules and the faster they will be moving apart (Kotz *et al*, 2015: 13). As the molecules move apart because of the kinetic energy the fluid becomes less dense. That is, the molecules move apart so that they are no more densely

populated but spaced out (i.e. occupying a larger volume). This causes the fluid density to decrease at high temperatures.

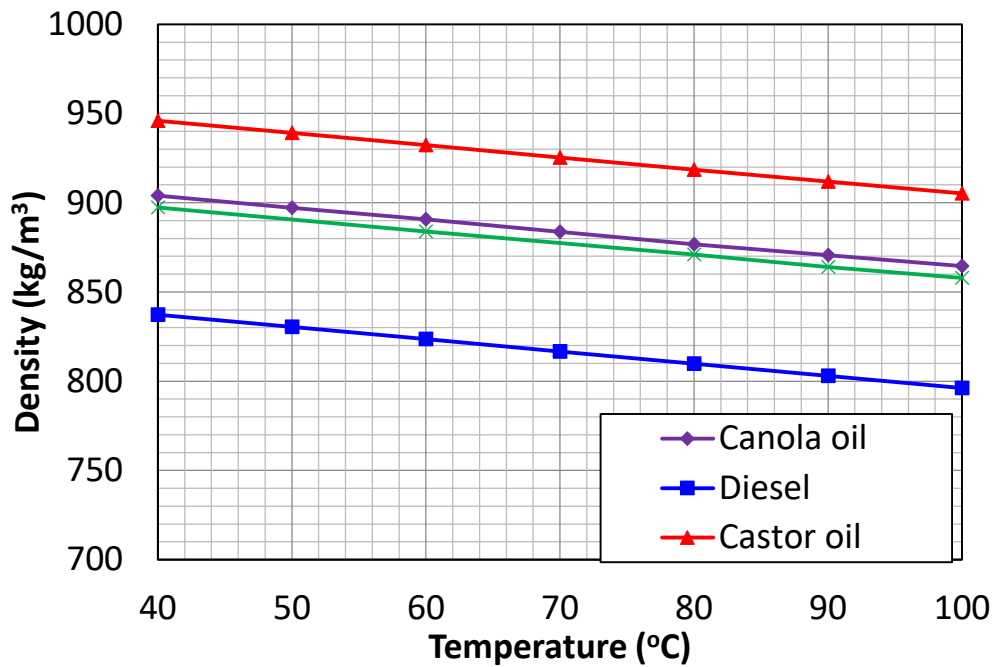


Figure 2.25: Relationship between density and temperature for diesel, castor oil, moringa oil and canola oil. These laboratory results were obtained using the Anton Paar SVM 3000/G2 Stabinger viscometer.

[Table 2.6](#) details the physical properties of castor oil, moringa oil and canola oil.

Table 2.6: Physical properties of castor oil, moringa oil and canola oil (Patel *et al*, 2016 and Mosarof *et al*, 2016, Herbst, 2015).

Physical properties	Castor oil	Moringa oil	Canola oil
Appearance	Pale yellow	Pale yellow	Yellow
Viscosity 40 °C (cP)	231.63	40.17	32.08
Viscosity 100 °C (cP)	17.12	7.88	7.04
Flash point (°C)	145	260	323
Boiling point (°C)	313	220	205
Pour point (°C)	2.7	4	-15
Melting point (°C)	-2 to -5	20.5	-10
Cloud point (°C)	-5	5	-13
Specific heat (kJ/kg/K)	0.089	1.520 to 2.516	1.910-1.916
Refractive index	1.480	1.45-1.46	1.465-1.467
Thermal conductivity (W/m·°C)	4.727	0.19	0.179-0.188
Iodine value (mg I ₂ /g)	82-90	66.83-69.45	121
Extreme pressure (Kg)	60	42	45
Smoke point (°C)	204.5	204.3-204.7	220-230
Saponification number	177-185	166.19-167.81	182-193
Peroxide value (meq/kg)	5	2.60	4
Free fatty acids (%)	0.8	6.678	0.15
Acid value (mg KOH/g)	1-1.6	0.012	0.071
pH value	6.10	5.93-5.99	5.5

To summarize, castor oil, moringa oil and canola oil were chosen as the lubricity enhancers for this study because these oils possess good lubrication properties.

Canola oil is popular in Europe for making biodiesel (Herbst, 2015). Castor oil has excellent lubrication and high viscosity which is desirable in automotive lubrication (Patel *et al*, 2016). Moringa oil on the other hand has a high percentage of unsaturated fatty acids and grows in arid (very dry) grounds (Mosarof *et al*, 2016).

Literature suggests these oils can act as lubricity enhancers in diesel fuel, due to strong interactions with lubricated surfaces. The oils show potential to function well either in the boundary lubrication regime or in the hydrodynamic lubrication regime because of long fatty acid chains and the presence of polar groups in the structure of the oils. The nature of the polar group enables either a physisorbed or chemisorbed layer to form on the surface depending on conditions such as temperature and pressure. If a chemisorbed layer forms more deterrence to high friction and wear will result. Diesel fuel treated with castor oil, moringa oil or canola oil as lubricity enhancing additives have potential to form stronger boundary films that reduces friction and wear. Fox (2007) proposes that the wear reduction in the diesel fuel follows the inverse sigmoidal curve. Castor oil, moringa oil and canola oil can be used to replace petroleum based oils because they possess good lubricating properties and are more environmentally friendly. Despite the benefits of using these plant oils they also have severe disadvantages such as low thermal and oxidative stability. The experimental work in the next chapter explores methodologies used in investigating these effects and techniques used to analyze their tribological properties.

3. Experimental work

In this section the methods that were used to explore the underlying principles of how boundary films are adsorbed, reacted, and desorbed as an effect of the concentration, temperature and load are discussed. The materials and equipment used in this investigation are also listed and discussed.

The HFRR tests conducted in this study examined the effects of temperature, load and concentration of castor oil, moringa oil and canola oil on diesel lubrication. Diesel fuel was treated with various quantities of castor oil, moringa oil and canola oil to improve fuel lubricity. The following plant oil concentrations were selected for the investigation: 0 %, 0.1 %, 0.2 %, 0.4 % and 1% (w/w). The test method followed was ISO 12156 ([Table 3.2](#) & [Table 3](#)).

The HFRR test conditions investigating temperature and load effects only had temperature or load being varied in their respective tests (refer to [Table 3](#)). The plant oil concentration selected for these tests was 0.5 % (w/w). This concentration was selected based on the results obtained from the trial runs. It was observed that at a concentration of 0.5 % (w/w) enough of each plant oil had been added as lubricity enhancing additive to the fuel that concentration should not influence the experiments done for temperature or load effects.

The HFRR has a limit of 120 °C for temperature and 1 kg mass for load. For this reason, the quantity of applied loads selected for investigating the effects of load on diesel lubrication were 200 g \approx 2 N, 400 g \approx 4 N, 600 g \approx 6 N and 800 g \approx 8 N (assuming gravitational acceleration is 9.8 m/s²). A summary of the experimental work is detailed in [Table 3](#).

Table 3: Summary of experimental work.

Parameter	Effect of concentration	Effect of temperature	Effect of load
Duration (min)	75	75	75
Frequency (Hz)	50	50	50
Stroke length (μm)	1 000	1 000	1 000
Load (g)	200	200	200, 400, 600 & 800
Temperature ($^{\circ}\text{C}$)	60	40, 60, 80 & 100	60
Concentration (% (w/w))	0, 0.1, 0.2, 0.4 & 1	0.5	0.5

3.1. Apparatus

The equipment used in this study are discussed below.

3.1.1. High frequency reciprocating rig (HFRR)

The HFRR is a reciprocating tribometer that was developed to test the lubricity of diesel fuels. The friction and wear tests performed in this investigation were carried out on the HFRR. The instrument can be programmed to accommodate the application of the diesel fuel being tested and can be operated at different temperatures.

The HFRR tribometer includes an upper specimen holder, a lower specimen holder that also serves as the lubricant reservoir, a heating block to maintain the necessary lubricant temperature, electromagnetic vibrator, and force transducer to measure the friction force. The instrument also generates a film percentage data. The film percentage data is a function of the electrical resistance across the ball–disk contact interface.

After each test run the generated wear scar on the ball is used as a measure of the fuel's lubricating ability. A model of the HFRR instrument used in this investigation is presented in [Figure 3.1](#) and its operating limits are detailed in [Table 3.1](#).

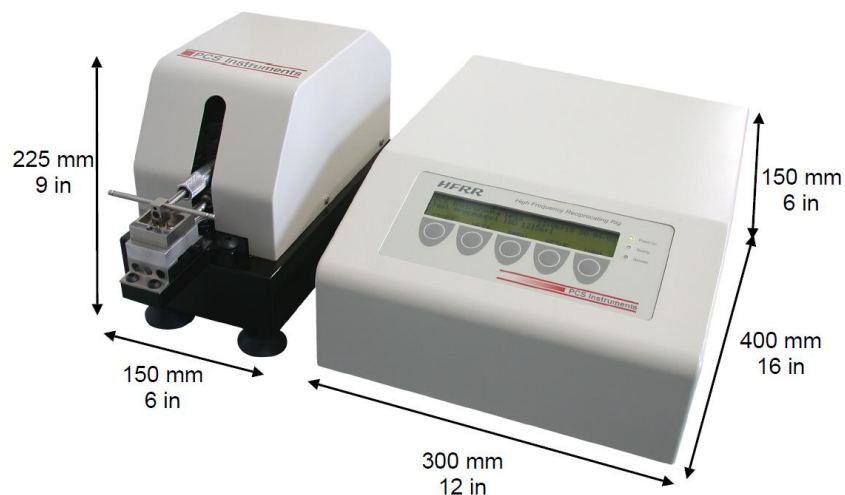


Figure 3.1: HFRR tribometer (PCS instruments, 2005)

In this study the test method used was ISO 12156. [Figure 3.2](#) shows the laboratory air conditions for ISO 12156. Although Figure 3.2 does not appear in the recent issues of ISO 12156. In situations where the HFRR is enclosed in an environmental chamber, the temperature and humidity inside the chamber must meet the specification in [Figure 3.2](#) for the test to be valid. [Table 3.2](#) summarizes the remaining test conditions and specimen properties.

Table 3.1: Limits of operation for the HFRR instrument (PCS instruments, 2005)

Parameter	Value
Frequency	10 -200 Hz
Stroke length	20 μm -2.0 mm
Temperature	Ambient to 150 $^{\circ}\text{C}$
Load	0.1 - 1.0 kg with supplied weight
Maximum frictional force	10 N

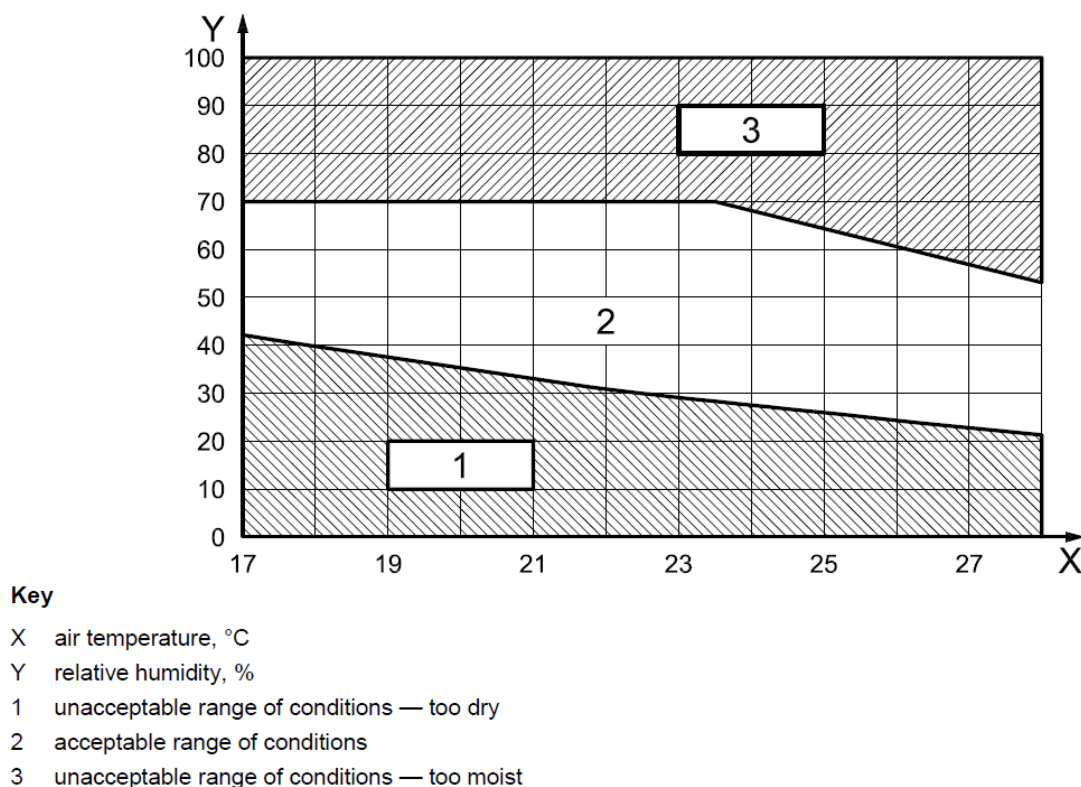


Figure 3.2: Laboratory air conditions (ISO 12156)

ISO 12156 provides only a single parameter which is used to assess the lubricity of the fuel. The test method requires that the diesel fuel produce a wear scar of no greater than 460 μm . The European specifications for diesel, EN 590 also stipulates a maximum wear scar diameter of 460 μm . However, the WWFC is more stringent and recommends the use of the HFRR, with a 400 μm maximum limit (Hultema *et al*, 2019: 59).

Table 3.2: Summary of ISO 12156 standard test method (ISO 12156, 2018).

Parameter	Value
Fluid volume	2 ± 0.2 mL
Stroke length	1 ± 0.02 mm
Frequency	50 ± 1 Hz
Laboratory air	Refer to Figure 3.2
Fluid temperature	60 ± 2 °C
Test mass	200 ± 1 g
Test duration	75 ± 0.1 min
Reservoir surface area	600 ± 100 mm ²
Ball (Top specimen)	
Material	Grade 28 (ANSI B3.12) of AISI E-52100 steel
Hardness	Rockwell hardness “C” Scale number 58-66
Surface finish (Ra)	$Ra < 0.05$ μm
Diameter	6 mm
Test disk (bottom specimen)	
Material	AISI E-52100 steel
Hardness	Vickers hardness “HV30” Scale number 190 - 210
Surface finish	Turned, lapped, and polished to $Ra < 0.02$ μm
Diameter	10 mm
Repeatability at 60 °C	63 μm
Reproducibility at 60 °C	102 μm

3.1.1.1. *WS1.4* correction

The HFRR instrument used in this investigation was enclosed in an environmental chamber, meaning the humidity and temperature inside the chamber could be controlled according to [Figure 3.2](#). The *WS1.4* correction in ISO 12156 considers humidity effect on tests and corrects the WSD to a

standardized water vapour pressure of 1.4 kPa. Reasons why this correction is applied and why 1.4 kPa was selected as a standard is discussed in [Section 2.7](#).

Other lubricity evaluating methods for diesel place different specifications on laboratory conditions. For example ASTM D6079 which is the American test standard for evaluating lubricity of diesel fuels stipulate humidity must only be greater than 30 % and the *MWSD* will be sufficient to characterize the lubricity of the diesel without any correction needed as in ISO 12156. ASTM D6079 also makes no mention of ambient temperature conditions.

Occasionally, it happens that a diesel fuel passes the ISO 12156 or ASTM D6079 test but the diesel engine still fails because of inadequate lubricity in the fuel. Upon inspection of the wear scar surfaces, it was found that friction and wear tests contain more information about a fluid's lubricating properties than can be obtained from the wear scar diameter alone. Oláh *et al* (2005) developed a visual rating system that aids in characterizing lubricating performance. This is termed the complementary rating (*CR*) system. Based on the appearance of wear scars, a six-graded visual rating is established, and laboratory tests obtained from ball-on-disk friction and wear tests are compared to these reference wear scars, and a CR value is given. [Figure 3.3](#) depicts the wear scars that will be used as a reference.

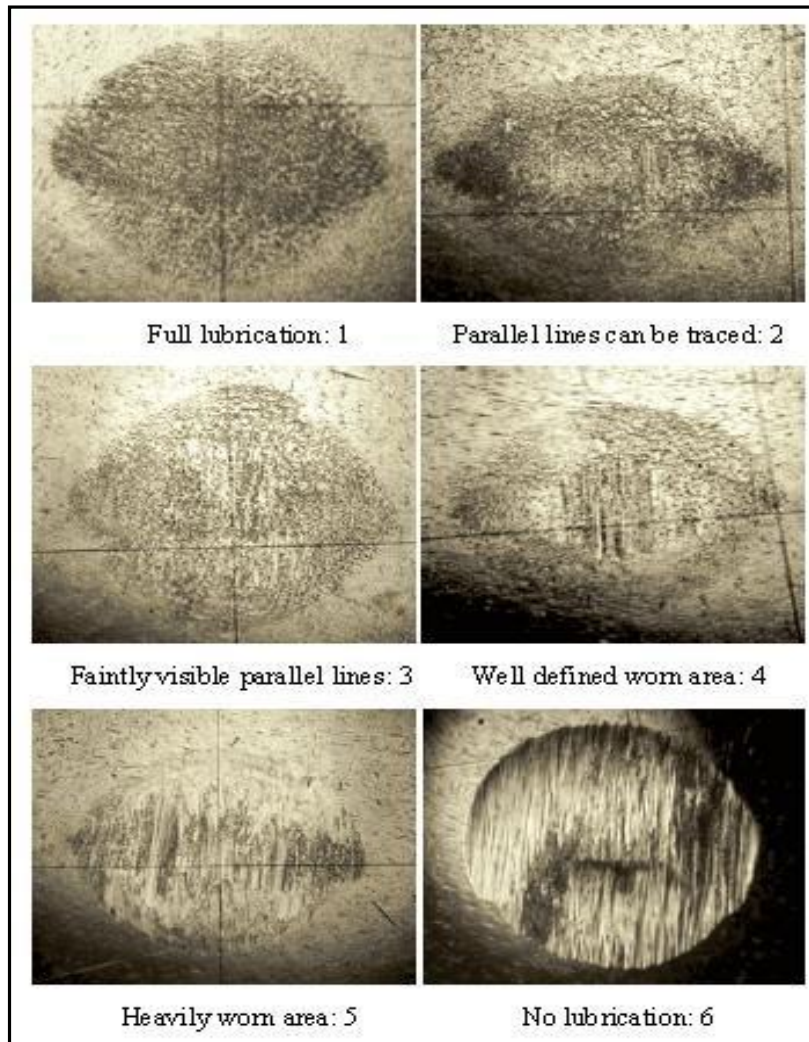


Figure 3.3: A visual rating method to assist in HFRR results evaluation (Oláh *et al*, 2005).

3.1.2. Ultrasonic cleaner

The ultrasonic cleaning instrument used in this work was the PS-40 ultrasonic cleaner. It was used to clean test specimens before and after experiments at atmospheric conditions (25 °C and 101.325 kPa). [Table 3.3](#) shows the operating limits for the PS-40 ultrasonic cleaner.

Table 3.3: Limits of operation for the PS-40 ultrasonic cleaner (Ultrasonic cleaners, 2017).

Parameter	Value
Timer	1-30 min
Heating power	400 W
Ultrasonic power	240 W
Tank capacity	10 L
Operating frequency	40 kHz

3.1.3. Viscometer

The Anton Paar SVM 3000/G2 Stabinger viscometer was used in this study to measure the viscosities of the diesel fuel, castor oil, moringa oil and canola oil at atmospheric pressure. The instrument performs the measurements according to ASTM D7042. The viscometer can operate at temperatures ranging from -56 °C to 105°C (Anton Paar, 2011: 14 - 33).

3.1.4. Relative humidity control

According to the work done by Langenhoven (2014) humidity and atmospheric water content influence the repeatability of the friction and wear tests. Therefore, to ensure good repeatability from the experiments and minor effects of moisture on friction in this study, an in-house built humidity control system was used. Moreover, it was equally important to keep the laboratory conditions compliant to ISO 12156 specification ([Figure 3.2](#)).

The relative humidity (RH) in the environmental chamber was kept between 50 - 55 % throughout this study. A schematic diagram and working principle of the in-house built humidity control setup is presented in [Appendix A](#).

3.1.5. Optical microscope

The Zeiss Axio scope A1 microscope was used to measure the wear scar diameters from the HFRR test runs. It has three objective magnifications of different strengths (5x, 10x and 20x). The magnification strength used for taking the wear scar photographs on the test ball was 10x and the magnification strength used to take the wear track photographs on the disks was 5x.

3.2. Materials and chemicals

The steel balls and discs used in these tribological tests were obtained from PCS Instruments (London, England). The specifications for the balls and discs are provided in [Table 3.2](#). Both chemicals and solvents were used exactly as they were received.

The fuel used in this research work was untreated diesel (i.e. contains no fuel additives) and three plant oils that serve as lubricity enhancing additives. The certificate of analysis (CoA) of the diesel fuel as received from the supplier is presented in [Table 3.4](#). The sulphur content in this diesel is 38 ppm. The fuel was sourced from the refinery and as a precaution was filtered upon arrival.

Castor oil, moringa oil and canola oil were purchased from commercial suppliers. All the plant oils were commercial grade oils and were used without being

purified further (refer to [Table 3.5](#) for product specification). Acetone (HPLC grade, 99.7 %), ethanol (95 %), and hexane (HPLC grade, 99.9 %) were purchased from Merck Chemicals (Pty) Ltd, South Africa.

Table 3.4: Certificate of analysis of the diesel fuel (without any fuel additives).

Test	Units	Result	Lower limit	Upper limit	Test method
Acid Number	mgKOH/g	0.06		0.25	D974
Appearance (Haze)		1		2	D4176
Ash	% m/m	<0.010		0.01	D482
Cetane No		55.0	45.0		ASTM 613
Cetane Index		52	48		D976
CFPP	°C	-4		3	IP309
Cloud Pt	°C	-3			D2500
Colour		1.5		2.5	D1500
Conductivity	Ps/M @ 20°C	173	100		D2624
Copper Corrosion		1		1	D130
Density @ 20 °C	kg/L	0.8483	0.80		D4052
90 % Rec	°C	346.9		362.0	ASTM D86
Fame	% vol	0.010		0.05	ENI 4078
Filter_Blk_Tendency		1.00		2.52	IP 387
Flash PMCC	°C	102.0	62		ASTM D93 MET
Oxidative Stability	mg/100 mL	1.20		2	D2274
RCR, 10 % res	%	0.01		0.30	D4530
Strong Acid Number	mgKOH/g	NIL	NIL	NIL	D974
Sulphur	ppm	38		40.00	ASTM D5453
Total Contamination Number	Mg/kg	10.5		12.0	IP440
Viscosity @ 40 °C	cSt	3.825	2.200	5.300	D445
Water, KF	ppm	32		250	D6304

Castor oil, moringa oil and canola oil were chosen as the lubricity enhancers for this study because these oils possess good lubrication properties. Canola oil is popular in Europe for making biodiesel (Herbst, 2015). Its popularity necessitates research into its performance as a lubricity enhancer. Castor oil has high viscosity which is desirable in automotive lubrication (Patel *et al*, 2016). Moringa oil on the other hand has a high percentage of unsaturated fatty acids and grows in arid (very dry) grounds. These grounds are not suitable for food cultivation. Hence, moringa oil does not take up lands used for food cultivation (Mosarof *et al*, 2016).

Table 3.5: Product specification for plant oils

Plant oil	Castor oil	Moringa oil	Canola oil
Appearance	Yellow	Golden Yellow	Light yellow
Appearance (Form)	Liquid	Liquid	Liquid
Extraction method	Expeller pressed, unrefined		
Infrared Spectrum	Conforms to structure		Conforms to structure
Refractive index at 20 °C	1.475 – 1.481	-	1.471 – 1.475
Free fatty acid			≤ 0.10 %
Peroxide (ppm)			≤ 10 ppm
Miscellaneous assay (Fatty acid composition)			Pass
Arsenic (As)			≤ 3 ppm
Cadmium (Cd)			≤ 1 ppm
Mercury (Hg)			≤ 1 ppm
Lead (Pb)			≤ 10 ppm
Optical rotation (C = 5 %, Ethanol)	4.0 – 6.0 degrees	-	
Specific gravity at 25 °C			0.90 - 0.92
Primary constituent	Ricinoleic acid (90.85 %)	Oleic acid (73.85 %)	Oleic acid (61.6 %)

3.3. Experimental method

3.3.1. Filtering process (ASTM D6217)

As a precaution the diesel fuel was filtered upon arrival from the supplier. All materials that will come in contact with the diesel fuel were rinsed thoroughly with heptane and then air dried. Two 0.8-micrometer nylon membrane filters were placed in an oven at 110 °C for 30 min to eliminate unwanted moisture.

After 30 min the nylon membrane filters were removed from the oven, weighed individually and their mass recorded. Both filters were then placed on the mesh with the heaviest one on top, as to distinguish between them. A funnel was fitted with the mesh and two bolts were used to tighten the setup. The setup was held in place by a clamp. 1 L of diesel was measured and poured into the funnel. The entire setup was now placed on a Buchner flask which was connected to a vacuum pump (shown in [Figure 3.4](#)). The pump was switched on for the filtering process to begin.

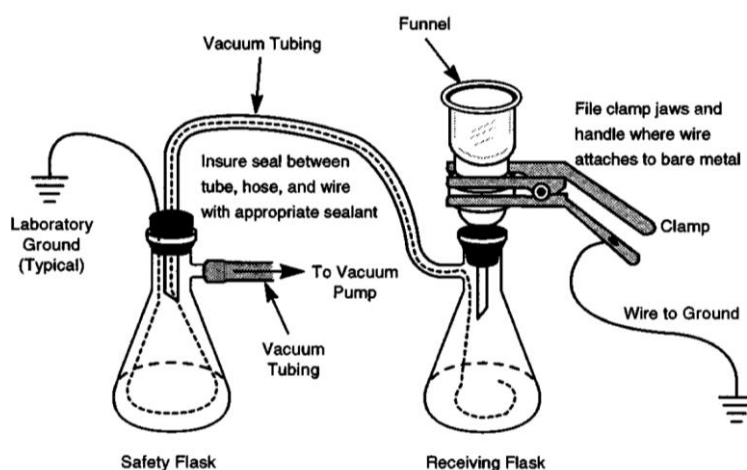


Figure 3.4: Schematic of filtration system (ASTM D6217)

After filtration was complete, the Buchner flask was disconnected, and the filtered diesel was poured into clean glass storage containers. The Buchner flask was again reconnected to the entire setup so that the funnel could be rinsed with heptane. Rinsing was done with the vacuum pump to transfer the heptane from the funnel into the Buchner flask. After rinsing, the setup was disassembled, and the nylon filter papers were dried in the oven for 15 min at 110 °C to remove heptane. The filter papers were now stored in the desiccator for 30 min before weighing. The new masses of the filter papers were then recorded.

3.3.2. Cleaning of test specimen

The disks and balls were placed in a clean beaker and covered with toluene for a minimum of 8 h before the test. Using clean forceps, the specimens, screws, and all hardware that came into contact with the test fluid was transferred into a glass beaker with toluene and ultrasonically stirred for 10 min. All the hardware and specimens were transferred to a beaker filled with acetone and ultrasonically stirred for another 10 min. The specimens were blow-dried, and the test was started immediately.

3.3.3. HFRR test procedure

After the holders and specimens were cleaned and dry the disk was placed in the reservoir and fastened with screws. Care was taken to ensure the disk was screwed tight to prevent movement during the test. The ball was also inserted into the upper specimen holder and was tightened. The top specimen holder containing the ball was now placed under a microscope to examine that no

scratches or scars were on the area of the ball surface that will be used for the test. The reservoir was then attached to the HFRR instrument and tightened, the same was done for the top specimen holder. Following this, the corresponding weight was loaded onto the bar of the upper specimen holder. 2 mL sample of diesel fuel was poured into the reservoir and the temperature probe was inserted. After this, the HFRR program was started.

The test proceeds and stops automatically at the end of the set test period. The specimen holders were then removed, washed clean, and used to measure wear scars after the instrument had cooled.

Using the HFRPC program on the device, the values were entered manually in the saved test data following the wear track calculation. Three (3) repeat runs on a fresh sample of the same test fuel were carried out together with freshly cleaned ball and disk specimens. More repeat runs were conducted if there was a suspicion of error or sample contamination. Average and standard deviation calculations were done using test averages produced under identical test conditions, and the results were recorded and used in further research.

3.3.4. Wear scar measurement

The upper ball specimen was placed under the ZEISS Axio Scope A1 microscope. Using the 10x magnification to focus the image, the horizontal (X) and vertical (Y) wear scar diameters was measured with the ruler.

Following this, the X and Y measurements for wear scars were manually inserted into the HFRR program on the computer. Under the comments section the

complementary rating by Oláh *et al.* ([Figure 3.3](#)) was inputted. The WS1.4 was then calculated by the HFRR program.

3.3.5. Calculating averages and standard deviations

Every experiment was repeated at least three times and each reported trend in the results section (i.e. [Chapter 4](#)) represents the average data from three experiments. The averages were calculated from the friction coefficient values obtained every second on the HFRR instrument. For wear scar sizes an average was taken between the three repeat experiments and this average was considered a true representation of the result under the given test conditions. The average standard deviation for friction coefficient and wear scar size were calculated in the same manner. The graphs displaying standard deviations for friction coefficient are presented in Appendix B.

In summary, the experimental design comprising of friction and wear tests carried out on the HFRR was aimed at establishing how well castor oil, moringa oil and canola oil perform as lubricity enhancers in diesel fuel under variations in concentration, temperature and load. The design was based on observations after the physical properties of castor oil, moringa oil and canola oil were determined as well as results from the trial runs. The next chapter brings to light findings on how these oils contribute to diesel lubricity.

4. Results and discussion

In this section of the work all experimental results are presented and discussed. The experimental and modelling results together bring an understanding to the behaviour of castor oil, moringa oil and canola oil in reducing wear.

According to the certificate of analysis obtained from the supplier the diesel fuel used in this investigation was refined and contained no fuel additives prior to the experiments. Friction and wear tests performed on the HFRR for untreated diesel fuel showed a case of severe wear on the metal surface. The diesel fuel had extremely poor lubricity from the test results ([Figure 4.1A](#)). The wear scar diameter was extremely high (i.e. 897 μm). This is about twice the acceptable wear scar diameter of 460 μm in ISO 12156. Clearly, the untreated diesel fuel needs a lubricity enhancer.

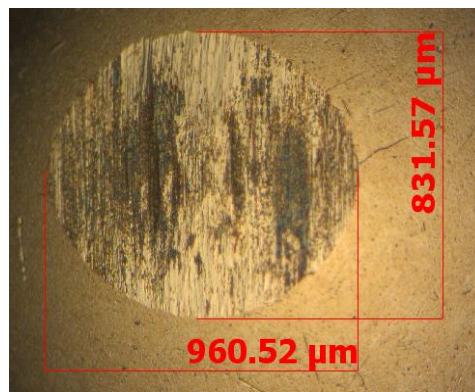


Figure 4.1A: Wear scar photograph for untreated diesel ($WS1.4 = 897 \mu\text{m}$ & $MWSD = 896 \mu\text{m}$).

The relative humidity for all tests conducted was between 50 - 55 % and the ambient temperature was between 19 – 23 °C. Careful attention was paid to keep the laboratory conditions within the ISO 12156 range shown in [Figure 3.2](#).

4.1. Effect of plant oil concentration on lubrication

In this section the effect of plant oil concentration on diesel fuel is presented and discussed. The discussion covers friction coefficient, effects of wear and diesel lubricity models. The HFRR test conditions were strictly ISO 12156 and are detailed in [Table 3](#). Concentrations of castor oil, moringa oil and canola oil in diesel selected for investigation were 0, 0.1, 0.2, 0.4 and 1 % (w/w).

4.1.1. Friction coefficient

[Figure 4.2](#) shows the friction coefficient for untreated diesel (i.e. 0 % (w/w) of plant oil). The three experimental runs are shown. The average standard deviation between the three runs ranged from 0 to 0.02 (details provided in [Appendix B](#)). From the curve the friction coefficient is significantly high and increases over time.

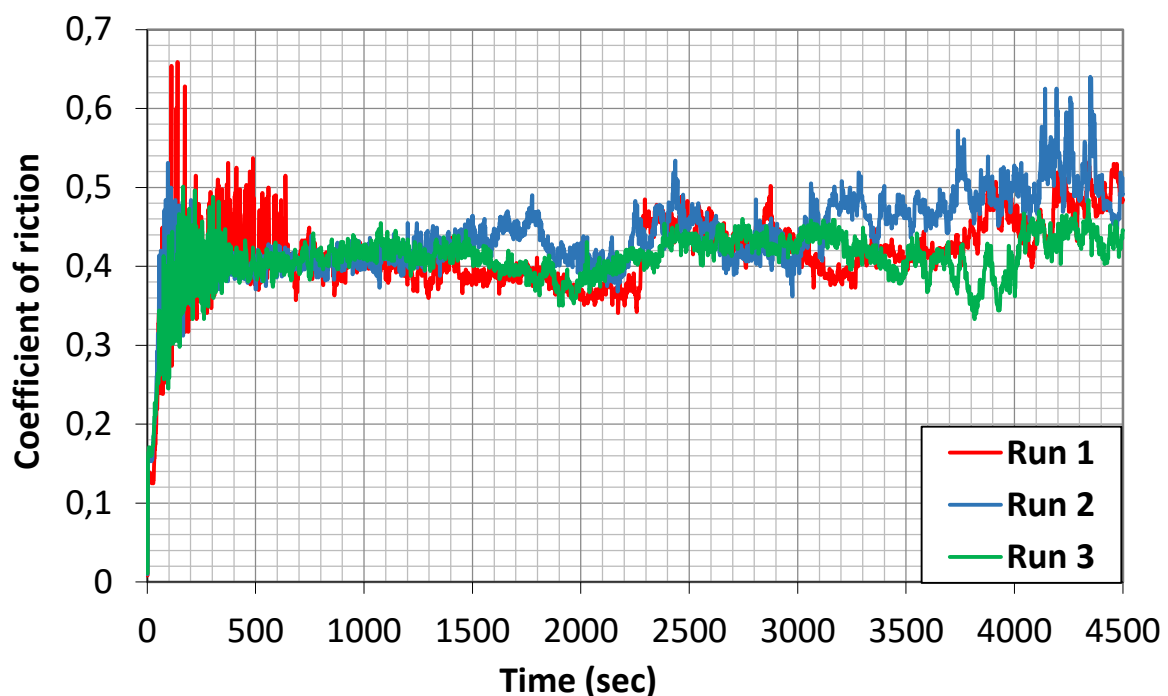


Figure 4.2: Friction coefficient for untreated diesel.

The HFRR forms a contact that operates in boundary lubrication conditions with extensive initial solid-solid contact. This behaviour of untreated diesel where the friction coefficient suddenly rises in the first minutes of the test signifies a change in regime from hydrodynamic to boundary lubrication. At 2 300 s there is a sudden rise in friction coefficient causing the friction coefficient curve to increase strongly. The sudden rise in COF is caused by the breakdown of the lubricant film formed by the untreated diesel (i.e. there is film failure). The film failure allows direct asperity (solid-solid) contact to occur, this explains why the COF keeps increasing strongly afterwards in [Figure 4.2](#). The wear scars obtained for untreated diesel shown in [Figure 4.1B](#) is consistent with the friction coefficient results. The high wear for untreated diesel in [Figure 4.1B](#) most probably occurred after 2 300s. At the end of the test run the wear scar diameters for the three runs were extremely high i.e. 894 μm on average.

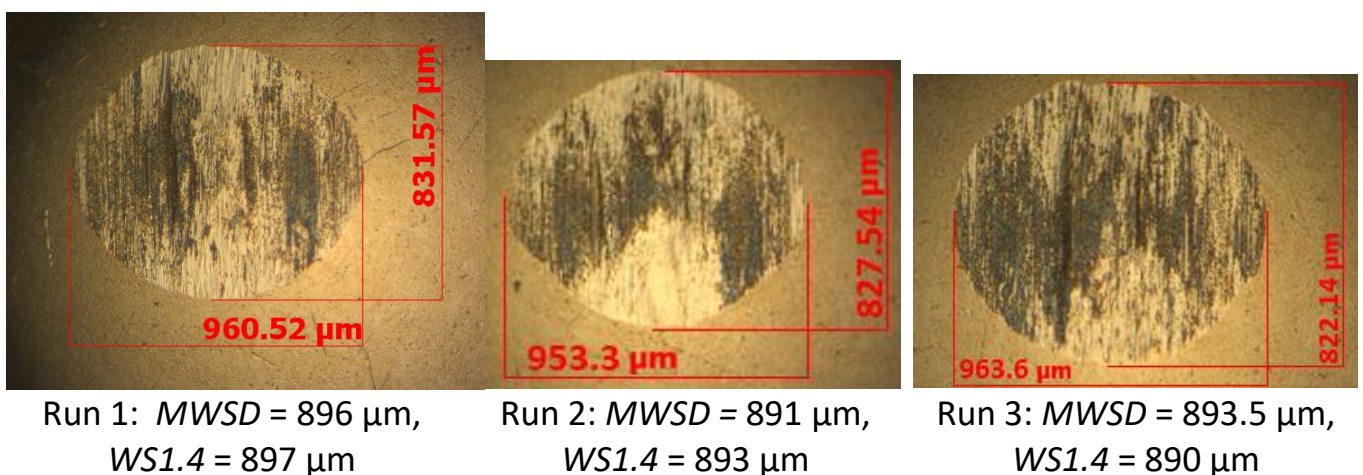


Figure 4.1B: Wear scar photos of untreated diesel for the three runs. CR is 6 in each case.

Figure 4.3 - Figure 4.5 shows the friction coefficient for diesel treated with 0.1, 0.2, 0.4 and 1 % (w/w) of castor oil, moringa oil and canola oil. [Figure 4.6](#) is a plot of the average friction coefficient values of the three experimental runs shown in Figure 4.3 – Figure 4.5 at the given concentration. The averages were

calculated from the friction coefficient values obtained every second between the three runs. The average standard deviation for COF between the three experimental runs ranged from 0 to 0.01.

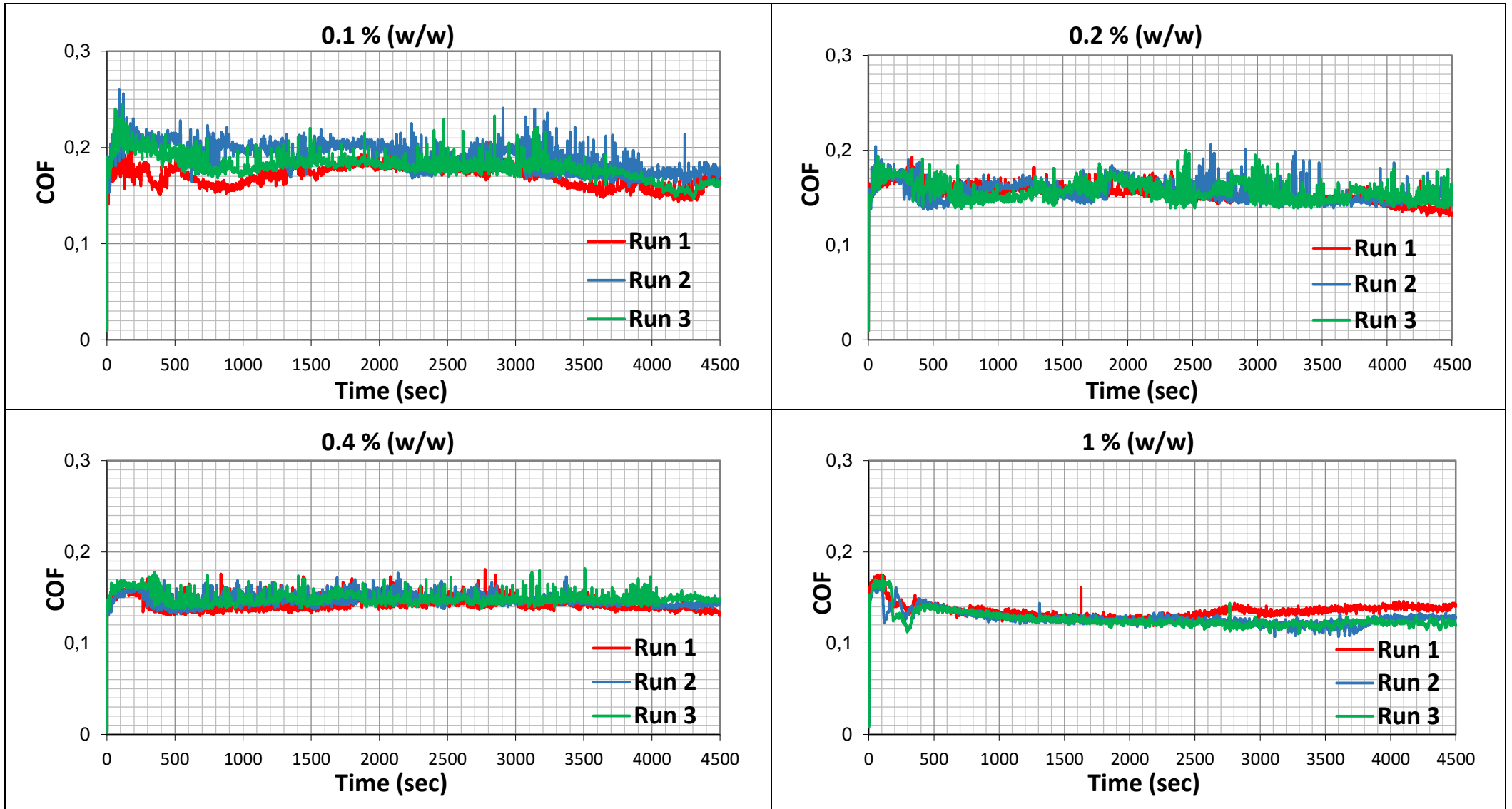


Figure 4.3: friction coefficient for diesel treated with different concentrations of castor oil.

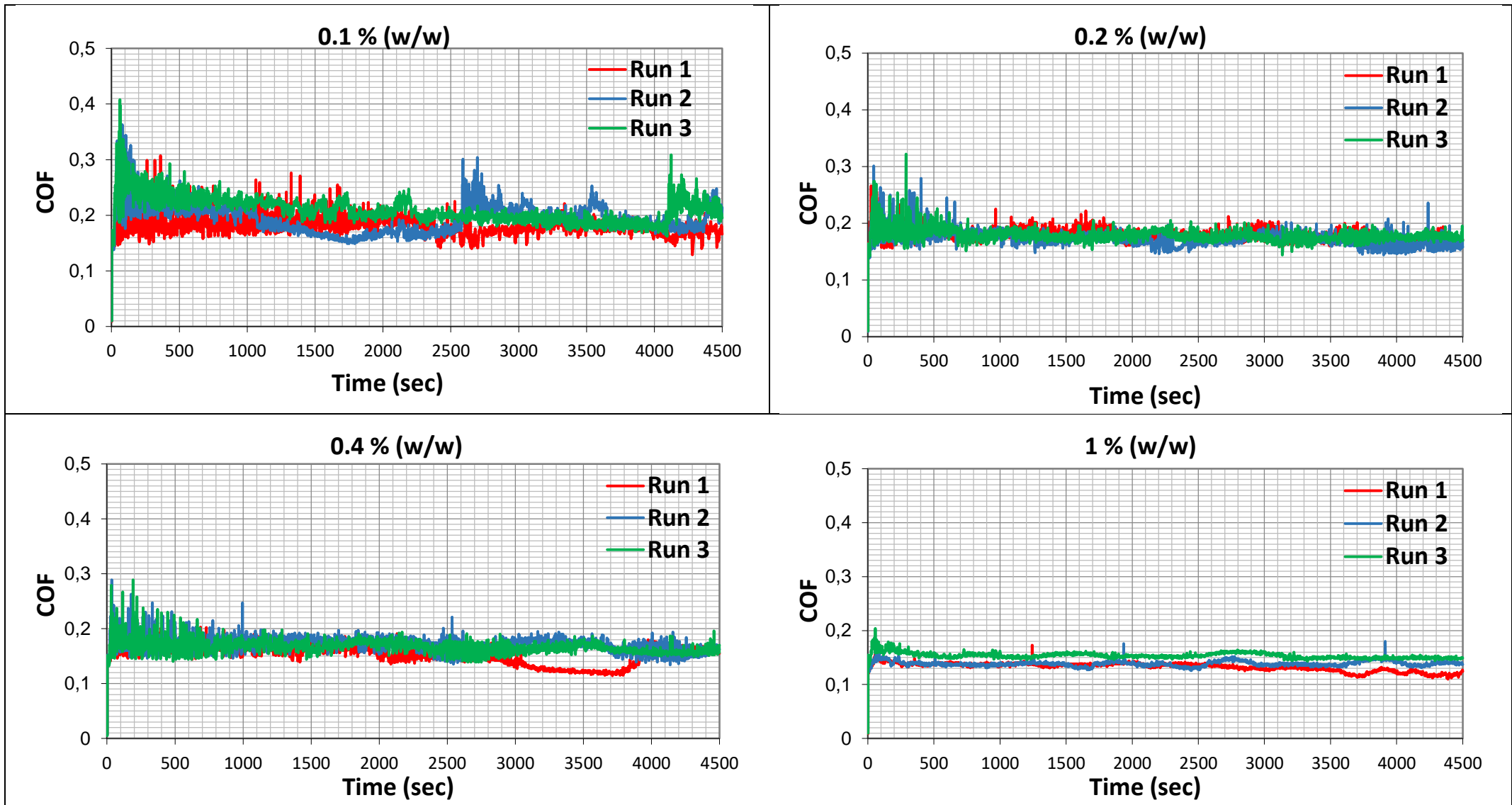


Figure 4.4: friction coefficient for diesel treated with different concentrations of moringa oil.

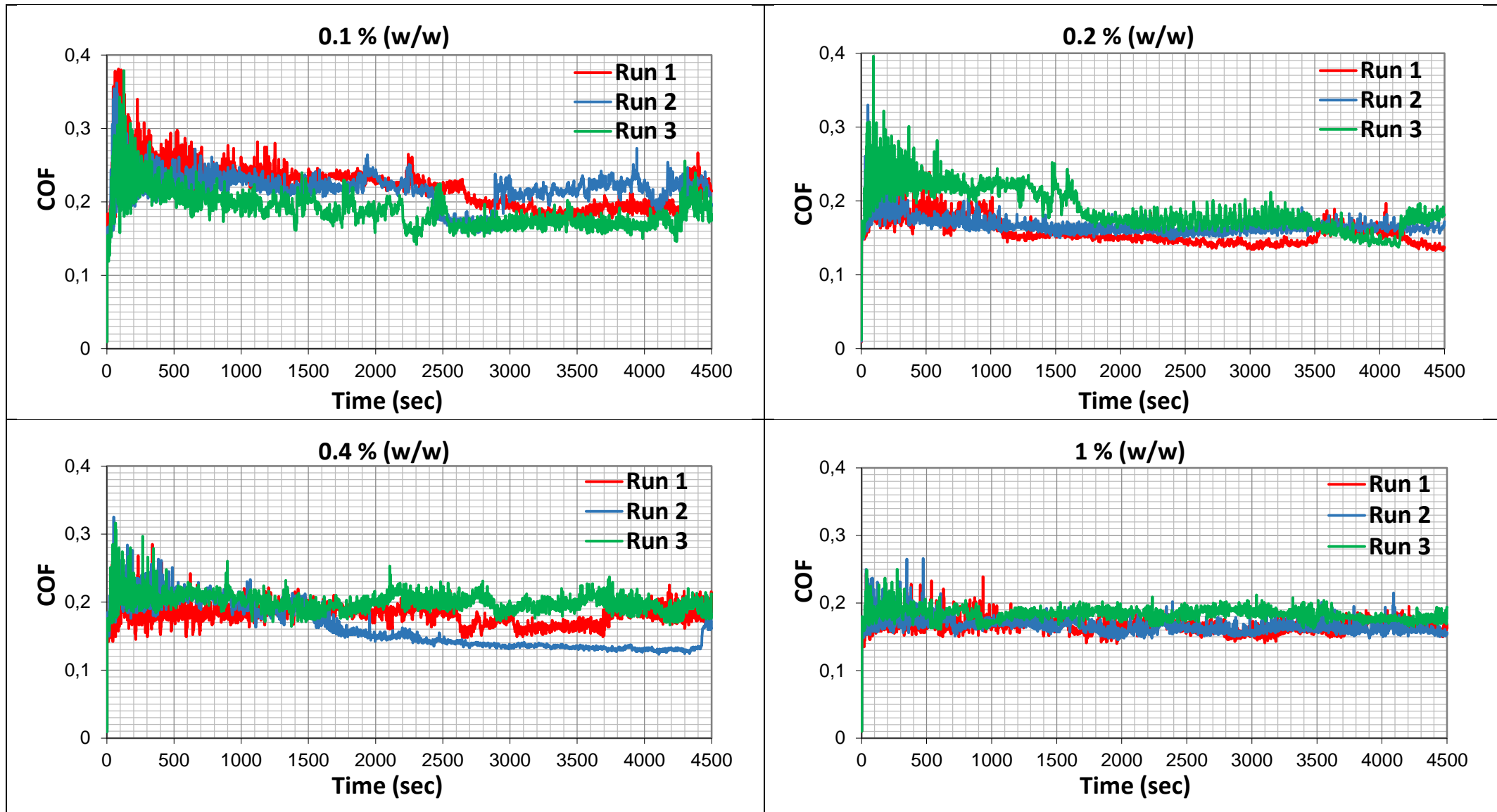


Figure 4.5: friction coefficient for diesel treated with different concentrations of canola oil.

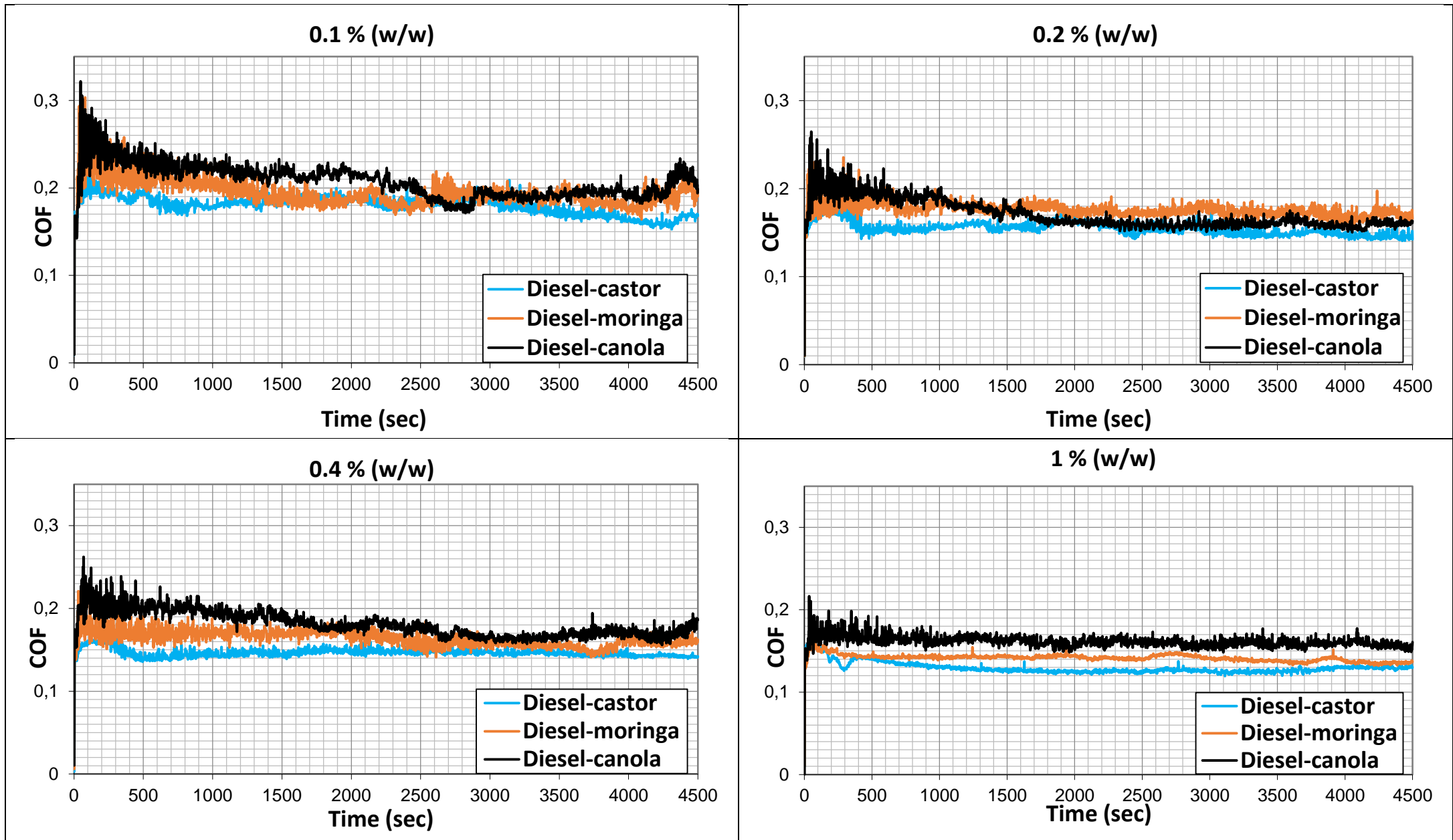


Figure 4.6: average COF over the three runs for diesel treated with castor, moringa and canola oils.

The friction coefficient for different concentrations of castor oil, moringa oil and canola oil in diesel under 200 g or 2 N load is shown in [Figure 4.6](#). As can be seen from the curves, the friction coefficient of the diesel fuel significantly decreased with the addition of castor oil, moringa oil and canola oil as lubricity enhancers (compare results in [Figure 4.6](#) with untreated diesel in [Figure 4.2](#)). The decrease in the friction coefficient of diesel containing the plant oils can be attributed to the formation of an adsorption film and/or reaction film by the oils on the sliding surfaces.

It is worth mentioning that the average friction coefficient of untreated diesel is 0.421, and at 0.2 % (w/w) it decreased by 63.35 % for castor, 58.19 % for moringa and 59.45 % for canola oil. Additionally, diesel treated with castor oil showed an excellent and stable friction coefficient compared to the other plant oils. This observation is in agreement with the work done by Quinchia *et al* (2014) on castor oil as a potential vegetable oil-based lubricant. Looking at [Figure 4.6](#) the COF curves for castor oil was the lowest among the plant oils investigated. Moringa and canola oil can only form an adsorption layer with the –COOH group in the fatty acid, whereas castor oil has an -OH group in addition to the –COOH group, thus enabling it to form stronger boundary films.

[Figure 4.6](#) further reveals that the friction coefficient decreased as the concentration of the lubricity enhancers increased. This suggests that sufficient molecules were now present in the diesel fuel that could migrate to the contact area and adhere to the steel surface to form a lubricating film that separates the sliding contacts. However, it is postulated that too much of the plant oil in the diesel will have a detrimental effect on performance because this will alter the

chemical and physical nature of the fuel (Minami, 2017). Nonetheless, the type of effect and the concentration at which this happens was not investigated.

4.1.2. Diesel lubricity model

The variation of wear scar diameter with concentrations of castor oil, moringa oil and canola oil in the diesel fuel under 200 g load is shown in [Figure 4.7](#). For each concentration the wear scar diameter was calculated by finding the average of three wear scar diameters obtained from three identical runs. The average standard deviation was 60 μm (details provided in [Appendix B](#)). Results for 0.2 % (w/w) concentration is arbitrarily chosen and provided in [Appendix C](#).

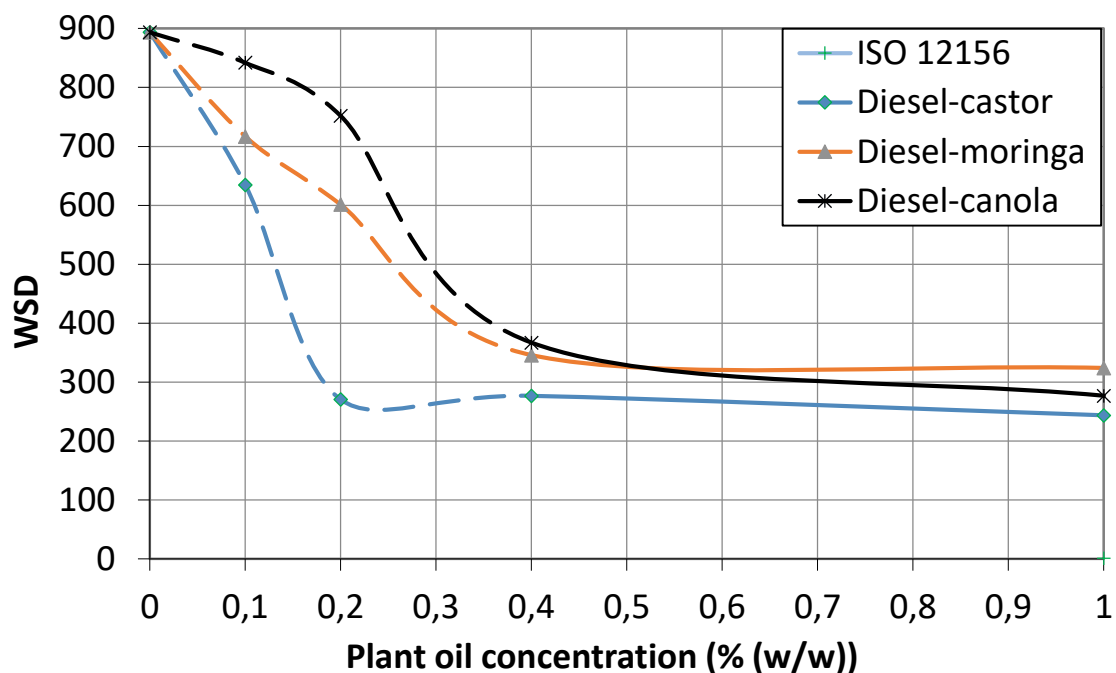


Figure 4.7: HFRR wear scar diameter reductions against diesel treated with castor oil, moringa oil and canola oil. (Test conditions: ISO 12156, 2018)

Castor oil, moringa oil and canola oil can improve the anti-wear property of diesel fuel and castor oil is the best at the same concentration. The reason for this is the presence of the hydroxyl group attached to the 12th carbon of the ricinoleic fatty acid. Agarwal *et al* (2013) makes a similar observation in his work on tribological behaviour of diesel fuels and the effect of anti-wear additives. According to Agarwal *et al* (2013) the hydroxylated fatty acid in ricinoleic acid (C18:1, OH) increases lubricity in diesel fuel more effectively than its non-hydroxylated counterpart, oleic acid (C18:1), which is the most common fatty acid in moringa and canola oil.

Fox (2007) put forward a general inverse sigmoidal model to explain the relationship between HFRR wear scar diameter reduction and fuel lubricity additive concentrations ([Figure 2.16](#)). In [Figure 4.7](#) region 'II' from Fox's model is indicated by the dashed line and region 'III' by the solid continuous line. Region 'III' of the curve in [Figure 4.7](#) includes a slight gradient, as this is more realistic for physical data. However, region 'I' of the curve was negligibly small, which shows that even the slightest amount of plant oil in diesel does cause a wear scar reduction.

Diesel-moringa oil met the 460 μm criterion (i.e. ISO 12156) at a lower concentration than diesel-canola oil according to [Figure 4.7](#) (see green dashed line). Diesel-castor oil was better with a 460 μm at only 0.13 % (w/w). At a concentration of only 0.2 % (w/w) the percentage reduction in the wear scar diameter was observed to be 69.72 %. This shows that castor oil has comparatively better lubrication than moringa and canola oil in diesel. Nonetheless, at a concentration of 1 % (w/w) moringa oil, canola oil and castor

oil in diesel the wear scar diameter was appreciably reduced. A percentage wear reduction of 62.2 %, 68.58 % and 75.34 % was observed at 1 % (w/w).

[Figure 4.8](#) shows the wear scar images at various concentrations of castor oil, moringa oil and canola oil in diesel. For each plant oil oxidative wear was observed but at different concentrations. Castor oil and moringa oil only exhibited oxidative wear at high concentrations i.e. 1 % (w/w) (indicated by white arrows). Canola oil on the other hand exhibited oxidative wear even from 0.1 % (w/w) (i.e. at low concentrations). Most likely because of high levels of polyunsaturation in canola oil. This observation is in agreement with the work done by Farahmandfar and Ramezanizadeh (2017) on oxidative stability of canola oils. In their work they suggest that the oxidation of canola oil is caused by polyunsaturation and can be retarded by the introduction of antioxidants such as *Barium bovei* (BBE) (Farahmandfar & Ramezanizadeh, 2017).

Moringa oil showed signs of high abrasive wear at low concentrations and this effect was also persistent at even higher concentrations. This suggests poor performance as a lubricity enhancer irrespective of how small the wear scar size is.

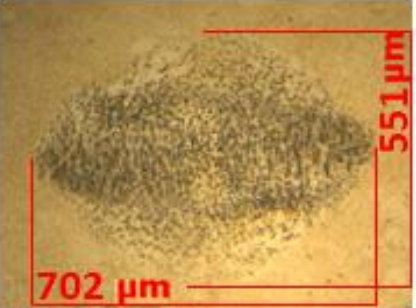
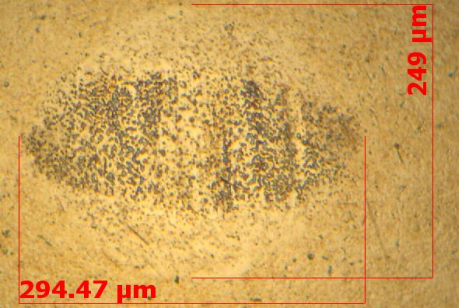
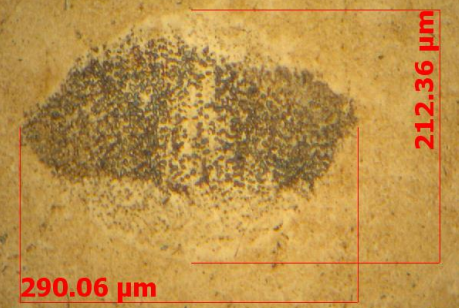
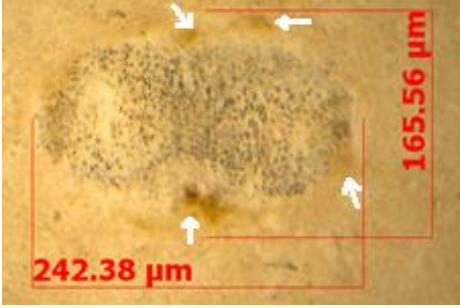
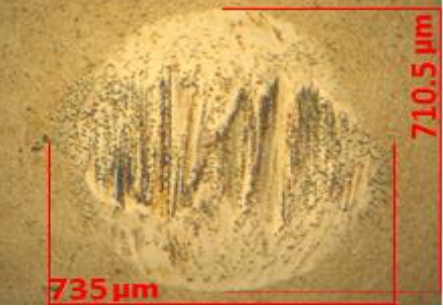
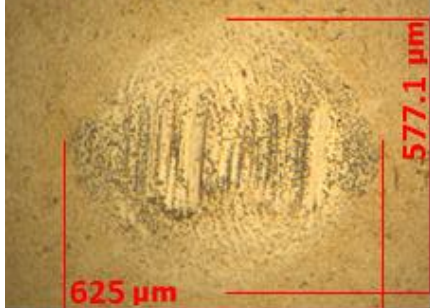
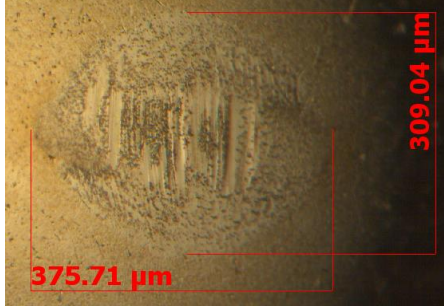
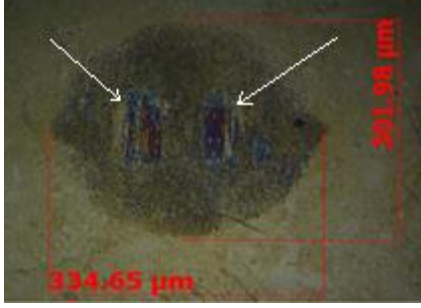
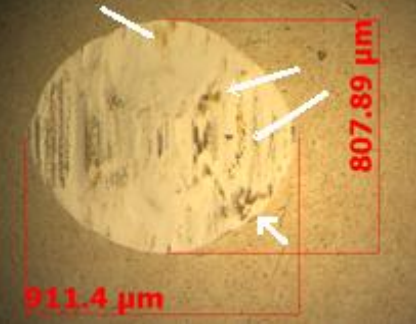
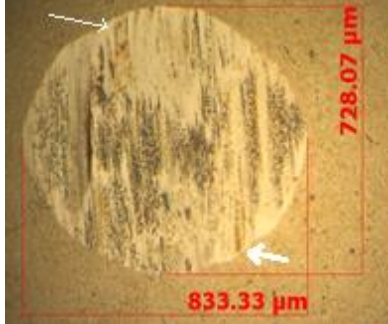
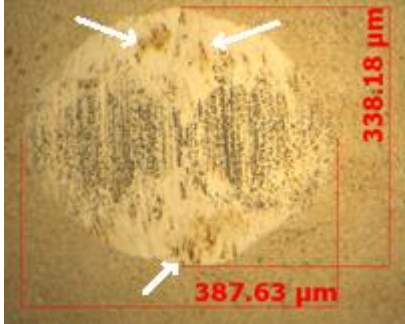
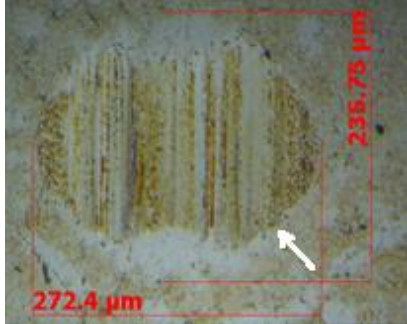
0.1 % (w/w) castor, $MWSD = 625.5 \mu\text{m}$, $WS1.4 = 615 \mu\text{m}$, $CR=3$	0.2 % (w/w) castor, $MWSD = 271.5 \mu\text{m}$, $WS1.4 = 277 \mu\text{m}$, $CR=2$	0.4 % (w/w) castor, $MWSD = 251 \mu\text{m}$, $WS1.4 = 264 \mu\text{m}$, $CR=2$	1 % (w/w) castor, $MWSD = 204 \mu\text{m}$, $WS1.4 = 214 \mu\text{m}$, $CR=2$
			
0.1 % (w/w) moringa, $MWSD = 723 \mu\text{m}$, $WS1.4 = 732$, $CR = 5$	0.2 % (w/w) moringa, $MWSD = 601 \mu\text{m}$, $WS1.4 = 597$, $CR = 4$	0.4 % (w/w) moringa, $MWSD = 342.5 \mu\text{m}$, $WS1.4 = 355$, $CR = 4$	1 % (w/w) moringa, $MWSD = 318.5 \mu\text{m}$, $WS1.4 = 327$, $CR = 3$
			
0.1 % (w/w) canola, $MWSD = 859.5 \mu\text{m}$, $WS1.4 = 864$, $CR = 4$	0.2 % (w/w) canola, $MWSD = 780.5 \mu\text{m}$, $WS1.4 = 781$, $CR = 4$	0.4 % (w/w) canola, $MWSD = 363 \mu\text{m}$, $WS1.4 = 371$, $CR = 3$	1 % (w/w) canola, $MWSD = 254.5 \mu\text{m}$, $WS1.4 = 267$, $CR = 3$
			

Figure 4.8: Wear scar photographs of diesel treated with different concentrations of plant oils

4.2. Effect of temperature on lubrication

The effects of temperature on the tribo-characteristics of diesel fuel treated with 0.5 % (w/w) of castor oil, moringa oil and canola oil are analysed and discussed. The discussion covers effects on friction coefficient and wear. Test conditions are detailed in [Table 3](#).

4.2.1. Friction coefficient

Figure 4.9 – Figure 4.11 show the COF for diesel treated with 0.5 % (w/w) castor oil, moringa oil and canola oil, respectively. The results are obtained from the HFRR tests done at 40 °C, 60 °C, 80 °C and 100 °C.

[Figure 4.12](#) is a plot of the average COF values of the three repeat runs shown in Figure 4.9 – Figure 4.11 at the given temperature. The averages were calculated from the COF values obtained every second between the three repeat runs. The average standard deviation for COF between the three experimental runs ranged from 0 to 0.01.

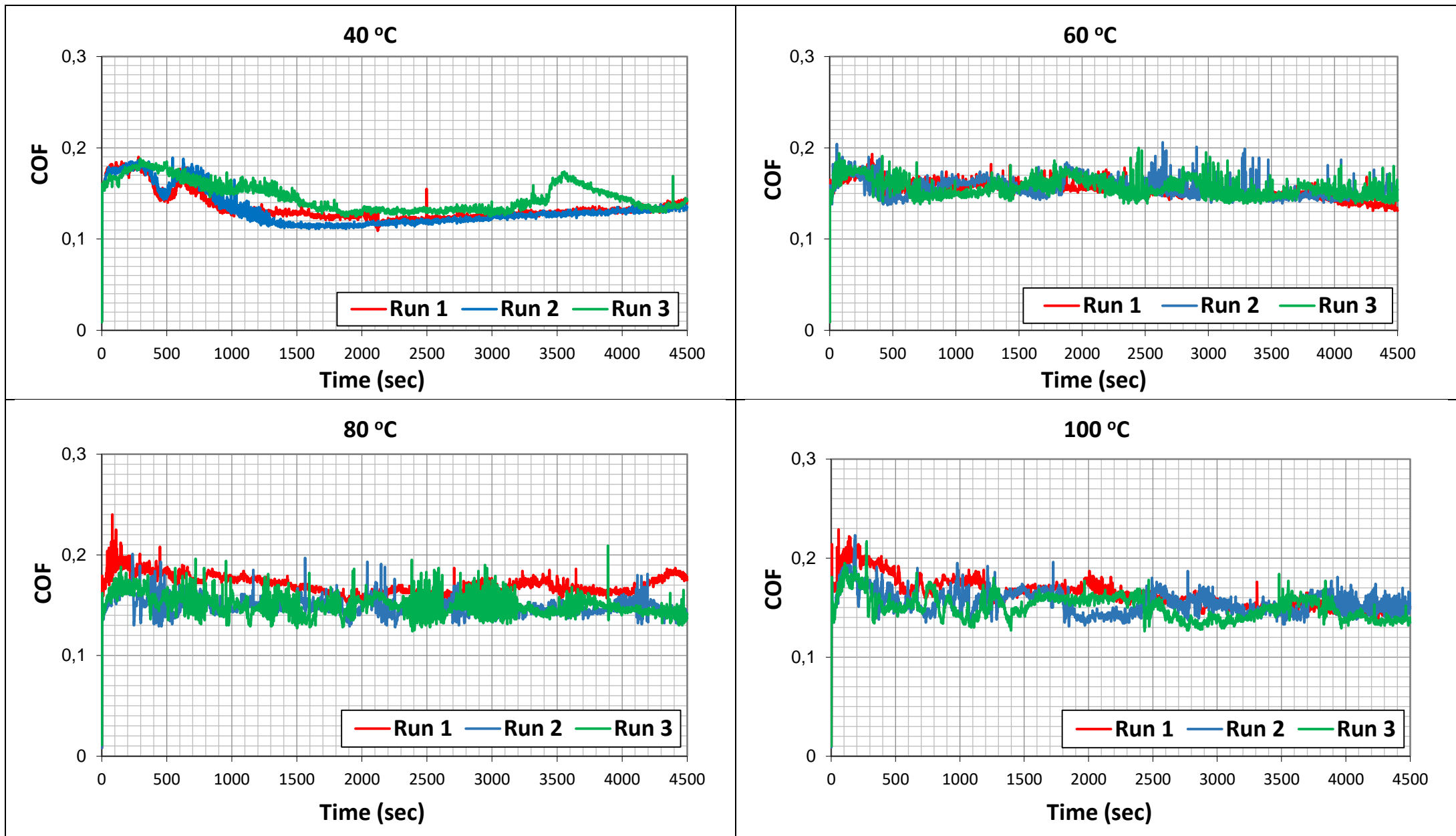


Figure 4.9: friction coefficient for diesel treated with 0.5 % (w/w) castor oil at different temperatures.

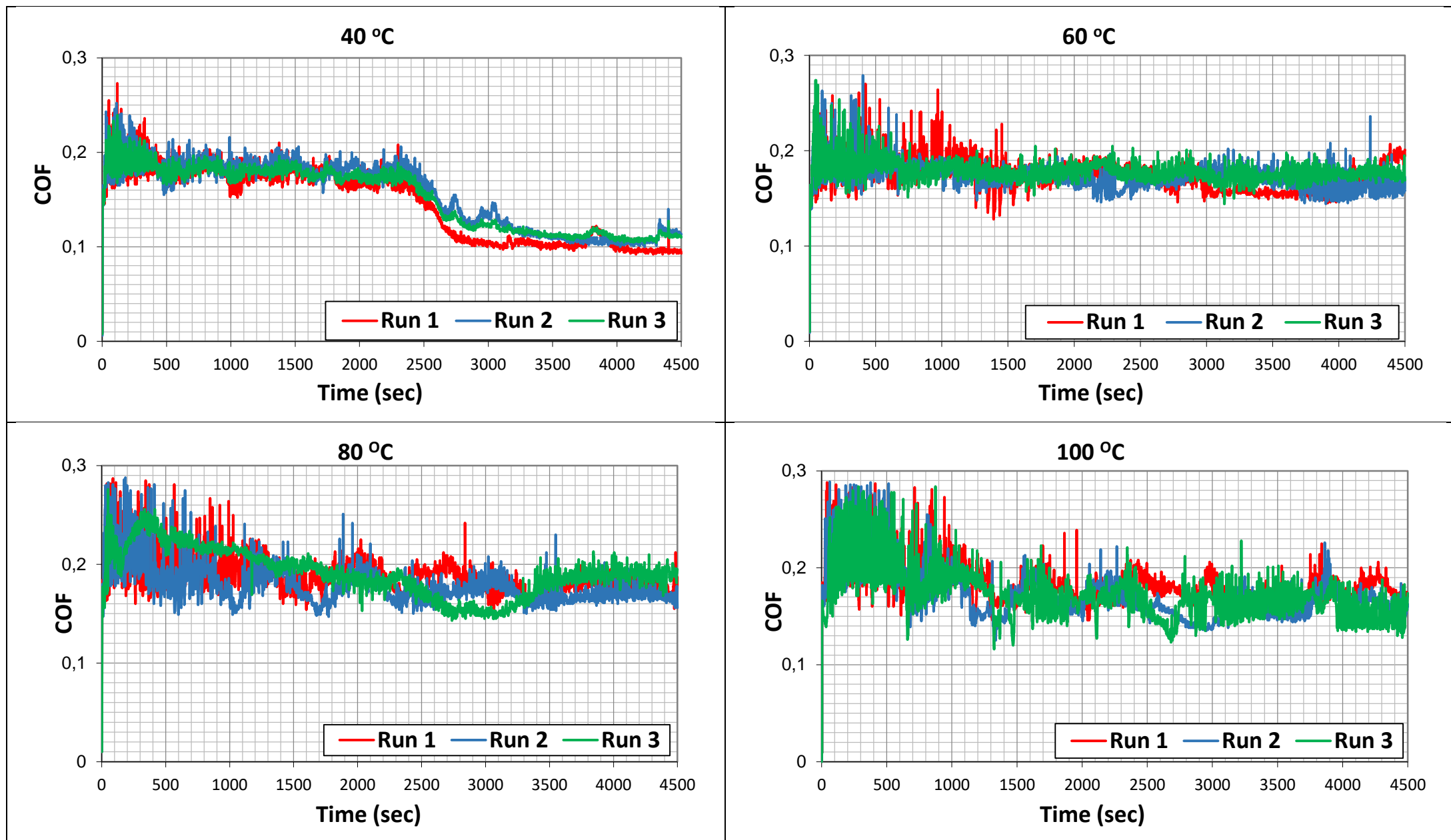


Figure 4.10: friction coefficient for diesel treated with 0.5 % (w/w) moringa oil at different temperatures.

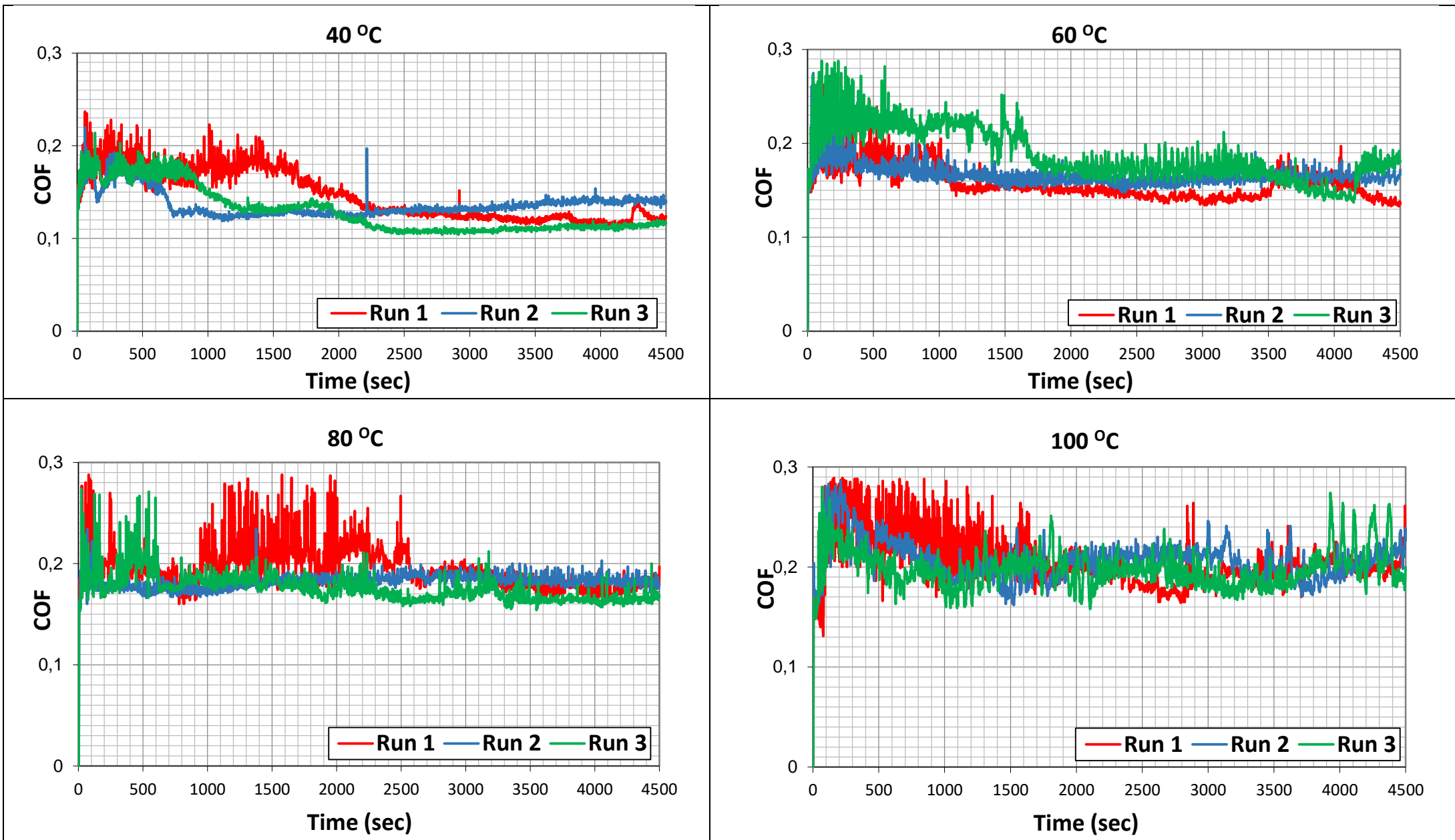


Figure 4.11: friction coefficient for diesel treated with 0.5 % (w/w) canola oil at different temperatures.

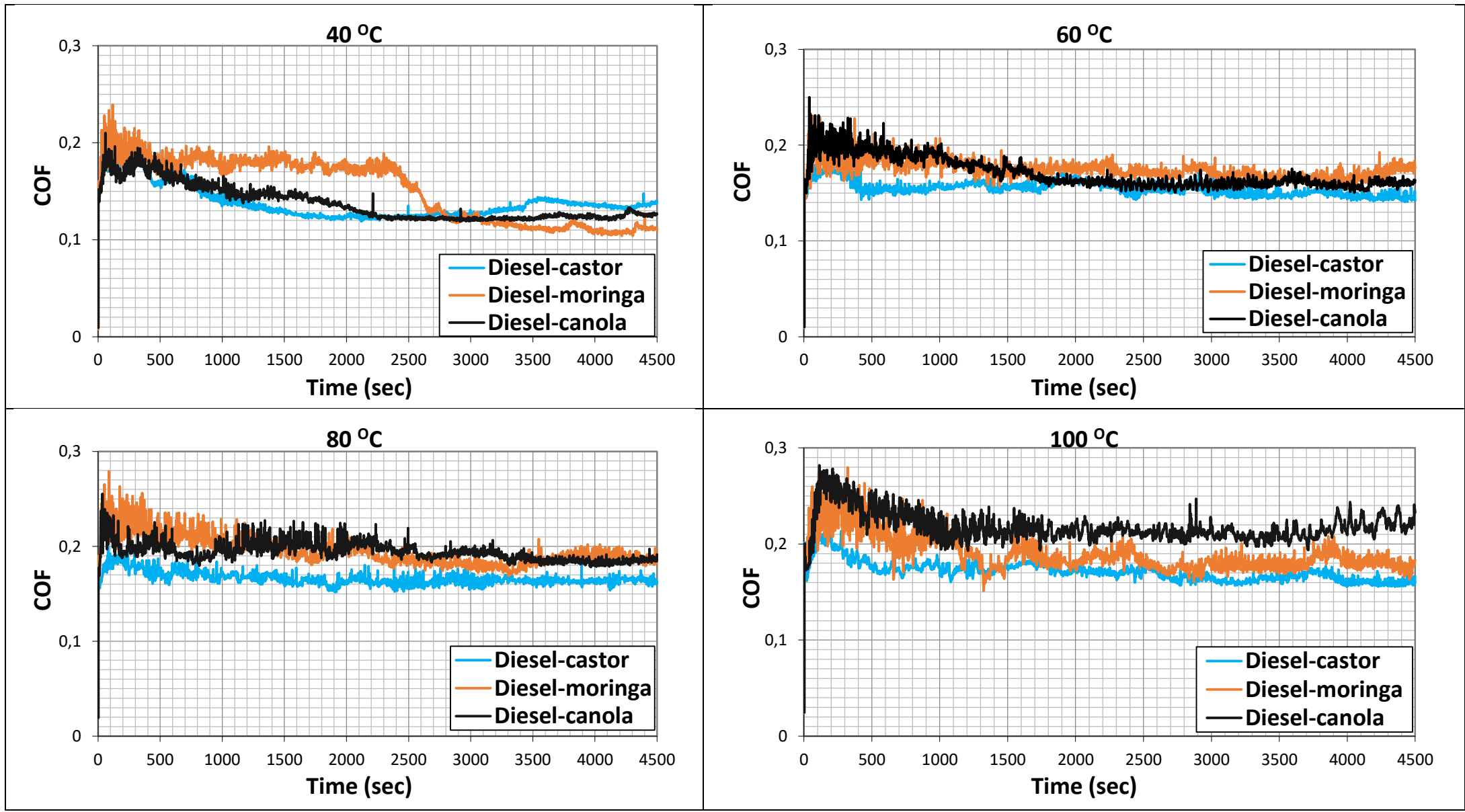


Figure 4.12: average COF over the three runs for diesel treated with castor oil, moringa oil and canola oil.

[Figure 4.12](#) shows the average friction coefficient of diesel treated with castor oil, moringa oil and canola oil. At 40 °C diesel treated with castor oil and canola oil had the lowest friction coefficient (≈ 0.138) with constant and stable behaviour over time. In contrast COF for diesel-moringa oil attained a higher steady-state boundary friction at the onset but dropped to a lower steady-state friction after 2 500 s. This behaviour is indicative of the formation of a more stable/complete surface film, promoted by tribochemical processes due to the sliding action. The plant oil molecules for moringa were able to migrate to the contact area and adhere to the steel surfaces to form a more stable film, thereby decreasing the friction coefficient as is seen from the results.

At 60 °C and 80 °C each of the plant oils in diesel showed a more constant COF behaviour with time, a fact that suggests good lubrication. Usually, if the COF fluctuates frequently over time it is a sign of bad lubrication. The friction coefficients obtained at 60 °C and 80 °C are higher than at 40 °C and those obtained at 100 °C are even higher than the preceding temperatures. This stems from the fact that plant oils suffer from a major drawback as lubricants in terms of their thermal stability (Bongfa *et al*, 2015). The monolayer lubricating film formed from the polar heads and hydrocarbon tails of the fatty acids found in plant oils deteriorates with heat. The effect worsens as temperature increases. This is because the fatty acid bonds break and become unstable, exposing the steel surfaces to direct metal – metal contact during the sliding action thereby increasing the COF.

The observed trend of increasing COF as temperature increases meets expectation if one considers the Stribeck curve closely. An increase in

temperature causes a decrease in oil viscosity ([Figure 2.24](#)). Load and speed are kept constant, as a result the Hersey number reduces in magnitude. In the boundary lubrication regime wherein the HFRR operates a decreasing Hersey number implies a rise in COF as can be seen from the results.

Another important observation in [Figure 4.12](#) is diesel-castor oil mixture showed the lowest values for friction coefficient over the tested temperature range. The wear scars obtained by HFRR (to be discussed in the next section) are consistent with the friction coefficient results seen here, with diesel-castor oil mixture having the lowest wear scar diameters of the three oils on average. The differences in performance observed at high temperatures, in both friction and wear reflect the strength of the boundary films formed by the oils on the surface. This observation is in agreement with the work done by Guo *et al* (2016) on the evaluation of lubrication performance of mixtures of castor oil and other plant oils on a high-temperature nickel based alloy. Guo *et al* explains how at high temperatures the performance of various plant oils is dependent on the strength of the formed boundary film.

The lubricating film formed by canola and moringa oil as lubricity enhancers in diesel are relatively weaker and thus less able to withstand sliding action at higher temperatures. It is most probable that the lubricating films formed by plant oils having many polyunsaturated fatty acids are weak and unstable over time and therefore less effective (Agarwal *et al*, 2013). Castor oil in diesel appears to form a much stronger film, because of its higher viscosity and polarity. The polarity creates a strong affinity to the metal at one end of the molecule (i.e. the polar end) and allows the non-polar hydrocarbon part to act as a tail projecting into the fuel. The polar end can form extra hydrogen bonds

from the hydroxyl group attached to the ricinoleic fatty acid (Agarwal *et al*, 2013). These results show that the frictional properties of castor oil, moringa oil and canola oil are largely determined by the composition of the oil. In this circumstance, the results obtained in the boundary lubrication regime show a beneficial influence of the hydroxyl group of the ricinoleic acid in the lubrication process, achieving lower and more stable friction coefficient for castor oil. Moringa and canola oil showed lower performances as lubricity enhancers because of higher levels of unsaturation in the oils.

4.2.2. Wear mechanism

[Figure 4.13](#) shows the effect of temperature on wear scar size for diesel treated with castor oil, moringa oil and canola oil. For each temperature the MWSD was calculated by performing at least three identical tests and finding the average of the three wear scar diameters. The average standard deviation was 20 μm (details provided in [Appendix B](#)).

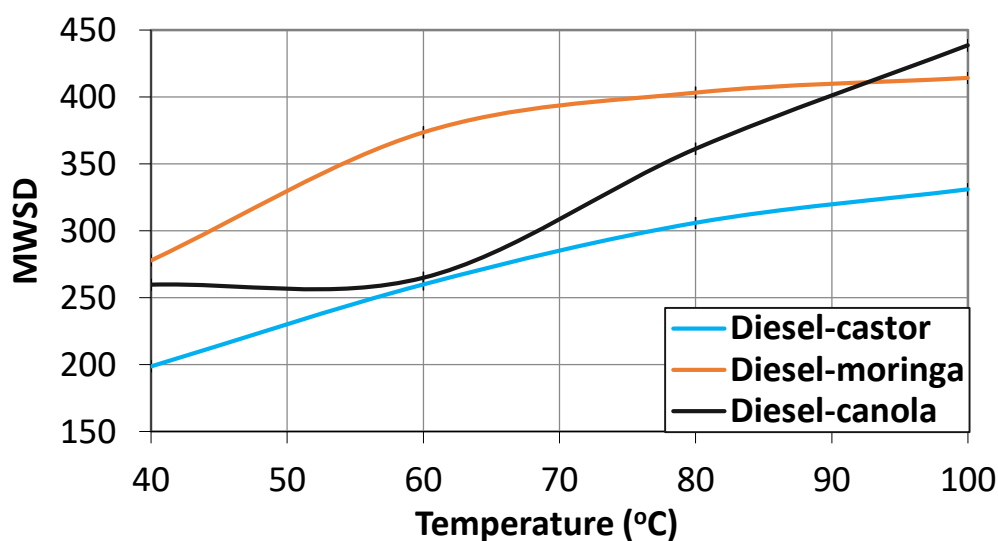
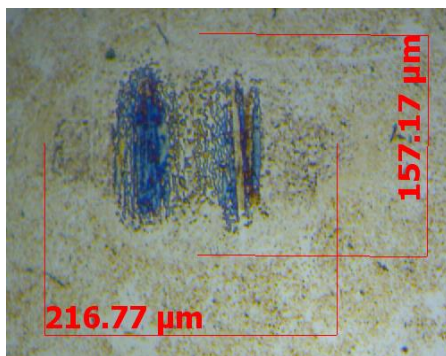


Figure 4.13: Effect of temperature on wear for diesel treated with 0.5 % (w/w) castor oil, moringa oil and canola oil.

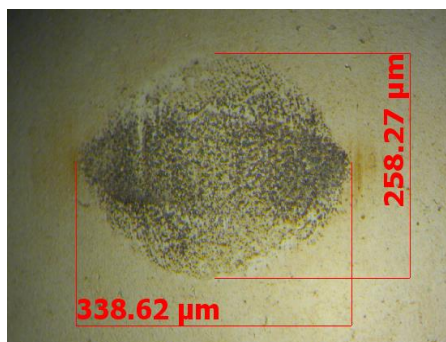
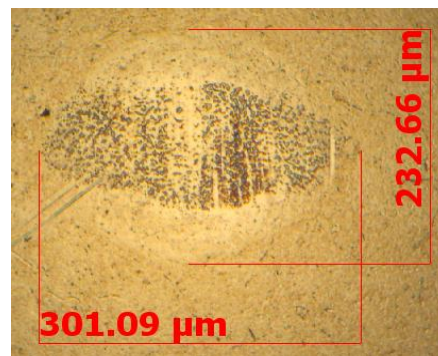
From [Figure 4.13](#) wear scar diameters for diesel treated with moringa oil, canola oil and castor oil increase with increasing temperature. This observed trend occurs because at high temperatures the formed lubricant film that is supposed to inhibit metal-metal contact deteriorates with increased temperature. As the temperature increases the viscosity of the oils decreases therefore the fatty acid molecules are less able to form a thermally stable film thus exposing the metal surfaces to direct asperity contact.

[Figure 4.14](#) shows wear scar photographs of diesel treated with 0.5 % (w/w) castor oil under varying temperature conditions. The complementary rating (CR) for each wear scar is also indicated.

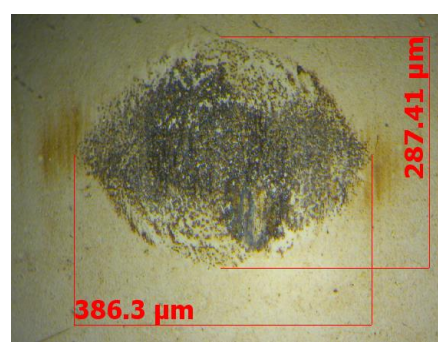
$T = 40\text{ }^{\circ}\text{C}$, $CR = 2$, $MWSD = 187.5\text{ }\mu\text{m}$



$T = 60\text{ }^{\circ}\text{C}$, $CR = 3$, $MWSD = 267\text{ }\mu\text{m}$



$T = 80\text{ }^{\circ}\text{C}$, $CR = 4$, $MWSD = 299\text{ }\mu\text{m}$



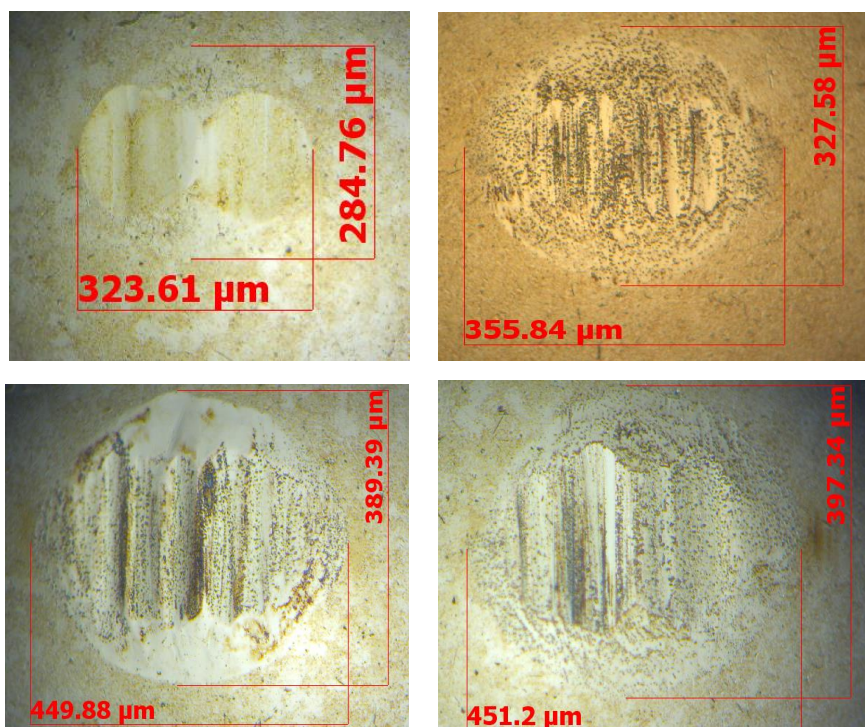
$T = 100\text{ }^{\circ}\text{C}$, $CR = 4$, $MWSD = 337\text{ }\mu\text{m}$

Figure 4.14: Effect of temperature on MWSD for diesel treated with 0.5 % (w/w) castor oil. Sliding direction is along the vertical axis.

The results obtained for castor oil in the boundary lubrication regime show a beneficial influence of the hydroxyl group (i.e. -OH) of the ricinoleic fatty acid in the lubrication process such that no severe abrasion marks are observed in [Figure 4.14](#). Even at the elevated temperature of 100 °C the *MWSD* is still below the 460 μm set by ISO 12156. Castor oil performed better as a lubricity enhancer than moringa oil.

The wear scar photographs for diesel-moringa mixture are shown in [Figure 4.15](#).

$T = 40\text{ }^{\circ}\text{C}, CR=3, MWSD = 304.5\text{ }\mu\text{m}$ $T = 60\text{ }^{\circ}\text{C}, CR=4, MWSD = 342\text{ }\mu\text{m}$



$T = 80\text{ }^{\circ}\text{C}, CR = 5, MWSD = 420\text{ }\mu\text{m}$ $T = 100\text{ }^{\circ}\text{C}, CR = 5, MWSD = 425\text{ }\mu\text{m}$

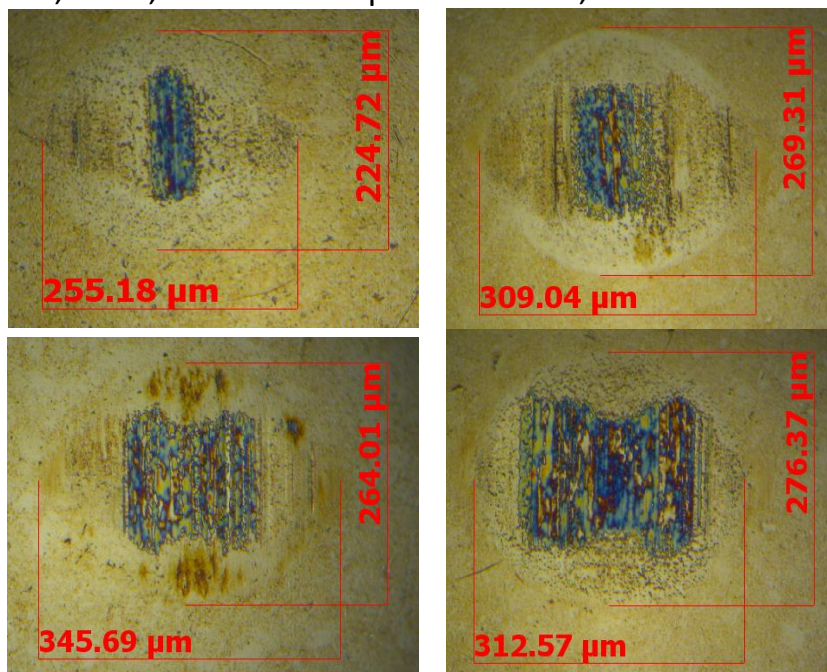
Figure 4.15: Effect of temperature on *MWSD* for diesel treated with 0.5 % (w/w) moringa oil. Sliding direction is along the vertical axis.

In [Figure 4.15](#) abrasive wear is dominant. Although little abrasion lines are observed at 40 °C, at elevated temperatures, such as 60 °C, 80 °C and 100 °C the abrasion lines become distinct parallel grooves showing severe abrasive wear. This makes a negative remark on the lubrication ability of moringa oil. Although

the wear scar sizes for diesel-moringa oil may be below 460 μm that speaks little compared to the type of wear mechanism seen in the wear photographs. This is because the wear scar diameter merely represents the “size of the contact” between the ball and disk. If there are signs of severe grooves or abrasion lines inside the wear, it generally indicates signs of bad lubrication irrespective of the wear scar size. This means a smaller wear scar size is not the only important criteria for assessing lubricant performance, the appearance of the wear scar also matters. This observation is in agreement with the work done by Oláh *et al* (2005) on micro and nano analysis of wear scar surfaces (see discussion on [Figure 3.3](#)). A *CR* of 5 suggests a heavily worn surface area and poor lubrication.

For diesel-canola oil mixture the wear scar photographs with varying temperature conditions are shown in [Figure 4.16](#).

$T = 40\text{ }^{\circ}\text{C}$, $CR=3$, $MWSD = 240\text{ }\mu\text{m}$ $T = 60\text{ }^{\circ}\text{C}$, $CR=4$, $MWSD = 289.5\text{ }\mu\text{m}$



$T = 80\text{ }^{\circ}\text{C}$, $CR=4$, $MWSD = 305\text{ }\mu\text{m}$ $T = 100\text{ }^{\circ}\text{C}$, $CR=4$, $MWSD = 295\text{ }\mu\text{m}$

Figure 4.16: Effect of varying temperature conditions on diesel fuel treated with 0.5 % (w/w) canola oil (showing oxidative wear). Sliding direction is along the vertical axis.

Oxidative wear is more dominant in diesel treated with canola oil from the wear scar photographs in [Figure 4.16](#). Oxidation occurs in the mixture because of high levels of polyunsaturation in the oil. The oil contains 29.4 % polyunsaturated fatty acids (i.e. 18.6 % linoleic containing 2 double bonds, 9.1 % linolenic containing 3 double bonds & eicosanoids) ([Table 2.4](#)). At elevated temperatures oxygen reacts with the double bonds to form peroxides. These oxide films on the metal surfaces cause the oxidative wear during the sliding action, as seen in the figure. The wear effect worsens when temperature is increased. The oxide films prevent the formation of a metallic bond between the sliding surfaces, resulting in fine wear debris and low wear rates (Bhushan, 2013: 359-360).

To summarize on wear, the observed effect of increasing temperature on diesel treated with castor oil, moringa oil and canola oil was increase in wear.

4.3. Effect of load on lubrication

The effects of load on the tribo-characteristics of diesel treated with 0.5 % (w/w) castor oil, moringa oil and canola oil are discussed in this section. The tribometer used was the HFRR.

The configuration on the HFRR is shown in [Figure 4.17](#). The applied load comprises of the test masses that are suspended on a suspension string hanging freely over the arms of the upper specimen holder. The contact load is a force exerted on the ball that pushes the ball against the disk as shown in the figure. The HFRR has a limit of 1 kg for load. For this reason, the quantity of applied loads selected for investigating the effects of load were 200 g \approx 2 N, 400 g \approx 4 N,

600 g \approx 6 N and 800 g \approx 8 N (assuming gravitational acceleration is 9.8 m/s²).
Test conditions are detailed in [Table 3](#).

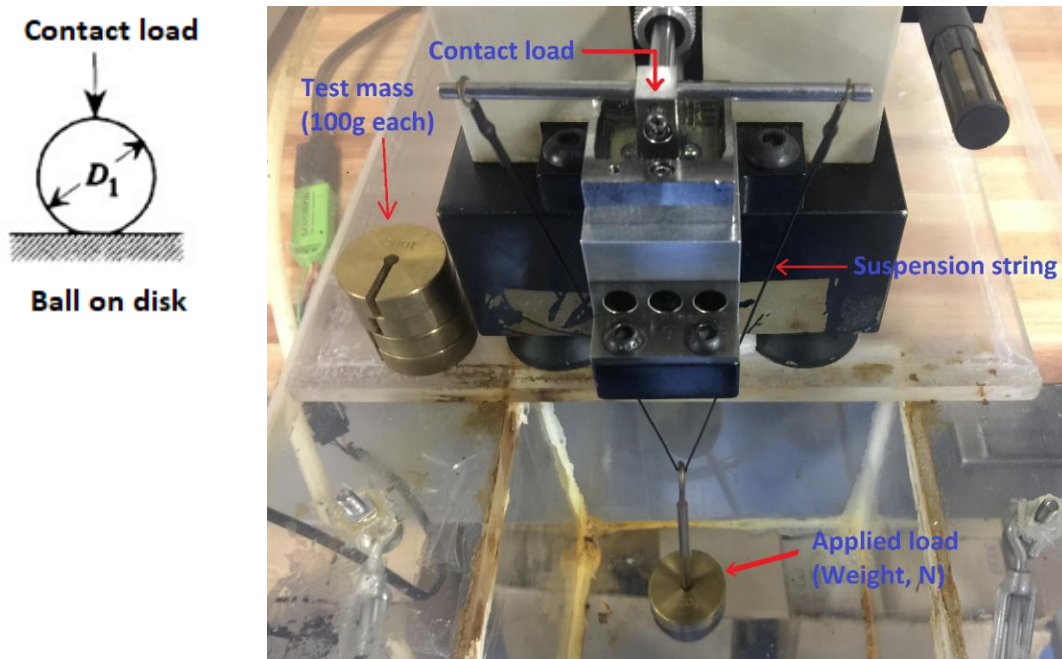


Figure 4.17: Image of the HFRR configuration and schematic view of the ball on disk configuration (PCS instruments, England).

When the selected loads are applied, the largest asperities make contact. If the load is increased, more asperities would make contact, and the contact areas of the plastically deformed asperities will increase.

4.3.1. Friction coefficient

Figure 4.19 – Figure 4.21 shows the friction coefficient for diesel treated with 0.5 % (w/w) castor, moringa and canola oil, respectively. The results are obtained from the HFRR tests done at 2 N, 4 N, 6 N and 8 N applied load. In each case the three experimental runs are shown at the given load. [Figure 4.22](#) is a plot of the average friction coefficient values of the three experimental runs shown in Figure 4.19 – Figure 4.21 at the given load. The averages were

calculated from the COF values obtained every second between the three runs. The average standard deviation for COF between the three experimental runs ranged from 0 to 0.02.

Beforehand, it is important to discuss the factors that generally influence friction coefficient behaviour regarding load. The fatty acids found in plant oils have hydrophilic heads that are polar by nature (Klein, 2017: 1200). The strong polarity of fatty acids that exist in plant oils contribute to the formation of a mono-molecular layer through the attraction of the carboxyl group (i.e. -COOH) to the metallic surfaces (Klein, 2017:1193-1199). This mono-molecular layer is expected to be one which still forces the two sliding surfaces apart to achieve "fluid bearing" conditions. Bahari *et al*, (2017) found that for most plant oils the composition of fatty acids in the oil is one of the determining factors for its COF behaviour. According to Bahari *et al*, (2017) for several plant oils investigated it was found that the friction coefficient increases with increase in level of unsaturation of fatty acids (i.e. double bonds). This indicates that a high content of unsaturated fatty acids in the plant oil denotes a high friction coefficient. Conversely, a high content of saturated fatty acids in the plant oil denotes low friction coefficient. A similar research done by Kumar *et al*, (2019) showed that stearic acid (a highly saturated fatty acid) exhibits lower friction coefficient than oleic and linoleic acid (unsaturated fatty acids). The reason for this behaviour in plant oils is explained in [Figure 4.18](#). Saturated fatty acids contain no double bonds in their chemical structure. They are only single bonds with linear chains; therefore, the molecules can easily align themselves in a straight chain formation. This means they can form an orderly stacking on the metal surface to form a protective layer which can withstand high loads (Kumar *et al*, 2019). Unsaturated fatty acids on the other hand have double bonds that produces

bends in their chemical structure, as a result fail to form an orderly stacking on the metal surface ([Figure 4.18b](#)).

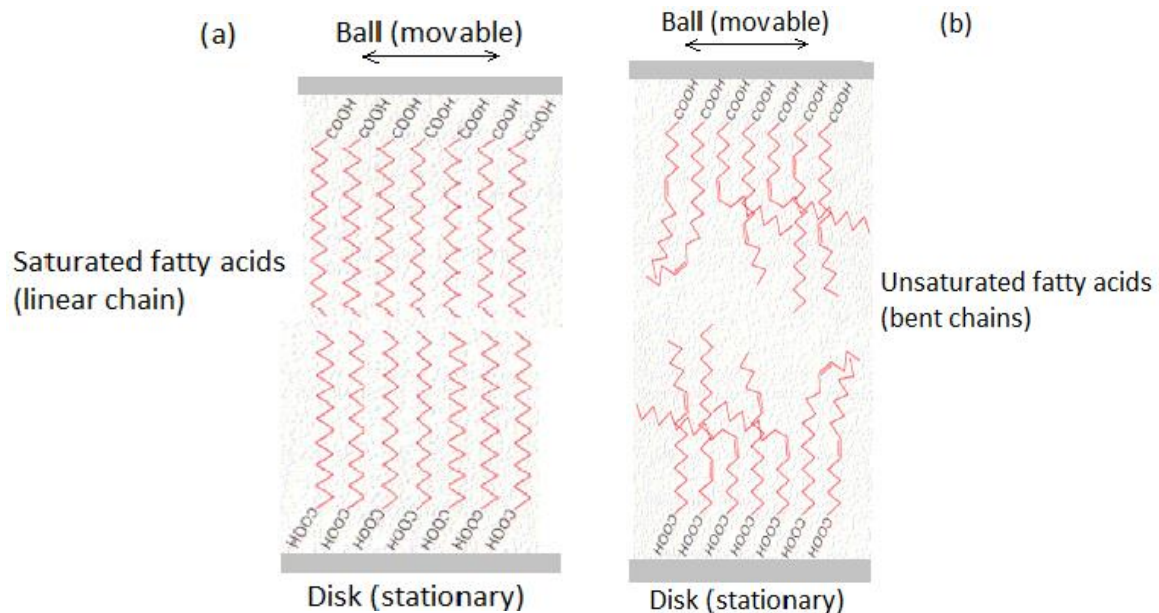


Figure 4.18: (a) Orderly stacking of saturated fatty acids results in better support for high loads. (b) Disorderly stacking of unsaturated fatty acids results in inadequate support for high loads (Bahari *et al*, 2017).

Therefore, under high loads, saturated fatty acids have a higher tendency to withstand load because of their compact nature as opposed to unsaturated fatty acids. This suggests that for plant oils, in terms of withstanding load, saturation level is especially important. Although when it comes to withstanding high temperature it may not necessarily be the case (Bahari *et al*, 2017).

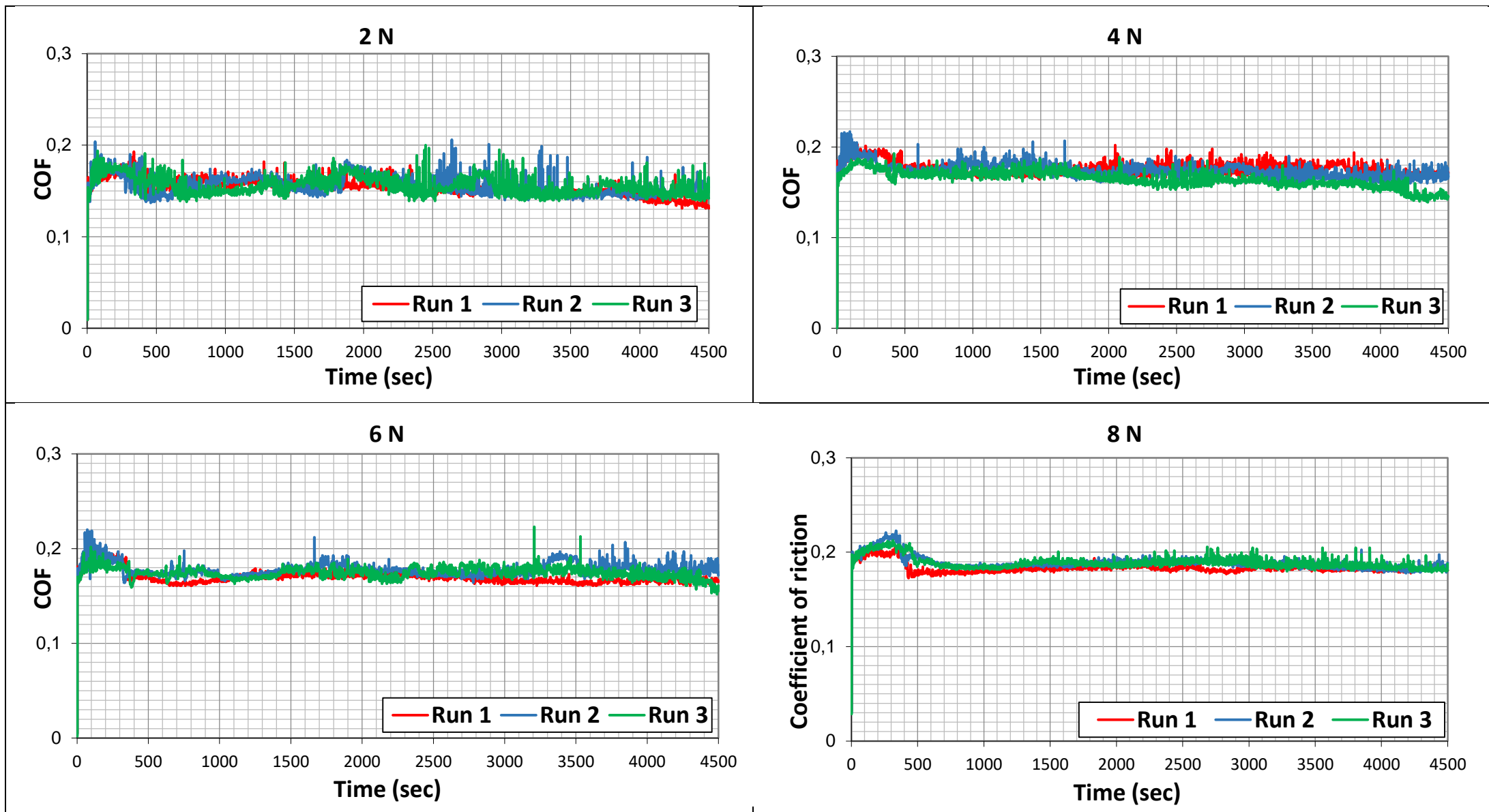


Figure 4.19: friction coefficient for diesel treated with 0.5 % (w/w) castor oil at different loads.

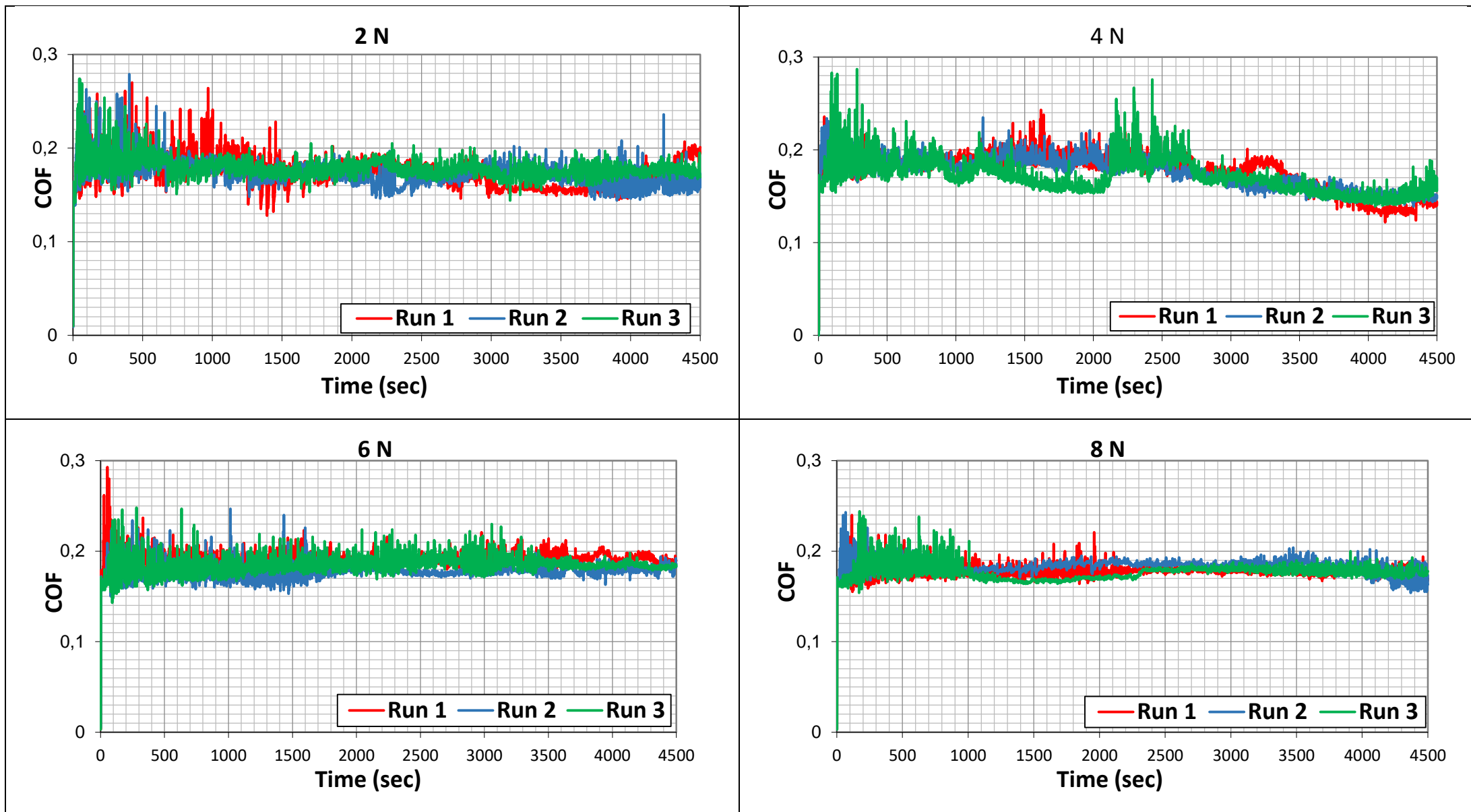


Figure 4.20: friction coefficient for diesel treated with 0.5 % (w/w) moringa oil at different loads.

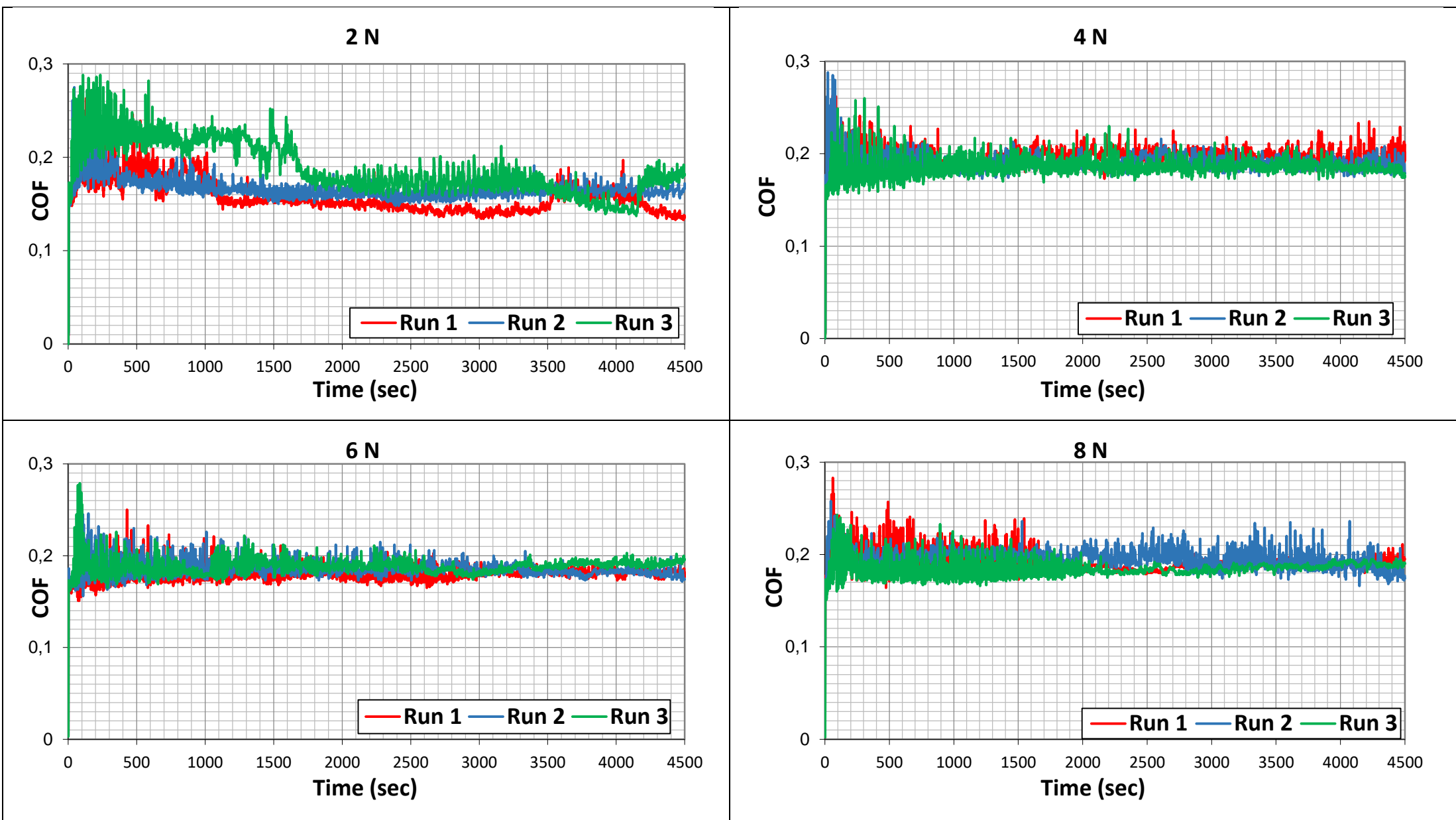


Figure 4.21: friction coefficient for diesel treated with 0.5 % (w/w) canola oil at different loads

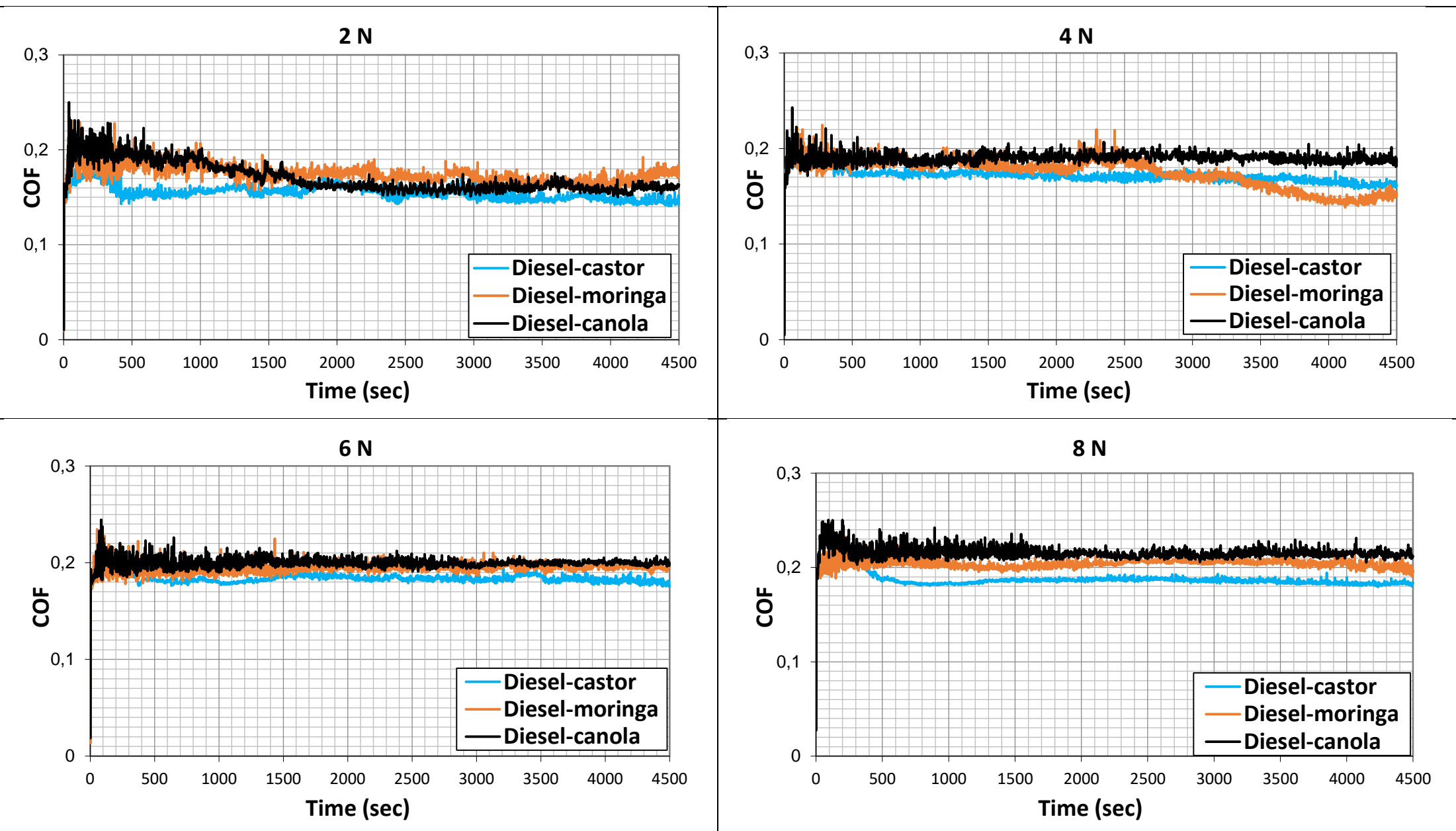


Figure 4.22: average COF over the three runs for diesel treated with castor oil, moringa oil and canola oil.

[Figure 4.22](#) shows the average friction coefficient of diesel treated with castor oil, moringa oil and canola oil. From the results, except at 2 N load diesel-canola oil mixture practically had higher friction coefficient than diesel-moringa oil for the reasons mentioned earlier ([Figure 4.18](#)). At 2 N Diesel-canola oil only performed better than diesel-moringa oil because of the formation of a physisorbed layer at lower loads. At higher loads, due to presence of polyunsaturation (i.e. highly bent fatty acid chains), diesel-canola oil begun to show poor lubrication with higher friction coefficient than diesel-moringa oil. Canola oil naturally contains 29.4 % polyunsaturated fatty acids whereas moringa oil contains only 1 % ([Table 2.4](#)). Therefore, the double bonds found in linoleic and linolenic fatty acids (i.e. highly bent chains) in canola oil contribute to the increment of the friction coefficient due to oxidation and irregularities in the stacking of the physisorbed layer at high loads.

The results in [Figure 4.22](#) further reveals that diesel-castor oil mixture showed the lowest values for friction coefficient over the tested load range. This is because unlike moringa and canola oils which contain only a $-\text{COOH}$ group, castor oil has an extra functional group (i.e. $-\text{OH}$ group) that works in its favour as a lubricity enhancer. The $-\text{COOH}$ and $-\text{OH}$ group found in castor oil enhances lubricity because of the ionic interactions of the lubricating molecules with the metal surface to form hydrogen bonding and this correlates with the fact that Debye orientation forces are considerably stronger than those based on dipole (Van der Waal's) forces (Agarwal *et al*, 2013). In plant oils different functional groups can be arranged in the order of lubricity as $-\text{COOH} > -\text{OH} > -\text{COOCH}_3 > -\text{C}=\text{O} > -\text{C}-\text{O}-\text{C}$ (Agarwal *et al*, 2013). $-\text{COOH}$ and $-\text{OH}$ are most effective because of hydrogen bonding.

Furthermore, an observed trend on [Figure 4.22](#) is that COF generally increases as load increased. This meets expectation if one considers the Stribeck curve. An increase in load while maintaining a constant speed and temperature reduces the magnitude of the Hersey number. In the boundary lubrication regime wherein the HFRR operates, a decreasing Hersey number implies a rise in COF as can be seen from the results.

4.3.2. Wear mechanism

[Figure 4.23](#) shows the effect of load on wear scar size for diesel treated with castor oil, moringa oil and canola oil. For each load, the MWSD was calculated by finding the average of three wear scar diameters obtained from three identical runs. The average standard deviation was 60 μm (details provided in [Appendix B](#)).

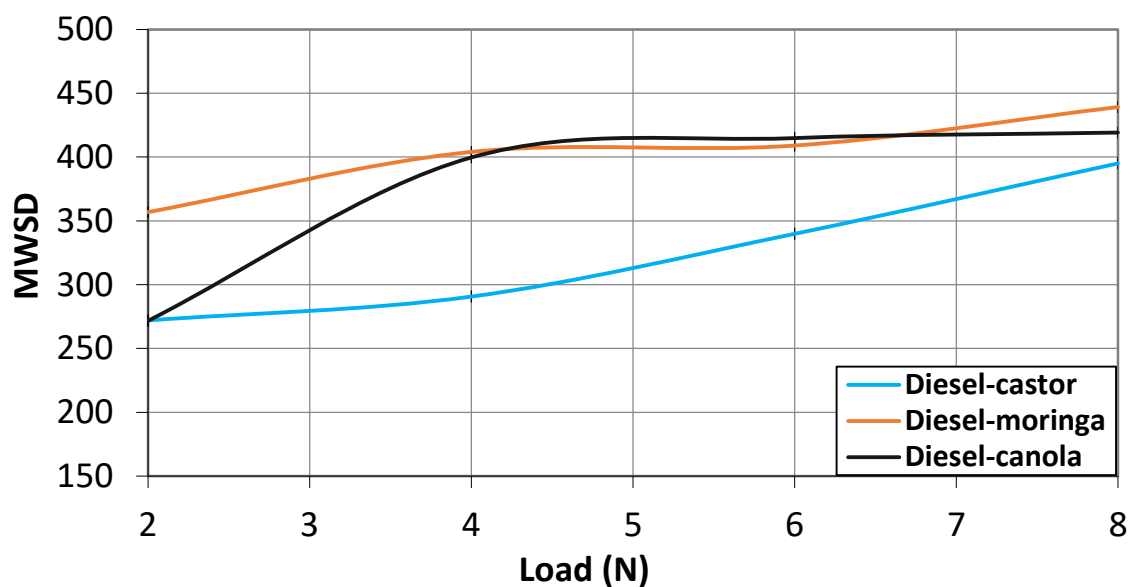


Figure 4.23: Effect of load on WSD for diesel treated with 0.5 % (w/w) castor oil, moringa oil and canola oil.

As was foreseeable, wear for diesel treated with castor oil, moringa oil and canola oil increased as load increased ([Figure 4.23](#)). The reason for this is because higher loads increase the contact pressure between the ball and disk. The increment of localized pressure causes temperature to increase thereby reducing the surface energy and this leads to the breakdown of the physisorbed layer formed by the fatty acid molecules.

[Figure 4.24](#) shows wear scar photographs of diesel treated with 0.5 % (w/w) castor oil under varying load conditions.

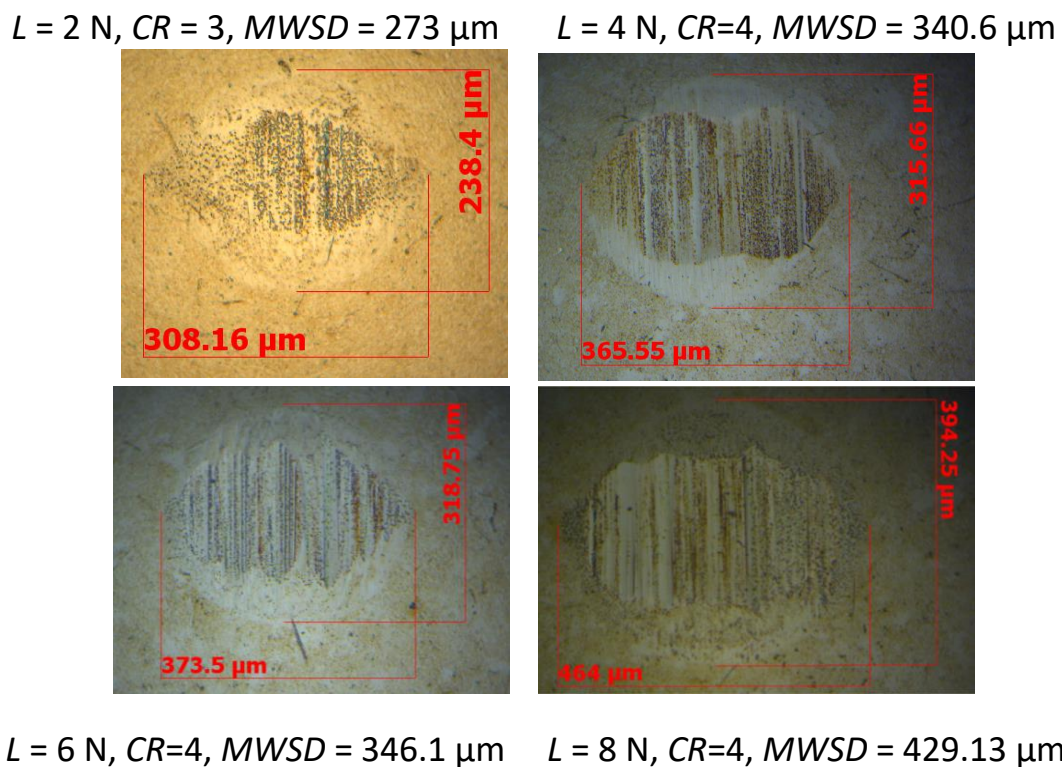


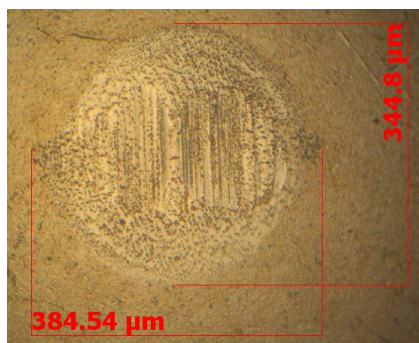
Figure 4.24: Effect of load on mean wear scar diameter for diesel treated with 0.5 % (w/w) castor oil. Sliding direction is along the vertical axis.

There are mild abrasion lines observed in the wear scar photographs. However, the abrasion lines are faint compared to those observed for moringa and canola

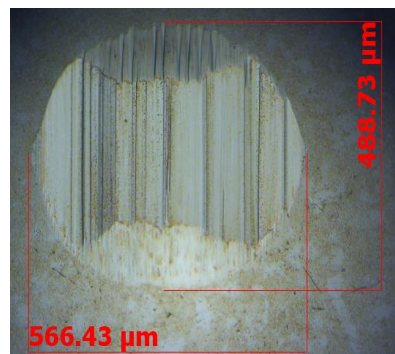
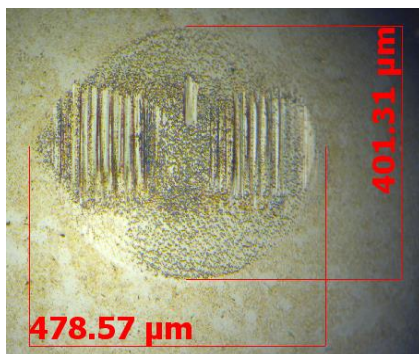
oil (to be shown later). This indicates castor oil performed better as a lubricity enhancer for diesel fuel compared to the other oils. The wear scar diameters are well below the 460 μm set by ISO 12156. This good performance reflects the strength of the boundary film formed by castor oil as a lubricity enhancer. The strong film formed by the oil is most probably assisted by its higher viscosity ([Figure 2.24](#)), higher polarity and low levels of polyunsaturation.

[Figure 4.25](#) shows wear scar photographs of diesel treated with 0.5 % (w/w) moringa oil under varying load conditions. Abrasive wear is once again dominant as was the case in temperature effect on diesel-moringa oil in [Figure 4.15](#). This signifies poor lubrication. In [Figure 4.25](#) the mild abrasion lines at 2 N load became distinct parallel grooves showing severe abrasive wear at higher loads such as 4N, 6N and 8N.

$L = 2 \text{ N}, CR=4, MWSD = 365 \mu\text{m}$



$L = 4 \text{ N}, CR=5, MWSD = 421.5 \mu\text{m}$



$L = 6 \text{ N}, CR=5, MWSD = 440.5 \mu\text{m}$

$L = 8 \text{ N}, CR=5, MWSD = 528 \mu\text{m}$

Figure 4.25: Effect of load on mean wear scar diameter for diesel treated with 0.5 % (w/w) moringa oil. Sliding direction is along the vertical axis.

As can be seen the wear effect worsens as load increases. At 8 N load the wear scar diameter surpasses the 460 μm set by ISO 12156. This suggests there were several asperity contacts during the sliding action. It is highly likely that adhesive wear led to the abrasive wear seen in the figure. Most lubricant failures in sliding metal contacts result from adhesive wear because this relates to a breakdown in the lubricant's basic function of providing some degree of separation between the sliding surfaces (Bhushan, 2013: 316). Although the WSD's may be below 460 μm a CR of 5 suggests poor lubrication because of many heavily worn areas.

[Figure 4.26](#) shows wear scar photographs of diesel treated with 0.5 % (w/w) canola oil under varying load conditions. Abrasive wear and oxidative wear are both present in the wear photographs.

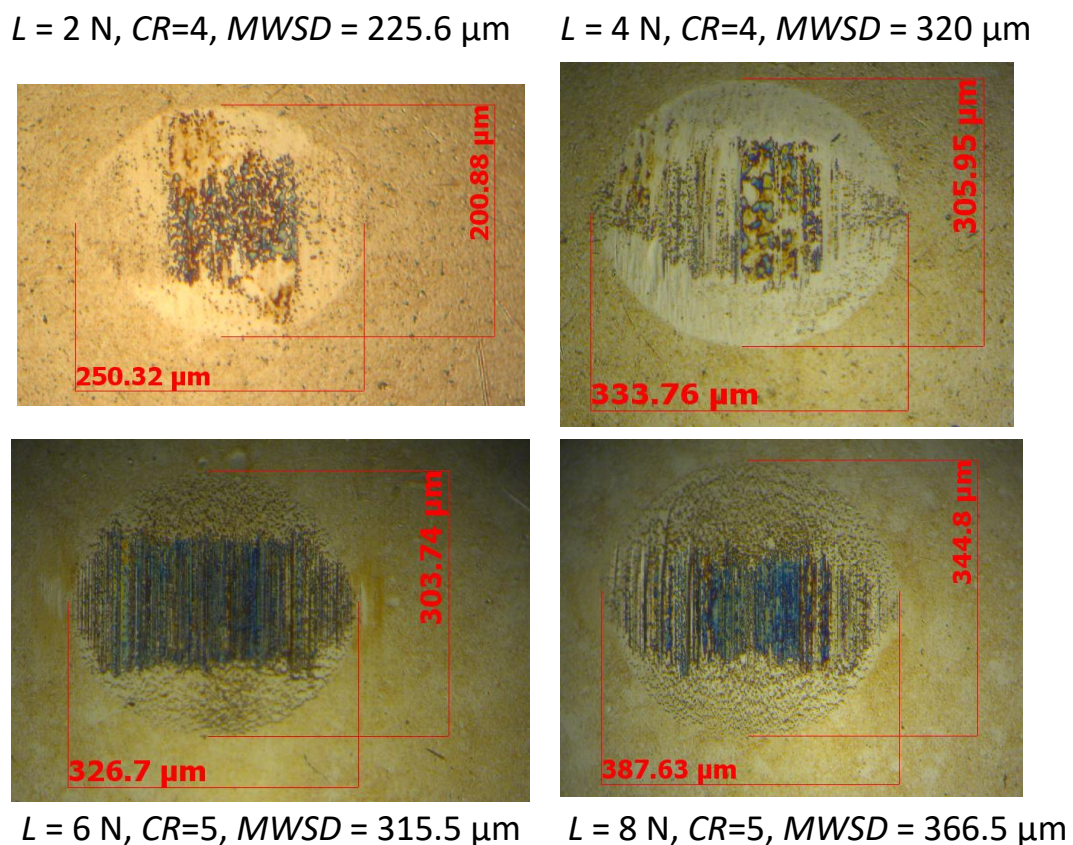


Figure 4.26: Effect of load on mean wear scar diameter for diesel treated with 0.5 % (w/w) canola oil. Sliding direction is along the vertical axis.

The lubricating film formed by the fatty acids in canola oil contain high levels of polyunsaturation (i.e. 29.4 %) and is therefore unstable due to oxidation and irregularities in the stacking at higher loads. At low loads such as 2 N, oxidative wear was dominant with almost no abrasion lines. However, as load increased the fatty acids also failed to form an orderly stacking of lubricating film between the sliding surfaces due to significant polyunsaturation (i.e. bent fatty acid chains because of double bonds). This caused abrasive wear to occur because of more direct asperity contact, (see wear scars for 6 N and 8 N load).

It is noteworthy that, the oxidation of the polyunsaturated fatty acids causes oxide films to form on the metal surface which causes the oxidative wear. These oxide films also prevent the formation of metallic bonds between the sliding metal surfaces, resulting in fine wear debris and low wear rates (Bhushan, 2013: 359-360). This means that the oxide layer in itself acts as a lubricating film which reduces the intensity of the abrasive wear. Canola oil contains 29.4 % polyunsaturated fatty acids, moringa oil 1 % and castor oil 5.7 % ([Table 2.4](#)). This explains why the intensity of the abrasive wear in diesel-canola oil is lower than diesel-moringa oil. In diesel-canola oil the presence of these oxide films that form on the metal surface because of polyunsaturation affect lubrication.

5. Conclusions and recommendations

Diesel fuel was mixed with castor oil, moringa oil and canola oil to examine the performance of these plant oils as fuel lubricity enhancers. Results for untreated diesel was adopted as a common benchmark for comparison purposes. The effects of temperature on diesel mixed with these plant oils was also examined at a temperature range of 40 °C – 120 °C. The same was done for load at a range of 2 N – 8 N. The physical properties of the fuel and the oils were also determined.

To conclude from the results realized, castor oil, moringa oil and canola oil can function as lubricity enhancers for diesel fuel. Mixing these oils with diesel can effectively reduce both friction and wear. Although, these oils have disadvantages like oxidative and thermal stability, they can be improved with addition of other specific additives. The key/significant outcome from this research work is it highlights a green approach to fuel lubrication. If we are to limit pollution from lubricants and hydraulic fluids based on mineral oils then these environmentally friendly and renewable plant oils are potential substitutes for petroleum-based oils.

5.1. Physical properties

Given the results from the experimental tests the following conclusions were made:

5.1.1. Molecular structure

The results obtained demonstrate that the frictional properties of different plant oils are largely determined by the chemical composition and molecular structure. In this sense, the results obtained in the boundary lubrication regime show a beneficial influence of the hydroxyl group of the ricinoleic acid in the lubrication process, achieving more stable lubricating conditions for castor oil in diesel. This hydroxyl functional group is responsible for the intermolecular interactions favouring the high viscosity of castor oil and gives the polar character to the oil.

5.1.2. Viscosity

1. Dynamic viscosity of castor oil, moringa oil, canola oil and diesel fuel decrease with increase in temperature.
2. Viscosity of plant oils have a significant effect on their performance as lubricity enhancers. Higher viscosity played an active role in the lubrication process. As a result, castor oil which possesses a higher viscosity attained a superior lubrication performance compared to the other plant oils in this study.

5.1.3. Viscosity index (VI)

1. In terms of viscosity index, the observed trend is as follows: canola oil > moringa oil > castor oil. Canola oil has the highest viscosity index among the three plant oils and consequently possesses the best viscosity-temperature relation.

2. To ensure better viscosity-temperature performance of castor oil, moringa oil and canola oil with diesel it is essential to operate at higher temperatures. Because under low temperatures the drop in fluid viscosity is steep and fast whereas at high temperatures the viscosity change is moderate.

5.1.4. Density

1. In terms of density the observed trend is as follows: castor oil>canola oil> moringa oil.

5.2. Effect of temperature on lubrication

Given the results from the experimental tests the following conclusions were made:

5.2.1. Friction coefficient

1. At low temperatures, the diesel-plant oil mixtures have low COF. However, as temperature increases the friction coefficient increases. This is because at high temperature, the lubricant film formed by fatty acids tends to be less stable and breaks down more easily.
2. In terms of temperature the trend for friction coefficient for diesel-plant oil mixture is as follows: canola oil>moringa oil>castor oil.

5.2.2. Wear mechanism

1. Canola oil is most affected by temperature with an increase in oxidative wear as temperature increases.
2. Increase in temperature generally causes increase in wear.
3. In terms of temperature the trend for wear scar diameter for the diesel-plant oil mixture on average is as follows: moringa oil>canola oil> castor oil.

5.3. Effect of load on lubrication

Given the results from the experimental tests the following conclusions were made:

5.3.1. Friction coefficient

1. With increase in the load the friction coefficient and wear scar diameters for diesel treated with castor oil, moringa oil and canola oil generally increase. Most affected are plant oils with high contents of unsaturated fatty acids.
2. In terms of load the trend for friction coefficient for diesel-plant oil mixture is as follows: canola oil>moringa oil>castor oil.

5.3.2. Wear mechanism

1. Wear scar diameter of the diesel-plant oil mixture increased with increase in load.

2. In terms of load the trend for wear scar diameter for diesel-plant oil mixture on average is as follows: canola oil>moringa oil>castor oil.
3. Moringa oil showed signs of severe abrasive wear, which suggests poor performance as a diesel lubricity enhancer.

5.4. Effect of plant oil concentration on lubrication

Given the results from the experimental tests the following conclusions were made:

5.4.1. Friction coefficient

1. Castor oil, moringa oil and canola oil can function as lubricity enhancers for diesel. Mixing these plant oils with diesel can effectively reduce both the friction coefficient and the wear of the tribo-contact surfaces. Nonetheless, plant oils suffer from major drawbacks such as oxidative and thermal stability, but these properties can be improved with addition of other specific additives.
2. Friction coefficient for diesel-plant oil mixtures decreases as concentration of plant oil increases.
3. In comparison to moringa oil and canola oil, castor oil has stronger boundary film-forming properties. The oil performs well in boundary friction and has strong anti-wear properties. Castor oil's improved lubricity is due to its hydroxyl functional group, which increases the viscosity and polarity of the oil. In terms of concentration the trend for friction coefficient for diesel-plant oil mixture is as follows: canola oil>moringa oil>castor oil.

5.4.2. Wear mechanism

Among the three plant oils investigated moringa oil appears less efficient as a lubricity enhancer because despite the wear scar diameters being below 460 μm the wear scar images show signs of severe grooves of abrasion lines for all different working conditions investigated. Castor oil on the other hand performed best of the three plant oils. The trend for lubricity enhancing ability for the three plant oils is as follows: castor oil > canola oil > moringa oil.

From these results the following recommendations are made for further research and study:

The HFRR has a maximum load capacity of 1 000 g (i.e. 10 N) therefore research work on load effects could only be done up to 10 N. For this reason it is recommended that research into lubrication performance of castor oil, moringa oil and canola oil as lubricity enhancers for diesel under extreme load conditions be carried out.

6. References

Agarwal, S, Chhibber, V and Bhatnagar, A (2013) "Tribological behaviour of diesel fuels and the effect of anti-wear additives", *Fuel*, 106(10), 21-29.

Ahmed, M, Jana, P, Taufiq, A, Liaquat, M, Farid, A and Jahangir, J (2016) "Oxidation of lipids in foods", *Sarhad Journal of Agriculture*, 32(3), 230-235.

Anton Paar (2011) *Instruction manual: SVM 3000/G2*, Stabinger viscometer, Anton Paar GmbH, Austria.

Arakeri, JH and Sreenivas, KR (1996) "Hydrodynamic lubrication", *Resonance*, 51-58.

Asadauskas, S, Perez, J, Duda, L (1997) "Lubrication properties of castor oil potential base stock for biodegradable lubricants", *Society of Tribologists and Lubrication Engineering*, 53(12), 35-40.

ASTM D2270 (1998) "Standard practice for calculating viscosity index from kinematic viscosity at 40°C and 100 °C", ASTM Int.

ASTM D6079 (2005) "Standard Test Method for Evaluating Lubricity of Diesel Fuels by the High-Frequency Reciprocating Rig (HFRR)", ASTM Int.

ASTM D6217 (1998) "Standard Test Method for Particulate contamination in Middle Distillate Fuels by Laboratory Filtration", ASTM Int.

ASTM D7042 (2011) “Standard Test Method for Dynamic Viscosity and Density of Liquids by Stabinger Viscometer (and the Calculation of Kinematic Viscosity)”, ASTM Int.

Bahari, A, Lewis, R and Slatter, T (2017) “Friction and wear response of vegetable oils and their blends with mineral engine oil in a reciprocating sliding contact at severe contact conditions”, *Journal of Engineering Tribology*, 232(3), 244-258.

Barnes, A (2017) “Canola Council of Canada”, <https://www.canolacouncil.org/media/image-gallery/seed,-oil-meal/> [2019, May 05].

Bhushan, B (2013) *Introduction to Tribology*, 2nd edition, John Wiley & Sons, New York.

Bongfa, B, Atabor, P, Barnabas, A and Adeoti, M (2015) “Comparison of lubricant properties of castor oil and commercial engine oil”, *Jurnal Tribologi*, 5, 1-11.

Davenport, J (1996) “Development and verification of the HFRR test for automotive diesel fuels”, Shell Research Ltd, Chester, UK.

Debnath S, Reddy M and Yi Q (2014) “Environmental friendly cutting fluids and cooling techniques in machining: A Review”, *Journal of Cleaner Production*, 1-38.

Dehaghani, A and Rahimi, R (2018) “An experimental study of diesel fuel cloud and pour point reduction using different additives”, *Petroleum*, 1-4.

Farahmandfar, R and Ramezanizadeh MH (2017) "Oxidative stability of canola oil", *Wiley*, 6, 342 - 347.

Fox, M (2007) "A model for diesel fuel additive lubricity", *Journal of Engineering Tribology*, 221, 161 – 164.

Guo, S, Li, S, Zhang, Y, Wang, Y, Li, B, Yang, M, Zhang, X, Liu, G (2016) "Experimental evaluation of the lubrication performance of mixtures of castor oil with other vegetable oils in MQL grinding of nickel-based alloy", *Journal of Clear Production*, 140, 1060-1076.

Herbst, M (2015), "Fact sheet on canola oil", <https://cansa.org.za/files/2021/02/Fact-Sheet-on-Canola-Oil-February-2021.pdf>. [2021-07-11].

Hironaka, S (1984) "Boundary lubrication and lubricants", *Three bond technical news*, 9, 1-8.

Hultema E, Schwletert D, Mandel J, Nagatsuka S (2019), "Worldwide fuel charter", <https://www.acea.auto/publication/worldwide-fuel-charter-2019-gasoline-and-diesel-fuel/> [2021-07-09].

ISO 12156 (2018) "Diesel fuel – Assessment of lubricity using the high-frequency reciprocating rig (HFRR) – Part 1: Test method", ISO.

IUPAC (2016) *Compendium of Chemical Terminology*, 2nd edition, Gold book, New York.

Janes, A and Chaineaux, J (2013) "Experimental determination of flash point of flammable liquid aqueous solutions", *Chemical Engineering Transactions*, 31, 943-948.

Jechura, J (2018) "Crude oil distillation", Colorado School of Mines, Colorado, United States.

Kajal (2019), "Benefits of moringa seeds for health, skin and hair", <https://www.stylecraze.com/articles/benefits-of-moringa-seeds-for-skin-hair-and-health/> [2019, May 09].

Klein, D (2017) *Organic Chemistry*, 3rd edition, Wiley, New York.

Knothe, G and Steidley, K (2005) "Lubricity of components of biodiesel and petrodiesel. The origin of biodiesel lubricity", *Energy & Fuels*, 19(3), 1192-1200.

Kotz, J, Treichel, P, Townsend, J and Treichel, D (2015) *Chemistry and chemical reactivity*, 9th edition, CENGAGE learning, New York.

Kumar, V, Wani, M, Mannekote, J and Kailas, S (2019) "Tribological properties of some fatty acids", *Journal of Physics*, 1-9.

Langenhoven, J (2014) *The effects of humidity and soluble water content on the lubricity testing of a N-Hexadecane and palmitic acid test liquids*, MEng Dissertation, University of Pretoria, South Africa.

Laurent, A (2010) “Botany blueprint: the castor bean”, <https://www.printmag.com/design-inspiration/botany-blueprint-the-castor-bean/> [2019, May 05].

LePera, M (2000) “Low sulfur and diesel fuel lubricity”, *LePera and Associates*, 1-2.

Minami, I (2017) “Molecular science of lubricant additives”, *Applied Sciences*, 7(17), 445-478.

Mosarof, M, Kalam, M, Masjuki, H and Ashraful, A (2016) “Evaluation of lubricating performance of biodegradable moringa oleifera oil”, *Modern Environmental Science and Engineering*, 2(8), 530-536.

Oláh, Z.S, Szirmai, L, Resofszki, G; *Micro and macro analyses of wear scar surfaces – A complementary rating method to the evaluation of HFRR test results*; International Colloquium on Fuels, Technische Akademie Esslingen (TAE), Ostfildern, 12 – 13 January, 2005.

Patel, V, Dumancas, G, Viswanath, L, Maples, R and Subong, BJ (2016) “Castor oil: properties, uses, and optimization of processing parameters in commercial production”, *Lipid Insights*, 9, 1–12.

PCS Instruments (2005) HFRR installation and test preparation manual, Hardware Version 1.

Quinchia, L, Delgado, M, Reddyhoff, T, Gallegos, C and Spikes H (2014) “Tribological studies of potential vegetable oil-based lubricants containing

environmentally friendly viscosity modifiers”, *Tribology International*, 69, 110-117.

Reedijk, J and Poepelmeier, K (2013) *Comprehensive Inorganic Chemistry II: From Elements to Applications*, 2nd edition, Elsevier Science, New York.

Rothbart, H and Brown, T (2006) *Mechanical Design Handbook*, 2nd edition, McGraw Hill Education, New York.

Rustan, A and Drevon, C (2005) “Fatty acids: Structures and Properties”, *John Wiley & Sons*, 1-7.

SANS 342 (2016), “Automotive fuels-Requirements and test methods for diesel”, SABS.

Schaschke, C (2014) *A dictionary of chemical engineering*, 1st edition, Oxford University Press, United Kingdom.

Stachowiak, G (2017) “How tribology has been helping us to advance and to survive “, *Friction*, 5(3), 233-247.

Stachowiak, G and Batchelor, A (2006) *Engineering Tribology*, 3rd Edition, Elsevier Butterworth-Heinemann, USA.

Stolten, D and Emonts, B (2016) *Hydrogen science and engineering: materials, processes, systems and technology*, 1st edition, Wiley, USA.

Surawski, N, Van, T, Ristovski, Z and Cong, N (2017) “Effect of sulphur and vanadium contents in diesel fuel on engine performance and emissions: principal component analysis”, paper presented at *The 11th Asia-Pacific Conference on Combustion*, 10 -14 December, 2017, Sydney, Australia.

Ultrasonic cleaners made in China (2017), “Jeken ultrasonic cleaner limited”, <http://www.ultrasoniccleaners.en.made-in-china.com> [2019, March 25].

Welty, J, Wicks, C and Forster, D (2014) *Fundamentals of momentum, heat, and mass transfer*, 6th edition, Wiley, New York.

Zhang, X, Zhao,Y, Kai, M and Wang Q (2016) “Friction behavior and wear protection ability of selected base lubricants”, *Friction*, 4(1), 72-83.

Appendix A - Humidity control

Figure A1 shows the mechanism of the humidifier in controlling the humidity inside the environmental chamber of the HFRR. In the setup compressed air flows through the particle trap and moisture trap wherein a particulate filter separates moisture and/or particles from the compressed air. This ensures that the compressed air that enters the dry and wet columns are clean. The wet column contains distilled water and the dry column, inert silica granules at 120 - 160 kPa.

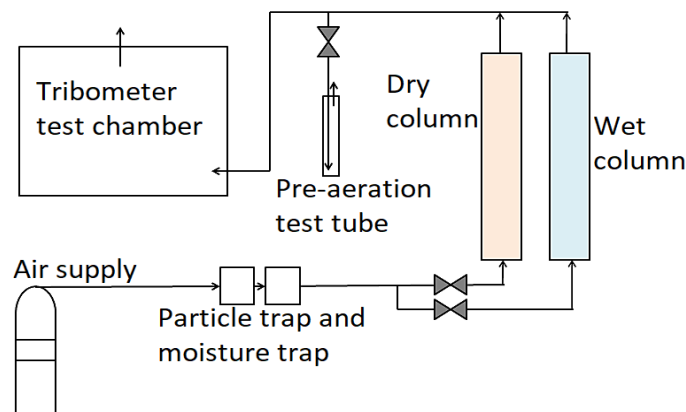
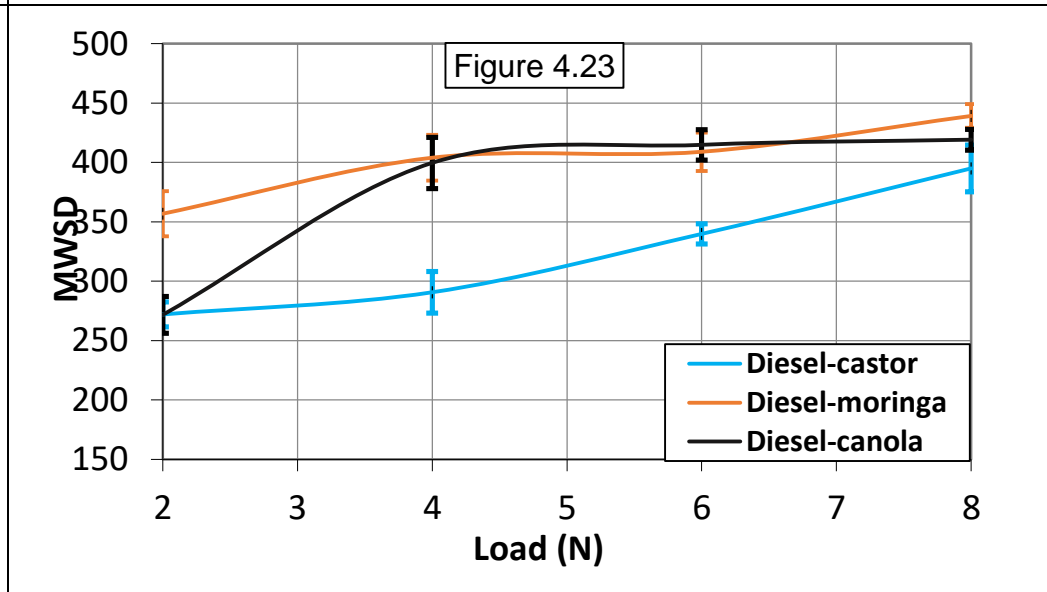
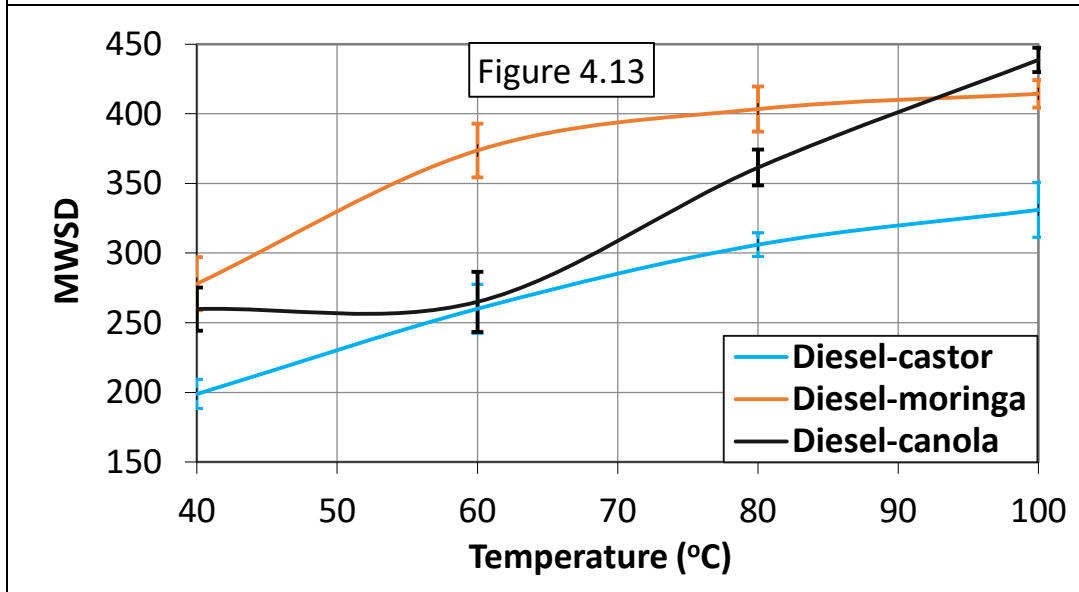
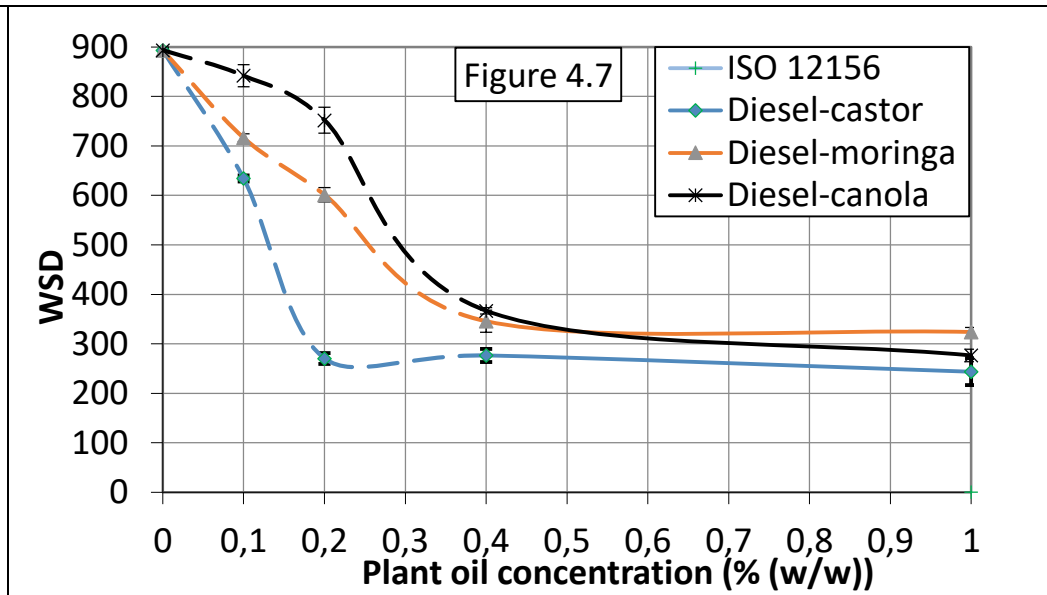
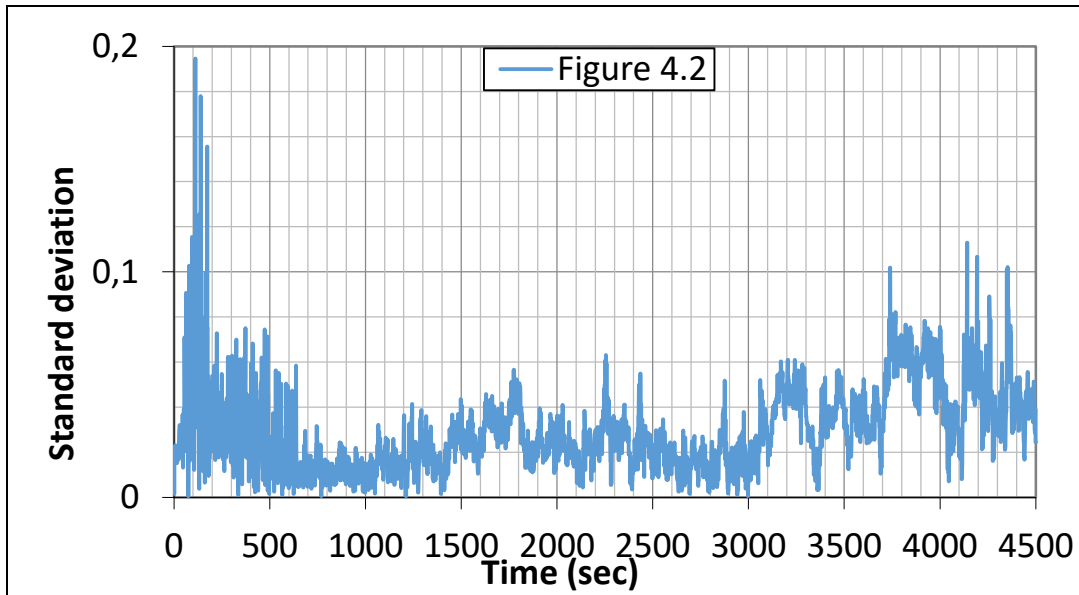


Figure A1: Humidity control setup (Langenhoven, 2014)

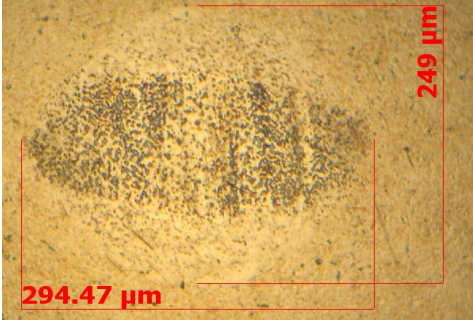
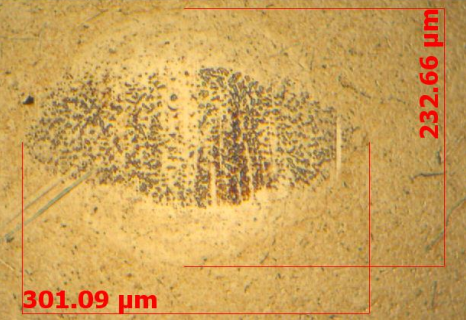
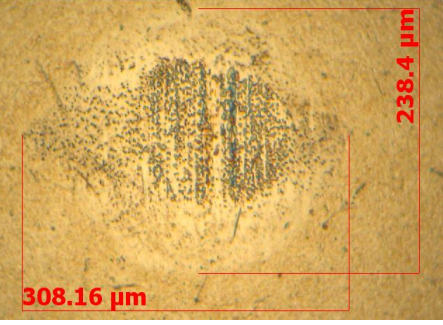
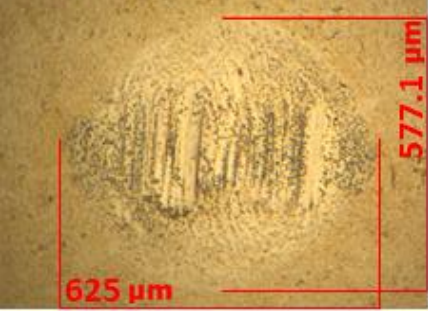

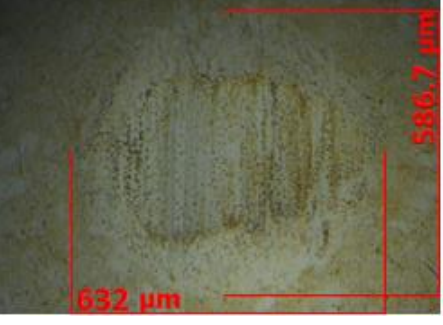
To supply conditioned air to the HFRR environmental chamber the compressed air is bubbled. Depending on whether moist air or dry air was needed in the environmental chamber, the wet column and/or dry column was regulated using a control knob attached to the rear of each column. This allows moist air or dry air to flow into the environmental chamber.

Appendix B – Standard deviations (error bars)

The standard deviation for the graphs in the results section are shown.



Appendix C – Wear scars at 0.2 % (w/w) plant oil in diesel

Run 1, castor oil, $MWSD = 271.5 \mu\text{m}$, $WS1.4 = 277 \mu\text{m}$, $CR = 2$	Run 2, castor oil, $MWSD = 267 \mu\text{m}$, $WS1.4 = 277 \mu\text{m}$, $CR = 2$	Run 3, castor oil, $MWSD = 273 \mu\text{m}$, $WS1.4 = 258 \mu\text{m}$, $CR = 2$
		
Run 1, moringa oil, $MWSD = 601 \mu\text{m}$, $WS1.4 = 597 \mu\text{m}$, $CR = 5$	Run 2, moringa oil, $MWSD = 593 \mu\text{m}$, $WS1.4 = 603 \mu\text{m}$, $CR = 5$	Run 3, moringa oil, $MWSD = 609.5 \mu\text{m}$, $WS1.4 = 625 \mu\text{m}$, $CR = 4$
		
Run 1, canola oil, $MWSD = 709 \mu\text{m}$, $WS1.4 = 735 \mu\text{m}$, $CR = 5$	Run 2, canola oil, $MWSD = 780.5 \mu\text{m}$, $WS1.4 = 781 \mu\text{m}$, $CR = 4$	Run 3, canola oil, $MWSD = 766 \mu\text{m}$, $WS1.4 = 780 \mu\text{m}$, $CR = 5$
